Université de Montréal

Decoding protein networks during porcine epidemic diarrhea virus (PEDV) infection through proteomics

Par Camila Andrea Valle Tejada

Département de pathologie et microbiologie
Faculté de médecine vétérinaire

Mémoire présenté à la Faculté de médecine vétérinaire
en vue de l'obtention du grade de *Maîtrise ès sciences* (M.Sc.)
En sciences vétérinaires
option microbiologie

Avril, 2019

Université de Montréal

Faculté de médecine vétérinaire

Decoding protein networks during porcine epidemic diarrhea virus (PEDV) infection through proteomics

Présenté par

Camila Andrea Valle Tejada

A été évalué par un jury composé des personnes suivantes :

Dr. Marcio Carvalho Costa, président-rapporteur

Dr. Levon Abrahamyan, directeur de recherche

Dr. Carl A. Gagnon, co-directeur de recherche

Dr. Francis Beaudry, co-directeur de recherche

Dre. Neda Barjesteh, membre du jury

Résumé

Le virus de la diarrhée épidémique porcine (VDEP) est responsable de graves pertes économiques. Les épidémies de VDEP ont détruit plus de 10% de la population porcine américaine au cours des 3 dernières années. Malheureusement, la compréhension insuffisante des interactions hôte-virus empêche la mise au point d'un vaccin efficace contre le VDEP. Les interactions hôte-virus sont très dynamiques et peuvent impliquer des complexes multiprotéiques. De plus en plus de preuves indiquent que les microvésicules extracellulaires (MVE) et la composition des particules virales jouent un rôle important dans la pathogenèse virale et la modulation de la réponse immunitaire de l'hôte à l'infection. De plus, on pourrait s'attendre à ce que la composition des virions de la diarrhée épidémique porcine (DEP) soit dépendante du type cellulaire, en raison de l'incorporation ou de l'association de protéines de cellules hôtes dans ou avec des virions. Par conséquent, la caractérisation des profils protéomiques des MVEs produits par les cellules infectées par le VDEP, et l'identification des protéines hôtes spécifiquement encapsidées dans les virions sont importantes pour notre compréhension plus approfondie des interactions virus-hôte. Pour atteindre cet objectif, nous avons produit et purifié des virions et des MVE de VDEP et analysé leur composition en protéines en utilisant une approche protéomique. Afin d'étudier la régulation spatio-temporelle de l'infection virale, une certaine optimisation de l'infection par le VDEP était nécessaire. Pour cela, nous avons synchronisé et augmenté l'entrée de virus dans les cellules et étudié les schémas protéomiques des cellules infectées par le VDEP selon un mode de résolution temporelle.

Nous avons constaté que l'infection par le VDEP affectait l'abondance de diverses protéines de l'hôte associées aux microvésicules produites par les cellules infectées. Plus précisément, nos données protéomiques ont révélé que les protéines impliquées dans la liaison aux acides nucléiques, les processus métaboliques et les voies de la réponse immunitaire étaient parmi les plus touchées par l'infection. Fait intéressant, les protéines de l'hôte impliquées dans la régulation du cycle cellulaire et du système cytosquelettique ont également été touchées en abondance, ce qui n'est pas étonnant, car plusieurs chercheurs ont rapporté que les protéines cytosquelettiques participent activement au déplacement des composants viraux vers le site d'assemblage et que de nombreux virus manipulent la réparation de l'ADN, ainsi que le cycle cellulaire. La présente étude a démontré

l’incorporation de nombreuses protéines cellulaires dans les virions de la DEP. De plus, nous avons démontré que les polycations (molécules à charge positive) eu augmente 9-fois l'efficacité de l'entrée et de l'infection du VDEP. Ainsi, les polycations peuvent être utilisés pour optimiser l’infection par le VDEP, et améliorer la production de vaccins.

À notre connaissance, il s'agit de la première étude de la composition des virions et des microvésicules de DEP produits par une infection par le VDEP.

Mots-clés : Le virus de la diarrhée épidémique porcine, protéomiques, polycation, polybrène, DEAE-dextran, composition du virion, microvésicules.

Abstract

Porcine epidemic diarrhea virus (PEDV) is responsible for severe economic losses. The PEDV epidemics have destroyed more than 10% of the US swine population in the past 3 years. Unfortunately, the insufficient understanding of virus-host interactions impedes the development of an effective vaccine against PEDV. Virus-host interactions are highly dynamic and may involve multiprotein complexes. Growing evidence indicates that extracellular microvesicles (EMV) and composition of the viral particles play an important role in viral pathogenesis and modulation of host immune responses to infection. Additionally, it could be expected that the composition of porcine epidemic diarrhea (PED) virions is cell type dependent, due to the differential incorporation or association of host cell proteins into or with virions. Consequently, the characterization of the proteomic profiles of the EMV, produced by the PEDV-infected cells, and identification of the host proteins that are specifically encapsidated into the virions are important for our further understanding of virus-host interactions. To accomplish this objective, we produced and purified PEDV virions and EMV and analyzed their protein composition using a proteomic approach. In order to investigate the spatial-temporal regulation of viral infection and due to the low overall infectivity of the virus, a certain optimization of the PEDV infection was needed. To this end, we synchronized and increased virus entry into the cells. This allowed us to study the proteomic patterns of the PEDV-infected cells in a time-resolved mode.

We found that PEDV infection affected the abundance of various host proteins associated with microvesicles produced by the infected cells. More precisely, our proteomic data revealed that proteins involved in nucleic acids binding, metabolic processes and immune response pathways were among the most affected by the PEDV infection. Interestingly, host proteins involved in cell cycle regulation and cytoskeletal system also were affected in abundance, which is not surprising since several investigators have reported that cytoskeletal proteins are actively participating in moving the viral components to the assembly site, and that many viruses manipulate DNA repair and cell cycle. The present study has demonstrated the incorporation of numerous cellular proteins into the PED virions. Additionally, we demonstrated that treatment of PEDV virions with polycations (positively charged molecules) induced a nine-fold increase in the efficiency of viral entry and infection.

Thus, polycations can be used for the optimization of PEDV infection and improved vaccine production.

To the best of our knowledge, this is the first study of the composition of PED virions and microvesicles produced by PEDV infection.

Keywords: Porcine epidemic diarrhea virus, proteomics, polycation, polybrene, DEAE-dextran, virion composition, microvesicles.

Table of content

List of tables

List of figures

List of acronyms and abbreviations

3C1: Poliovirus 3C-like proteinase

ABPP: Activity-based protein profiling

ANOVA: One-way Analysis of variance

ASFV: African swine fever virus

B2M: β-actin

Bcl-2: B-cell lymphoma 2

BtCo: Bat coronavirus

cAMP: Cyclic adenosine monophosphate

CDV: Canine distemper virus

CHIKV: Chikungunya virus

CPE: Cytopathic effect

CREB: cAMP responsive element binding

CRIPA : Le centre de recherche en infectiologie porcine et avicole

CsCl: Cesium chloride

DENV: Dengue virus

DEP : Diarrhée épidémique porcine

DHBV: Duck hepatitis B virus

DMEM: Dulbecco Modified Eagle Medium

DTT: DL-dithiothreitol

EBOV: Ebola virus,

EBV: Epstein-Barr virus

EDTA: Ethylene-diamine-tetra acetic acid

EGF: Epidermal growth factor

ELISA: Enzyme-linked immunosorbent assay

EMCV: Encephalomyocarditis virus

EMV: Extracellular microvesicles

ER: Endoplasmic Reticulum

ERGIC: Endoplasmic reticulum Golgi intermediate compartment

ESI: Electrospray ionization

EV: Extracellular vesicles

FACS: Fluorescence-activated cell sorter

FBS: Fetal bovine serum

FDR: False discovery rate

FRQNT : Fonds de recherche du Québec – Nature et technologies

FT-ICR: Fourier-transform ion cyclotron resonance

FWHM: Full width at half maximum

GAPDH: Glyceraldehyde-3-phosphatase dehydrogenase

Gfl: One Growth factor-like motif

GREMIP : Le Groupe de recherche sur les maladies infectieuses en production animale

h.p.i: Hours post infection

HBV: Hepatitis B virus

hCMV: Human cytomegalovirus

HCoV: Human coronavirus

HCV: Hepatitis C virus

Hel: Helicase motif

HIV: Human immunodeficiency virus

HPLC: High Performance Liquid Chromatography

HPLC-MS/MS: High Performance Liquid Chromatography tandem-mass spectrometry

HPV: Human papilloma virus

HSV: Herpes simplex virus

HTLV: Human T-cell leukemia virus

IAA: Iodoacetamide

IFA: Immunofluorescent assay

IFN: Interferon

IgY: Immunoglobulin Y

IKK: IκB kinase

IL: Interleukin

IPEC: Intestinal porcine epithelial cells

IRFs: Interferon regulatory factors

iTRAQ: Isobaric tags for relative and absolute quantitation

JAK-STAT: Janus kinase- signal transducer and activator of transcription

JEV: Japanese encephalitis virus

kDa: Kilo Daltons

KSHV: Kaposi's sarcoma-associated herpesvirus

LC: Liquid chromatography

LFP: Label-free proteomics

LFQ: Label free quantification

LIT: Linear ion trap

LTQ: Linear trap quadrupole

MALDI: Matrix-assisted laser desorption /ionization

MARV: Marburg virus

Mb: Metal ion binding domain

MeV: Measles virus

MOI: Multiplicity of infection

mRNA: Messenger RNA

MS: Mass spectrometry

mTOR: Mammalian (or mechanistic) target of rapamycin, a serine/threonine kinase

MVBs: Multivesicular bodies

MVE : Microvésicules extracellulaires

MW: Molecular weight

NDV: Newcastle disease virus

NF-κB: Nuclear factor kappa-light-chain-enhancer of activated B cells

NK: Natural killer cell

NSERC: Natural Sciences and Engineering Research Council of Canada

Nsp: Non-structural proteins

ORF: Open reading frame

p.i.: Post-infection

pAPN: N aminopeptidase

PBS: Phosphate-buffered saline

PCR: Polymerase chain reaction

PED: Porcine epidemic diarrhea

PEDV: Porcine epidemic diarrhea virus

PFA: Paraformaldehyde

PI3K-AKT: Phosphoinositide 3-kinases- Protein kinase B

PIN: Protein interaction networks

Plp: Papain-like proteinase

PMF: Peptide mass fingerprinting

PML: Promyelocytic leukemia

PPIA: Peptidylprolyl isomerase

PPIs: Protein–protein interactions

PPRV: Peste des petits ruminants' viruses

PRCoV: Porcine respiratory coronavirus

PRD: Positive regulatory domain

PRRs: Pattern recognition receptors

PRRSV: Porcine reproductive and respiratory syndrome virus

PVRL4: Poliovirus like receptor 4

PVX: Potato virus X

RdRp: RNA-dependent RNA polymerase domain

RIPA: Radioimmunoprecipitation assay buffer

RLRs: RIG-I-like receptors

RNA: Ribonucleic acid

RNP: Ribonucleic protein complexes

RSV: Respiratory syncytial virus

RT-qPCR: Real-time quantitative reverse transcription polymerase chain reaction

RTC: Replication and transcription complex

SARS-Co: Severe acute respiratory syndrome-related coronavirus

SCX: Strong cation exchange chromatography

SFV: Simian foamy virus

sgRNA: Subgenomic RNA

SILAC: Stable isotope labeling by amino acids

SINV: Sindbis virus

ssRNA: Single strand RNA

SV40: Polyomavirus simian virus 40

TBK1: TANK-binding kinase 1 Serine/threonine-protein kinase

$TCID_{50}$: 50% Tissue culture infective dose

TFA: Trifluoroacetic Acid

TGEV: Transmissible gastroenteritis coronavirus

TLR: Toll-like receptor

TMEV: Theiler's encephalomyelitis virus

TMT: Tandem mass tags

TMV: Tobacco mosaic virus

TNE: Tris-NaCl-EDTA buffer

TNF: Tumor necrosis factor

TOF: Time of flight

TRIS-HCL: tris-hydrochloric acid

TTV: Transfusion-transmitted virus

UPR: Unfolded protein response

VDEP : Virus de la diarrhée épidémique porcine

VEEV: Venezuelan equine encephalitis virus

VSV: Vesicular stomatitis virus

VZV: Varicella-zoster virus

WNV: West Nile virus

WT: Wilde-type

YFV: Yellow fever virus

ZIKV: Zika Virus

Acknowledgments

First, I will like to start with acknowledging my director, Dr. Levon Abrahamyan, for giving me the opportunity to work on this project initially as an intern and then as a master student. I will also like to thank my co-directors, Dr. Carl A. Gagnon and Dr. Francis Beaudry.

I would like to thank the member of both virology labs for the help in the laboratory as well as for suggestions regarding my oral presentations. Special thanks to Dr. Chantale Provost and to Yaima Burgher, for giving me tips for some techniques.

Thanks to all the members of my «comité-conseil» and jury: Dr. Levon Abrahamyan, Dr. Carl A. Gagnon, Dr. Francis Beaudry, Dr. Christopher Fernandez-Prada, Dr. Mariela Segura, Dr. Marcio Costa, and Dr. Neda Barjesteh.

I would like to acknowledge all institutions for their financial support: FRQNT, GREMIP, CRIPA, NSERC, and the University of Montreal.

Particular thanks to my professors at the Pontificia Universidad Javeriana, for making me fell in love with research, and, more specifically, with research in virology field.

I am forever thankful to my family in Colombia, Mom, Poff, Susan, Sebas. Thank you for making the path easier for me, as well as for all the long-distance emotional support.

I thank the Cuban team for making the lunch-time funnier and more interesting.

And finally, I thank my closest friends in St- Hyacinthe: Catarina, Agustina, and Vincent, for the advices, the laughs, love, and support. Without you this journey wouldn’t have been the same.

I. Introduction

Porcine epidemic diarrhea virus (PEDV) is considered as an emerging pathogen of swine. It is the causative agent of an enteric disease characterized by severe diarrhea, vomiting, dehydration, anorexia, and death on newborn piglets (1). It was first reported in England in 1971, then virus has spread to different European and Asian countries. Nowadays, PEDV circulates on the Asian, American and European continents and causes outbreaks in Asia and North America, resulting in a tremendous impact on the swine industry (1). PEDV-caused diarrhea is clinically indistinguishable from other diarrhoeal diseases such as the transmissible gastritis-enteritis virus infection. Therefore, to diagnose PEDV, several sensitive and specific laboratory-based techniques have been developed (2). Despite significant efforts to develop safe vaccines for controlling the epidemics of PEDV, the development of an effective vaccine remains elusive. Thus, a better understanding of the molecular interactions between PEDV and host cells and the evidence-based improvements of vaccine technological platform are indispensable for a cost-effective anti-PEDV vaccine.
PEDV is a member of the order *Nidovirales*, *Coronaviridae* family, genus *Alphacoronavirus*, and belongs to the group IV, according to the Baltimore classification. It is an enveloped virus with a positive sense ssRNA of 28 kb. PEDV genome consists of 7 open reading frames (ORFs) encoding 3 non-structural proteins: replicases 1a and 1b, and ORF 3; and four structural ones: spike protein (S), the envelope protein (E), membrane protein (M), and the nucleocapsid protein (N) (1, 3). Recent studies have shown close similarities between PEDV and bat coronavirus (BtCo), suggesting that PEDV might have originated from coronavirus present in bats, a natural reservoir for coronaviruses (4).

Despite that just one serotype of PEDV has been reported, studies of the S protein (also known as the Spike protein) gene have proposed that, PEDV could be classified in two groups G1 (classical strains) and G2 (epidemic or pandemic strains). Among G1, strains containing insertions or deletions in the sequence of the S gene have been described, which could have implications on the levels of PEDV virulence (2). The M (membrane) protein is the most abundant protein on the PEDV virions membrane. It not only serves as a structural protein for the virions, but it was reported that M protein can induce the production of antibodies (5). Another component of the viral membrane is the E (envelope) protein, which also can induce immune response (6). The N (nucleocapsid) protein is known to form a complex with the genomic RNA and provides a helical shape to the viral capsid (7). Finally,

the ORF 3, an accessory protein, is believed to function as an ion channel. It was shown that ORF 3 gene is dispensable for the PEDV replications in cell cultures, but it is tightly related to cell adaptation and virulence (1).

PEDV infection disrupts the absorption capacity of the villus of the small intestine, by damaging the integrity of the cells (8). Both PEDV M and E proteins can arrest the host cell in the S phase of its growing cycle through the cyclin A pathway. This probably provides a more favorable intracellular environment for viral replication, and virus takes advantage of the replication machinery of the cell, available at this cellular step. Furthermore, it was reported that N protein suppresses the IFN (interferon) type I and III response (9), while S protein is known for promoting cell apoptosis by interacting with PARP9 (10). Thus, evidence from numerous studies suggests that, similar to other viruses, PEDV infection is mediated by multiple protein–protein interactions (PPIs), which globally can be represented as molecular networks (protein interaction networks, PIN). Understanding the complex dynamics of the virus-host cell interaction will provide the necessary knowledge for the design of effective strategies against this enteric swine coronavirus. This is fundamental to our understanding of the PEDV epidemiology and pathogenesis. Proteomic-based approaches are used at increasing rates to characterize the dynamic virus–host molecular interplay. However, only a very few studies used proteomics tools to characterize the PEDV-host molecular interactions (11–16). Furthermore, for some viruses, it has been reported the incorporation or association of host cell proteins into or with virions, which could have an implications in viral life cycle and pathogenicity (17). Importantly, incorporation or association of viral proteins into or with exosomes/microvesicles has been largely studied, and it was shown that they have an important impact on viral assemble, antigenicity, viral spread, cell signaling, etc. (18).

At cellular level, PEDV viral growth kinetics have shown a peak of viral production at 15 hours post infection (h.p.i.), reaching a titer of $10^{5,5}$ virus/mL (19, 20). Routinely, PEDV production in simian cells yields up to $10^{5,5}$ to $10^{6,5}$ virus/mL, which could be considered low and not ideal for variety of downstream applications.

Based on the aforementioned findings, we hypothesized that: a) PEDV can change the intracellular levels of host proteins in order to modify the intracellular environment, to escape host defenses and facilitate their own replication and spread, and b) that host-virus

interactions are highly dynamic and may involve viral-host-protein complexes. Thus, it could be expected that the compositions of PED virions are cell-type dependent.

Accordingly, the main objectives of this work are to investigate the changes in the intracellular levels of host proteins during PEDV infection, and to identify the host cell proteins associated with or encapsidated into PEDV and microvesicles/exosomes of infected cells.

To this end, the next specific aims were proposed:

1. To optimize PEDV infection, using polycations;
2. To produce and purify PEDV progeny virions using simian cell lines that are routinely used for PEDV production and studies;
3. To analyze the composition of virions and microvesicles/exosomes through proteomics approach.

II. Review of the literature

1. Introducing porcine epidemic diarrhea virus (PEDV)

Porcine epidemic diarrhea virus is a member of the *Alphacoronavirus* genus in the *Coronaviridae* family of the *Nidovirales* order (categorize in the group I). It is an enveloped virus, with a positive sense non-segmented ssRNA of 28 kb. Its genome contains 7 open reading frames (ORFs) that codify 16 non-structural and 4 structural proteins. The structural proteins are the spike protein (S), the envelope protein (E), the membrane protein (M), and the nucleocapsid protein (N) (Figure 1) (1, 3).

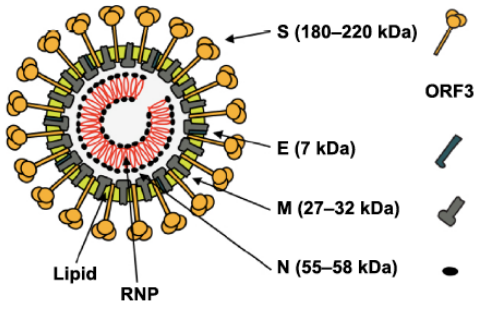

Figure 1. Schematic representation of the structure of porcine epidemic diarrhea viral particle. Structural proteins forming the virion are indicated, with their respective molecular weights (MW) (2).

1.1. Porcine epidemic diarrhea

PEDV is the etiological agent of porcine epidemic diarrhea (PED), a re-emergent virus, of enormous impact on the porcine industry. This virus was reported for the first time in England, and it was mistaken with transmissible gastroenteritis virus (TGEV) due to the similar symptoms produced by both viruses (21).

The primary sign of infection with PEDV is a watery diarrhea. It can affect pigs of all ages. Following the major symptom, the vomiting accompanied by anorexia and depression are common. Depending on the pigs' age, severity and morbidity could vary and reach 100% in piglets, but for sows it can have a lower impact (2). The incubation period is from 1 to 8 days, and viral particles can be detected during the first 48h of infection in a fecal sample.

Symptoms can last between 3 and 4 weeks. In adult animals, the disease is self-limiting, and recovery is within 7-10 days. Nevertheless, PED can have a significant impact on the growth of weanling piglets and on the reproductive performance of gilts and sows (reproductive failure) (22).

At the intestine level, PEDV completes its cycle in the cytoplasm of the villous epithelial cells, disrupts the lamina propria, and affects the intake of nutrients and electrolytes, which results in the characteristic diarrhea and deadly dehydration. Severe consequences on piglets could be due to the low rate of regeneration of the intestinal epithelial cells (23).

1.2. Biology of PEDV

1.2.1. Genome organization

PEDV has a positive sense non-segmented ssRNA genome of about 28 kb. Viral genome contains 7 ORFs that are organized in the following way: 5' ORF 1a/1b-(S)-ORF3-(E) -(M) -(N) 3'. The extreme 5' is capped, and the 3' tail is polyadenylated. 70% of the PEDV genome is occupied by the ORF 1a/1b, which codifies the non-structural polyproteins pp1a and pp1ab. These polyproteins are translationally processed into the 16 non-structural proteins (nsp) that play a key role in viral RNA replication, sub-genomic (sg) mRNA transcription and translation, besides, having an important function in the mechanisms of viral evasion of the host immune response. On the other hand, the genes encoding the structural proteins are a nested set of subgenomic RNAs (sgRNA) that perform a discontinuous transcription (Figure 2) (2).

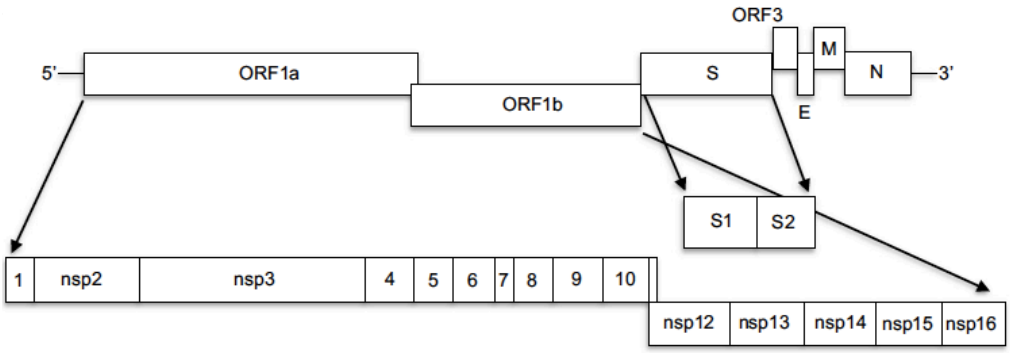

Figure 2. Schematic representation of porcine epidemic diarrhea viral genome.PEDV genome contains 7 ORFs. ORF1ab codifies for 16 nsp. ORF S codifies for the spike proteins; ORF3 results in an accessory protein. ORF E, M, N results in the expression of envelope, membrane and nucleocapsid proteins, respectively (6).

1.2.2. Non-structural proteins

The polyproteins pp1a and pp1ab encoded by the ORF1ab and the accessory protein encoded by ORF3 are the non-structural proteins found in the PED virions (2). Pp1a and pp1ab are cleaved internally by proteases into the 16 other proteins: poliovirus 3C-like proteinase (3C1), papain-like proteinase (Plp), one growth factor-like motif (Gfl), X domain (X), metal ion binding domain (Mb), an RNA-dependent RNA polymerase domain (RdRp) and a helicase motif (Hel), among others, which are highly conserved among coronaviruses (2). Interestingly, the accessory protein ORF3 has a high level of genetic diversity. Even though this protein is not essential for the PEDV replication, it has been associated with cell culture adaptation and strain pathogenicity (24).

1.2.3. Structural proteins

Similar to coronaviruses, PED virion is composed of the structural spike (S), membrane (M), envelope (E), and nucleocapsid (N) proteins. They are essential for viral life cycle and stimulation of antiviral host response. These genes and the corresponding proteins are important antiviral targets for viral diagnostics and for the vaccine's development.

1.2.3.1. Spike protein (S)

The spike protein plays an essential role in PEDV life cycle (2). The S protein is a key factor in the host receptor-virus interaction and virus-cell fusion. It is a class I fusion glycoprotein and has an apparent molecular mass of about 180 to 200 kDa. In order to activate the fusogenic properties of the S protein, it should be cleaved by trypsin-like proteases, after virus attachment (3). The cleavage results in two subunits S1 and S2. The S1, also called the N-terminal, binds to the cellular receptor. The S2, also called the C-terminus, contains the fusion peptide, allowing the virus to enter into the cell by membrane fusion. Successful entry of PEDV depends on this step (3). Additionally, the cell-surface associated S proteins, cleaved by exogenous proteases, can mediate cell-cell fusion and produce multinuclear cells (syncytium), inducing an obvious cytopathic effect (CPE) (25).

Aside from the attachment and fusion, the spike protein of the PEDV is implicated in other steps of viral replication. Wicht et al., in 2014 (26) showed that S protein of PEDV is an essential factor for viral progeny release. Authors infected Vero cells with PEDV classical strain CV777 (wild type WT) and mutant strain (cell cultured adapted and trypsin independent strain), in presence of trypsin or not. After 16 h.p.i they collected the supernatant and measured the amount of virion released. They found that WT strains' progeny was released in higher quantities, due to its dependency to trypsin (26).

The S protein is also a key factor of the cell adaptation and PEDV virulence. Sato et al., in 2011 (27) described that PEDV adapts to the Vero cell line by acquisition of several mutations in the S protein encoding gene. On the contrary, other structural proteins of the virus remained conserved over time. Interestingly, strains with mutations in the S protein showed attenuated phenotype during *in vivo* experiments. Thus, authors concluded that S protein is important for PEDV pathogenesis and virulence. The less was the amount of mutations in the S gene the more virulent the strain was. However, after long passage history PEDV S-mutants may revert in virulence and show a milder virulence (27). Insertion and deletion of nucleotides in the S gene are implicated in the PEDV pathogenic variability and facilitate the PEDV vaccine evasion. These strains were designated as S-Indel. As it was discussed earlier, deletions and insertions in S gene can attenuate the stain or enhance its

virulence and cause high mortality in suckling piglets. Thus, these strains are becoming a serious problem for the swine industry. Similar to what was observed for classical strains, severity of clinical signs of S-Indel strains also depends on the age of the animals (28).

The PEDV tropism is defined by the viral S protein. The N-terminal of S protein confers PEDV tropism to respiratory and intestinal tracts of the pigs. Virus with the deletions in this domain is able to replicate only in the enterocytes or in the respiratory tract, but not in both tissues. Similar phenotype has been observed for porcine respiratory coronavirus (PRCoV) and for the natural deletion variant of the TGEV (respiratory tract tropism) (15).

1.2.3.2. Membrane protein (M)

The membrane protein (M) is a type III glycoprotein with a molecular mass of 27-36 kDa. The M protein is the major component of the PED virions. Hence, the M protein is highly conserved among all strains, it is an excellent antiviral target. This feature of the M has important implications in the diagnostics (5). Antibodies produced against M protein of PEDV have been reported to be specific to the PEDV, when they were compared to other coronaviruses M protein (5). This protein plays an important role in PEDV viral life cycle, particularly, in viral assembly through its interaction with the viral E protein of virus (24).

1.2.3.3. Nucleocapsid protein (N)

The nucleocapsid protein (N) is a 58 kDa phosphoprotein. N protein plays a fundamental role in viral genome management (24). For instance, together with the viral RNA it forms the nucleocapsid of PEDV and provides a stable helical shape to the genome. This complex binds to the M protein, in this way protecting the viral genome (29). The N protein is produced in abundance during the early stages of infection and along the viral life cycle. It can be readily detected at the early time of infection (i.e. 6 h.p.i) (30). It has been shown that N protein mainly localizes in the endoplasmic reticulum, interacts with the several molecules involved in the cell cycle, and arrest host cells in S phase (29). Additionally, it has been reported that PEDV inhibits the host immune response by blocking the interferon (IFN)

signal signaling through its nucleocapsid protein. These strategies will be further explained in the section describing the PEDV-host interactions (13).

Recently (in 2019), a group of researchers from the National Science and Technology Development Agency (NSTDA) of Thailand, demonstrated that PEDV N protein can accelerate the growth ratio of a slow-growing PEDV strain. Additionally, authors observed a slight enhancement of infection of porcine reproductive and respiratory syndrome virus (PRRSV), on stable protein PEDV N protein-expressing Vero cells. On the contrary, they didn't observed any positive effect of PEDV N protein on Influenza virus replication (31).

1.2.3.4. Envelope protein (E)

The envelope protein (E; 7 kDa), a small transmembrane protein of PEDV, is a key component of the viral membrane. It has ion-channel properties and plays an important role in virion morphogenesis and maturation (24). In the infected cells, the E protein is located in the nucleolus or endoplasmic reticulum (ER). The ER localization of E protein induces ER stress, which can lead to unfolded protein response (UPR) and stimulation of inflammatory antiviral responses (14).

1.2.4. Viral life cycle

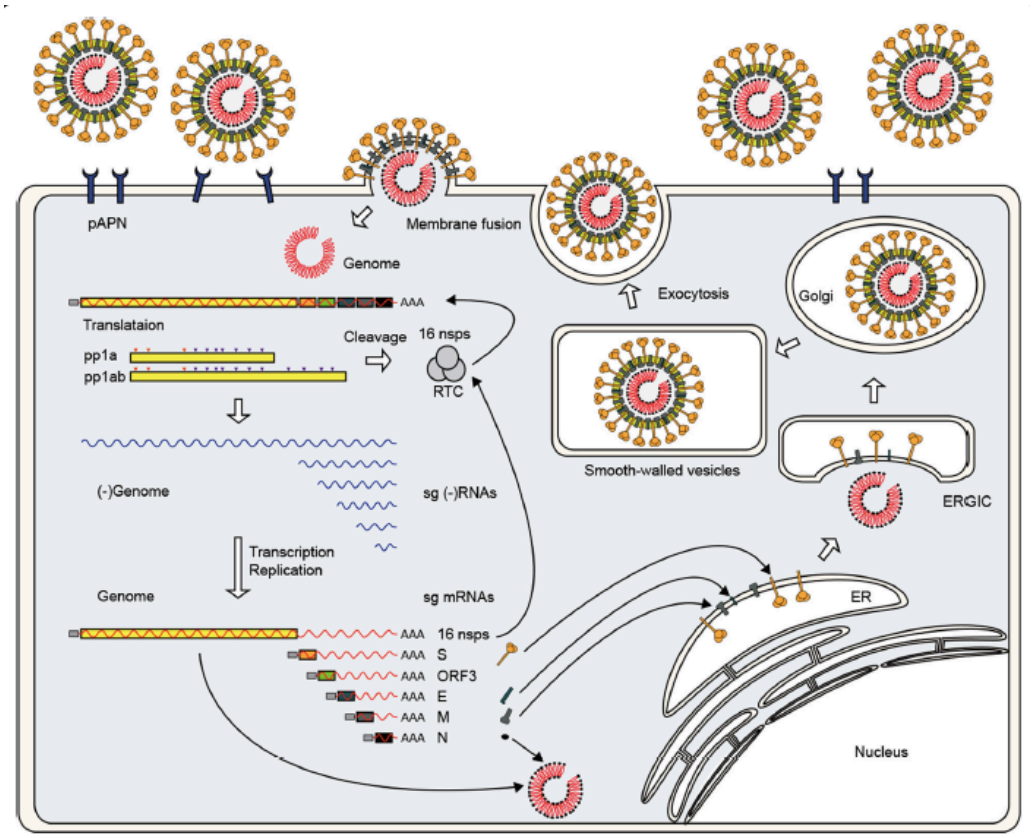

Figure 3. Overview of porcine epidemic diarrhea viral life cycle. PEDV binds its host cell using he spike protein. Translation of replicases pp1a and pp1ab starts immediately. Then, polyproteins are proteolytically cleaved into 16 non-structural proteins (nsp), which are part of the replicase-transcriptase complex (RTC). Transcription and replication of the genome takes place. Next, the envelope proteins are inserted in the endoplasmic reticulum (ER) and fixed in the Golgi apparatus. Finally, the progeny virus is assembled at the ER-Golgi intermediate compartment (ERGIC) and virions are released by the exocytosis-like fusion (2).

1.2.4.1. Cellular receptors

Until 2016, the N aminopeptidase (pAPN), a receptor abundantly expressed on the epithelial cells (particularly, in the small-intestinal microvillar membrane), was believed to be a principal host receptor for PEDV. Several studies showed that the presence of N aminopeptidase on the surface of permissive cell lines is essential for the PEDV biding and

cell entry. Moreover, in 2010, Nam and Lee reported that overexpression of pAPN in the non-expressing and non-permissive cell lines conferred them a susceptibility to PEDV infection (33). Earlier, Li and Li in 2007, demonstrated the blockage of PEDV infectivity when pAPN was masked by antibodies (34). Additionally, biochemical interactions between the S1 domain of the S protein with the pAPN has been also reported (35). But contrary to what was described for other permissive cell lines, Vero cells, which are widely used for the PEDV propagation, don't express pAPN. Nonetheless, Vero cells are permissive to PEDV (cell-adapted strains) infection, a fact that suggests the existence of different receptor for the PEDV. For example, PEDV was reported to bind to the sialic acid (15). Shirato et al. in 2017 (36) showed that pAPN was not a cellular receptor for the PEDV, but it could act as a promotor of the infectivity. In order to prove this, authors created a HeLa cell line stably expressing pAPN and infected them with PEDV or TEGV, known to use pAPN as main cellular receptor. Their experiments revealed that recombinant cell line was resistant to the PEDV infectivity but was susceptible to the TEGV. On the contrary, cell transfected with PEDV genome were able to produce infectious PEDV particles. Interestingly, overexpression of pAPN in porcine cells had a positive effect on PEDV infectivity, but it was attributed to the enzymatic activity of the receptor (36).

In 2016, Li et al. (37) showed that overexpression of porcine APN in non-susceptible cells didn't change their susceptibility towards the PEDV infectivity. They also didn't find any interaction between PEDV S1 and pAPN using fluorescence-activated cell sorter (FACS)-based assays. All their experiments were performed with multiple PEDV strains to exclude strain-specific artifacts (37), thus, there are no robust evidences that PEDV infects pAPN-expressing cells.

The ability to bind to specific cellular receptors is an important factor in determining the host range and tropism of viruses. It is well-documented that PEDV has tropism for small and large intestinal epithelial cells. However, additional studies are critical for better understanding the cellular tropism and evolution of PEDV. Nevertheless, in the process to discover the main cellular receptor for PEDV, co-receptor molecules or entry enhancement proteins have been found; such as occludin protein, member of the tight junctions of the small intestine (38).

1.2.4.2. Viral entry

After viral attachment via S protein to the cellular receptors, the spike protein undergoes conformational changes, which expose its trypsin cleavage site. Next, the trypsin cleaves the S protein at two sites: first, at the borderline between the subunits S1 and S2, and, second, at the S2, activating the exposure of the fusion peptide and positioning it in a close proximity to the host cell membrane. Then, cellular and viral membrane merge and PEDV genome is delivered into the host cells (Figure 3). This step might result in formation of syncytia, which is a characteristic CPE of the PEDV (25).

Occludin is a protein present in the tight junctions of the epithelial barrier, located in the intestinal epithelium cells (39). Luo et al., in 2017 (38), suggested that overexpression of the occludin in target cells enhanced susceptibility to the PEDV infection. Additionally, authors showed that reduction of occluding expression in target cells through RNAi assay, decreased significantly their susceptibility to PEDV infection. It has been observed that macropinocytosis inhibitors impeded occludin internalization and virus entry, indicating that virus entry and occludin internalization are tightly linked. Yet, the macropinocytosis inhibitors didn't impede virus replication, once the virus was inside the cells. This finding suggested that occludin internalization by macropinocytosis or a macropinocytosis-like activity is implicated in PEDV entry, but occludin is not involved in the initial attachment of virus to the cell (38).

1.2.4.3. Genome replication

Immediately after membrane fusion, the viral genome is released into the cytoplasm. It is translated into the first 2 replicases pp1a and pp1ab, which are proteolytically cleaved into the 16 non-structural proteins (nsps) that are part of the replication and transcription complex (RTC). Then, the RTC synthetizes the negative-strand RNA using genomic RNA and produces full-length genomic RNA and subgenomic mRNAs. Each subgenomic mRNA is translated into a structural protein (Figure 3) (2).

1.2.4.4. Assembly and viral spread

During viral replication, the viral envelope proteins, S, E, and M are inserted into the endoplasmic reticulum and attached to the Golgi apparatus. The N protein interacts with the genomic RNA to form helical ribonucleic protein complexes (RNP). The progeny virus is assembled after maturation of the RNP in the endoplasmic reticulum Golgi intermediate compartment (ERGIC), and then freed by the exocytosis-like fusion of smooth-walled vesicles with the host cell plasma membrane (Figure 3) (2).

1.2.4.5. Microvesicles and exosomes

Extracellular vesicles (EV) are vesicles release by the cells into the media. They are classified in three mayor groups according their size; exosomes, microvesicles and multivesicular bodies (MVBs) (40). Microvesicles are cell-derived membrane vesicles that mediate the cellular signaling and transport of various molecules. Their main objective is to communicate by delivering molecules to the cells. Exosomes are the most studied and well-characterized EVs. They are derived from the MVB and they play an important role in intercellular communication via RNAs and proteins between neighbor cells (41). Different cellular and extracellular processes and signals can trigger production of the exosomes, such as cell differentiation, activation, stress, cell death, and viral infection have been reported (40). The function of each type of EVs varies among them, besides cells communication, exosomes contain RNases, trypsin, or any degradative substance, due the composition of its bilipid membrane (42). Microvesicles on the other hand, are strictly related to the cell communication processes (40).

Coronaviruses replicate their genomes in the cytoplasm, in the specific replicative structures associated with cellular membranes. Viral infection induces formation of the cell-derived organelle-like membranous structures, where the viral replication-transcription complexes (RTCs) localize. Initially, the intracellular rearrange results in two types of organelle-like replicative structures: the double membrane vesicles (DMV) and convoluted membranes (CMs). Later, highly organized cubic membrane structures, the large virion-containing vesicles (LVCVs) and condensed tubular bodies are formed (43). These microvesicles have been recently described for PEDV infection. More specifically, PEDV

non-structural proteins trigger the synthesis of these microvesicles, appearing after 24 h.p.i, with a peak after 60h post infection. It was suggested that the endoplasmic reticulum, which plays a key role in late viral assembly, is the mostly likely source of DMVs (44).

Porcine reproductive and respiratory syndrome virus (PRRSV) is a nidovirus, part of the *Coronaviridae* family. Recently in a study, exosomes purified form PRRSV-infected cells were analyzed through proteomics, showing that these particles contained genomic viral RNA and viral proteins. Interestingly, infection of PRRSV-susceptible and -non susceptible cells with the purified exosomes, performed successful infection. Authors conclude that exosomes can be a mechanism of PRRSV to evade host immune response (45). Importantly, exosomes have been proven as a vaccine mechanism against PRRSV. Authors have report that exosomes isolated form non-viremic animals (animals previously exposed with PRRSV but free of virus at the moment of isolation) contained antigenic viral proteins. Moreover, the serum of non-viremic pigs reacted against the purified exosomes. Authors conclude that exosomes could be a new approach to control PRRSV infection (46).

Little is known about PEDV infection stimulating the use of microvesicles and exosomes. Demonstrating the utility of these molecules for PEDV viral life cycle, could help us to identify a new antiviral therapy strategy, as well as to fill the knowledge gap of PEDV-host molecular interactions.

1.3. Global distribution

Diarrheal disease resulted from PEDV infection in pigs was first reported in England in 1971. Initially, due to the typical symptoms shown by sick pigs, it was proposed that the causative agent is the transmissible gastroenteritis coronavirus (TGEV), due to the typical symptoms shown by sick pigs. Five years later, an outbreak of PEDV was reported in Belgium, and subsequently, in the 1980's and 1990's, PEDV was identified throughout Europe.

With the time, the outbreaks decreased on this continent and PEDV crossed borders to Asia, where it became endemic. Since 2010, several Asian countries such as Korea, Vietnam, China and Japan, large outbreaks causing major impact on the porcine industry have been observed (47). Significant outbreaks of PEDV with 50 to 90% mortality and 80 to

100% morbidity in suckling piglets emerged (48). In 2013, PEDV was reported for the first time in United States, and within a year it extended all over the country and neighbors (Mexico and Canada). It was shown that the strains isolated in the US are genetically related to the strains from China, with a distinguished U insertion. One year later, the PEDV strains isolated in the US showed different deletions and insertions in the S gene, suggesting a possible recombination event between the Chinese and US strains (2). Thus, taking in the consideration the phylogenetic studies of the S gene of PEDV, it was proposed that PEDV strains can be classified into 2 genotypic groups: genogroup 1 (G1; the classical) and genogroup 2 (G2; the field epidemic or pandemic). Each genogroup was additionally divided into the subgroups 1a and 1b, and 2a and 2b, respectively. G1a includes the classical PEDV strain CV777, vaccine strains, and viral strains adapted to the cell cultures. G1b contains new variants identified initially in China and then in the US and South Korea. The G2 genogroup contains global field isolates, which are grouped into 2a and 2b subgroups, responsible for previous epidemic outbreaks in Asia and current pandemic outbreaks in North America (2).

1.4.Strategies for the control of PEDV

1.4.1. Diagnostics

Because of PEDV similarities to any pathogen causing diarrhea, vomiting and anorexia; diagnostic of porcine epidemic diarrhea virus can't be based on symptoms presented by the animal. Diagnostic approaches such as direct and indirect immunofluorescence, ELISA are routinely performed, however, the RT-qPCR is the standard technique to diagnose PEDV-infected pigs. Immunohistochemical assay and direct electron microscopy are other additional techniques, which help determining the presence of PEDV in the samples. Depending on the type of samples, one or other type of technique could be more suitable. ELISA is used generally to study the presence of IgG or IgA in the sera of PEDV-infected piglets (49, 50). For the diagnostics purposes, an indirect ELISA, based on the PEDV structural protein M, has been designed as well, showing no cross-reactivity with the M proteins of other Coronaviruses (5).

RT-qPCR is the most commonly used technique, because of its sensitivity, specificity, and rapid time to results. Primers for the conserved regions of PEDV genome such as M gene, N gene, and ORF 1 are utilized to analyze samples for the PEDV presence (49). Since the S gene is the least conserved and undergoes through insertions and deletions processes, it is not used for diagnostics purposes (28).

1.4.2. Treatment

Four strategies have been described to treat PEDV outbreaks (Table I). Although, most of these options could work, majority of them have important disadvantages, that can't be ignored. The best approach to overcome and avoid any PEDV outbreak seems to be safe and effective vaccines.

On the conventional side, farmers treat suckling piglets with oral electrolyte solutions, to overcome dehydration. For adult pigs, it is recommended drop the intake of dry food upon 12–24 h and then, water should freely available for the pigs (48).

Table I. Strategies for PEDV-infection treatment

Strategy	Advantages	Disadvantages	reference
Exposure of the sow to the intestinal content of a PED dead pigs.	Generation of artificial immunity.	The viral load in the intestine content was unknown. Other pathogens could be transmitted and generate a larger outbreak, such as PRRSV and PCV2.	Song and Park., 2012 (51)
Treatment of pigs with anti-PEDV immunoglobulin (IgY) produced in egg yolk or with the	Shown to increase survival rate on treated pigs.	It is a strategy of prevention. Once the animal is infected with PEDV, this strategy won't be useful.	Song and Park., 2012 (51)

colostrum of immunized cow.			
Expression of neutralizing anti-PEDV antibodies in *E. coli* to block or treat viral infection *in vivo.*	Demonstrated to neutralize PEDV *in vitro.*	Performed only *in vitro.* *In vivo* approaches are necessary to validate the treatment. No indication of effectiveness was concluded.	Pyo et al., 2009 (52)
Inoculation to PEDV-infected pigs with epidermal growth factor (EGF)	Stimulates epithelial crypt cells growth, largely destroyed during the viral infection. Helping to recover the animal from the dehydration.	Further toxicological analyses are needed to determine safety level of the approach. It is expensive compared to the already mentioned strategies.	Jung et al., 2008 (53)

1.4.3. Vaccination

Vaccine development against PEDV began earlier in Asia compared to Europe and North America. PEDV is endemic in several Asian countries; therefore, it was a constant demand for effective vaccines against the PEDV. In Europe, the frequency of PEDV outbreaks decreased by 2007, however, mild symptoms in pigs of all ages have been reported in positive farms. In North America, PEDV appeared in 2013 in the United States and has been around since then (54).

Table II. Available vaccines for PEDV prevention in Asia and North America

Location	Type of vaccine	Administration	Specifications	Efficacy	Reference

North America	iPED: Inactivate particle	Two intramuscular doses within three weeks, in young pigs. Three oral inoculation to sows	Truncated in the S gene, produced in SirraVax℠ RNA Particle.	Viral shedding reduced in young pigs. Mortality drop from 91% to 63% in sows	Fredrickson et al., 2014 (55)
	Porcine Epidemic Diarrhea Vaccine (Zoetis): Inactivated whole virus	Two oral doses within three weeks for pregnant sows	Liquid from with an adjuvant that claims to increase the immune response	Increase titer of neutralizing antibody in sows compared to the control group	Schwartz et al., 2016 (56)
	Vaccine developed by InterVac: Inactivated virus	Two intramuscular doses within two weeks for pregnant sows (pre-farrowing)	Liquid from with an adjuvant that claims to increase the immune response	High levels of neutralizing antibodies were found in the milk and serum of piglets born to vaccinated sows	Makadiya et al., 2016 (57)
Asia	Trivalent vaccine (PEDV, TGEV and porcine rotavirus	One-time intramuscular inoculation to piglets	Based on the classical CV777 (G1-a) strain, produced on Vero cells	Resulted in partially protected piglets against PEDV	Chen et al., 2010 (58)

): Attenuated vaccine				
Bivalent (PEDV and TGEV): Attenuated Vaccine	One-time intramuscular inoculation	Contained the PEDV strain ZJ08 (G1-b) or AJ1102 strain (G2-b).	Still under evaluation	Song et al., 2015 (1)
P-5V vaccine: live Vaccine	Two-time intramuscular inoculation	PEDV strain 83P-5 (G1-a) attenuated through several passages on Vero cells	The vaccinated sows displayed PEDV specific antibody responses, containing neutralizing antibody in the colostrum. Reduction of clinical signs and mortality on piglets fed with the immunized sows-colostrum was observed.	Sato et al., 2018 (59)
South Korean G2-b vaccine: Inactivat	Two-time intramuscular inoculation of Pregnant sows	based on G2-b strain KOR/KNU-141112/2014	piglets born to vaccinated sows had reduced morbidity, mortality after	Song et al., 2015 (1)

ed vaccine	(pre-farrowing)	challenge with PEDV	

The most common approaches are to inoculate the sows before farrowing, in order to generate lactic immunogenicity, or direct inoculation to the young pigs. In general, the reduction of mortality, the morbidity and virus shedding, in orally inoculated young pigs were higher than in new born piglets. In comparison, sows inoculated with either viral genome or attenuated virus, produce a higher titer of neutralizing antibodies in the milk and colostrum. New generation of vaccines, directed against the PEDV strains G2, showed increased significantly pig's survival (54).

1.5. PEDV-host interactions

1.5.1. Immunogenic interactions between host cells and PEDV

To any pathogen invasion, cells will display several strategies such as cytokines and chemokines production to eradicate or control infection. One of the most important cytokines to restrict viral replication is the interferon (IFN) production (60). However, viruses have developed strategies to supress IFN production through their viral proteins (61–63). The activation of IFN response can be mediated by toll-like receptors (TLRs) and RIG-I-like Receptors (RLRs), which recognize viral RNA or DNA in the endosomes or cytosol. Then, activation of Serine/threonine-protein kinase (TBK1)-mediated phosphorylation of the IRFs (interferon regulatory factors) take place, activating the IFN transcription (Figure 4) (64). Serine/threonine-protein kinase (TBK1), a member of the IKK protein kinase family, is one of the many molecules that play key roles in the IFN regulation. TBK1 is a member of the IKK protein kinase family.

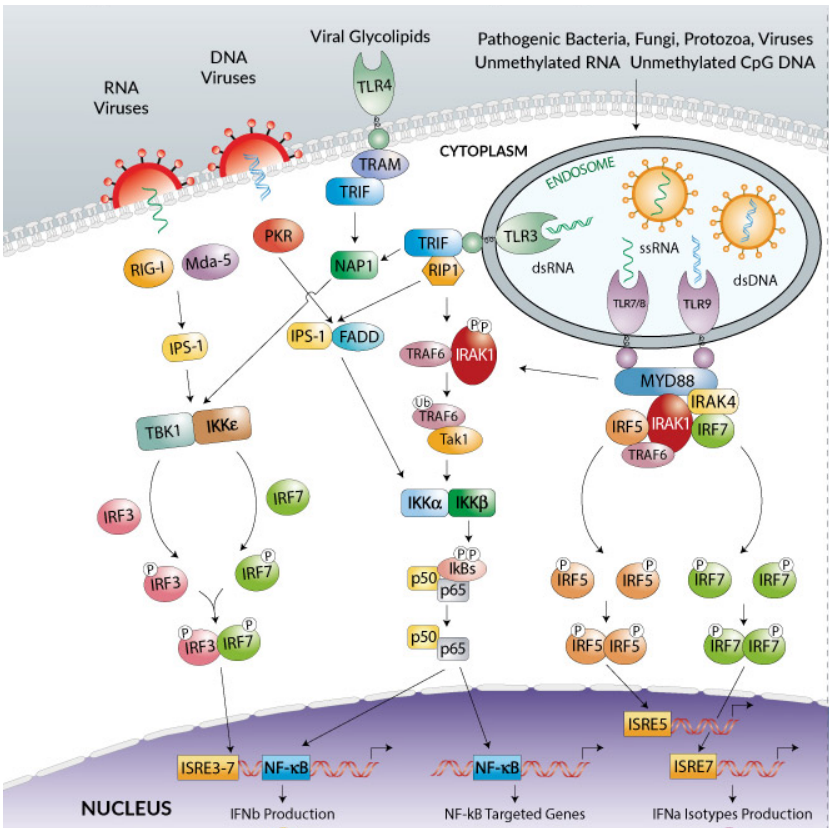

Figure 4. Inflammatory response to cytosolic or endosomal nucleic acid sensors.Recognition of nucleic acids through endosomal or cytosolic sensors, will activate a cascade of transcription of different molecules (IFRs, NF-kB). This process promotes cell activation as well as expression of different genes, resulting in TNF, IFN and IL responses (65).

Since TBK1 plays an important role in the IFN signaling pathway, viruses evolved mechanisms aimed at inhibition of the IFN production (66). This immune response evasion has been shown also for the PEDV. Its structural protein N impairs the IFN production by interacting with TBK1, sequestering this molecule and avoiding vital interaction between TBK1 and IRF3. The precise mechanism of this interaction is yet to be investigated, but several theories are proposed (9). Moreover, PEDV can interfere with type I INF production not only through its structural proteins but also through its non-structural proteins like nsp1(6). As it was mentioned earlier, the interaction between TBK1 and IRF3 is important for regulation of IFN expression. Upon PEDV infection the IRF3 displays a signal to form a

complex with the transcription co-activator CREB (cAMP responsive element binding)-binding protein (CBP)/p300. The IRF3-CBP/p300 complex then binds to the positive regulatory domain (PRD) regions of the IFN-β promoter, assembling together with NF-κB and other factors, to stimulate the transcription of type I IFN genes. The IRF3–CBP/p300 interaction is vital for IFN transcription. The nsp1 of PEDV causes the CBP degradation by the proteasome-dependent pathway (6).

Moreover, little is known about the pro-inflammatory response (chemokines) against PEDV. It has been shown that PEDV down-regulates different chemokines (IL-1α, IL-1β, CXCL8) to promote its own replication (67). Yu el al., in 2019 (67) further showed that PEDV nsp4 contributed to the up-regulation of IL-1α, IL-1β, TNF-α, and CXCL8, inhibiting PEDV viral life cycle *in vitro* (67). Additionally, Xu et al. in 2013 (68) demonstrated that cells overexpressing PEDV E protein were significantly up regulating IL-8. Authors related the up regulation of the IL-8 with the fact that E protein is normally and mainly localized on the ER, where it causes ER stress and IL-8 activation. At the same time, overexpression of E protein causes high expression of B-cell lymphoma 2 (Bcl-2) protein, a cell survival anti-apoptotic factor. Additional findings will be essential to elucidate the exact role of E protein in the antiviral host response against PEDV (68).

Likewise, it has been described that N protein up-regulates IL-8, causes ER stress and prolongs cell cycle phases, which are beneficial for viral infection. The S phase of cell cycle provides an optimal cellular environment for viral replication. Interestingly, the N protein of PEDV is able to inhibit the cell proliferation and prolongs the S-phase cell cycle (29) . Cyclin A is an important molecule for cells to pass from the S phase to G2/M phase. It has been shown that in PEDV N protein-expressing cell lines, cyclin A is significantly lower than in control cell lines (29). Also, it was found that PEDV N protein significantly inhibits the transcription of cyclin A. Since the PEDV N protein is mainly localizes in the ER and up regulates the chaperon GRP78, the ER stress response during PEDV infection (at least partially) is attribute to this protein. Finally, because PEDV N protein induces ER stress, it significantly activates NF-kB, which leads to induction of IL-8 transcription (29). Further studies are needed for understanding the roles of pro-inflammatory response in PEDV replication and host immune response.

2. Proteomic analyses

During the past three decades, mass spectrometry (MS) based proteomics has become one of the preferred methods for identifying **protein-protein interactions** and gaining insights into the complex networks of molecular interactions between the host and pathogen (69–72). There are different types of proteomic approaches: structural, functional, quantitative, and comparative expression profiles. These approaches can be performed through labeling proteomics, or label-free proteomics (Figure 6) (73). In general, the proteomic strategies involve following common steps: production and extraction of the proteins of interest from the sample, preparation of the protein samples for chemical or enzymatic digestion, digestion of proteins followed by the cleanup or desalting of the final peptide mixture prior to MS, analysis of the produced peptides by different types of mass spectrometers (Table III). The final step of proteomics workflow is the performing a database search to identify the proteins based on the peptides discovered in the sample.

Proteomics approaches proved to be effective at characterizing the composition of viral composition, **studying** viral life cycle, and changes in the virally-infected cells. Furthermore, proteomic tools are widely employed for searching new targets for antiviral strategies (74, 75).

2.1. Key steps in proteomic analysis

Once proteins have been produced, they can be separated or not prior to MS analysis. Separation before the MS analysis is most commonly done through one-dimensional or two-dimensional gels. Depending on the complexity of the sample, separation of proteins can be reasonable or not (76).

Prior to MS, proteins are enzymatically or chemically digested into peptides. There are two ways digest proteins; the first one is directly with proteases (in-solution), and the second one is in gel digestion, if gel electrophoresis separation was performed before (77). Then, the resulted peptides are ionized and desalted through a mass spectrometer. The mass spectrometers are typically composed of four elements: an ionization source, mass analyzers, an ion mirror, and a detector. Variety of mass spectrometer configurations are used, either

simple or hybrid (Table III). Recently, a new generation of mass spectrometers has been developed combining segmented quadrupole and Orbitrap mass analyzer, called the Q-Exactive. It designed to make easier the measurement and coupled with a higher sensitivity, compared to older generation of spectrometers (78). Among the new features of the Q-Exactive instrument are the high ion currents, fast high-energy collision-induced dissociation peptide fragmentation, double mass spectrometric resolution, 1 s for a top10 higher energy collisional dissociation (79).

Table III. Variety of mass spectrometer configurations commonly used for quantitative proteomic analysis

Mass spectrometer	Specifications	Reference
Electron spay ion source (ESI)	Involves 3 phases: a dispersal of charge droplets in a delicate spray, then a solvent evaporation, and, finally, an ion ejection of the very charged droplets, resulting in the foundation of desolvated ions	Ho et al., 2008 (80)
Matrix Assisted Laser Desorption/Ionization (MALDI)	The technique involves the following three steps: first, a low organic compound matrix is added to the digested sample, and the mixture is applied to a metal plate and dried; then, the sample plate is subjected to a laser irradiation for a short time, forming molecular ions; third, the resulting ionized peptides are analyzed by a mass analyzer to reveal characteristic information about the composition of the sample based on their mass-to-charge ratios.	Clark et al., 2013 (81)
Triple-quadrupole mass spectrometers	Often used to obtain amino acid sequences. This system performs the tandem mass spectrometry (MS/MS). Called that way	Graves and Hystead 2002 (77).

	because it involves two stages of mass analysis by two different mass analyzers	
Quadrupole-time-of-flight (QqTOF)	This is a combination of a quadrupole mass spectrometer with a TOF analyzer. The principal application of a Qq-TOF mass spectrometer is the protein identification by amino acid sequencing, including any potential post-translation modifications that those amino acids might have undergone.	Graves and Hystead 2002 (77).
Matrix Assisted Laser Desorption/Ionization-time-of-flight (MALDI-TOF)	Is a combination of matrix-assisted laser desorption/ionization and time-of-flight mass analyzers. Its main application is mass fingerprinting of peptides. It is completely automatic, which makes it easier to work with a large scale of samples.	Graves and Hystead 2002 (77).
Fourier transform ion cyclotron resonance (FT-ICR)	Is a Fourier transform ion cyclotron resonance mass spectrometer. It reaches a high mass resolution and mass accuracy. Similar to others, this technique identifies the amino acid sequences and protein fingerprints	Perry et al., 2008 (82)
Linear trap quadrupole (LTQ)-Orbitrap	Can pull up a mass resolution up to 150,000 ions. It has a high mass accuracy, and a larger capacity of ion trapping compared to FT-ICR, among other characteristics. This system is less expensive compare to others, smaller and easier to manage.	Perry et al., 2008 (82)

The last step in a proteomic analysis is the data analysis. After the processing the sample by a mass analyzer, the peptides are identified through peptide mass fingerprinting (PMF). This technique uses the masses of peptides derived from the analyte's spectra as to

check against the database of predicted peptide masses from databases of known proteins. If they overlap, the identification and changes can be assessed. There are different data searching programs such as MASCOT, SONAR, SEQUEST that are available for this task. MASCOT seems to be the most complete database. The main disadvantage of these programs is their vagueness, when identifying proteins due to peptide redundancy. In other words, similar amino acid sequences with small differences in the post-translational changes will have comparable peptide masses (77, 83).

2.2. Types of mass spectrometry analyses

As it was discussed before, there are two types of quantitative proteomics: label-free or label-based proteomics (Figure 6). For the labeling techniques, peptides are tagged metabolically, chemically, or enzymatically. The label-free quantitation technique determines ion quantity or peak intensity (73).

Among the metabolic labeling based techniques, the stable isotope labeling in cell culture (SILAC) is one of the best developed approaches. This technique relies on growing cells in culture media containing "light" and "heavy" isotopically labeled amino acids, which are going to be incorporated into the cell proteins by metabolic processes of protein synthesis. Heavy-labeled proteins are going to be distinguished from the pool of the proteins, and the difference between the peak's intensities will reflect the relative abundance of proteins labeled with the same amino acid (Figure 6. B) (84).

Along chemical labeling, isobaric tags for relative and absolute quantitation (iTRAQ) and the tandem mass tags (TMT), are the most used techniques. These tags are distinguished by their abundance and scores in the mass spectrometers. There are 12 available isobaric tags, which mean that at least 12 conditions can be compared (85). Additionally, trypsinization of samples can't be performed, because trypsin is unable to cleave modified lysine, so protein digestion step becomes complex (73).

Labeled proteomics has major advantages when studies are targeting a known group of proteins. Nevertheless, when performing a discovery proteomics approach, labeling is limited to a certain number of labels. Economically, these types of studies are high-priced, so limitation on number of samples would be a concern (84).

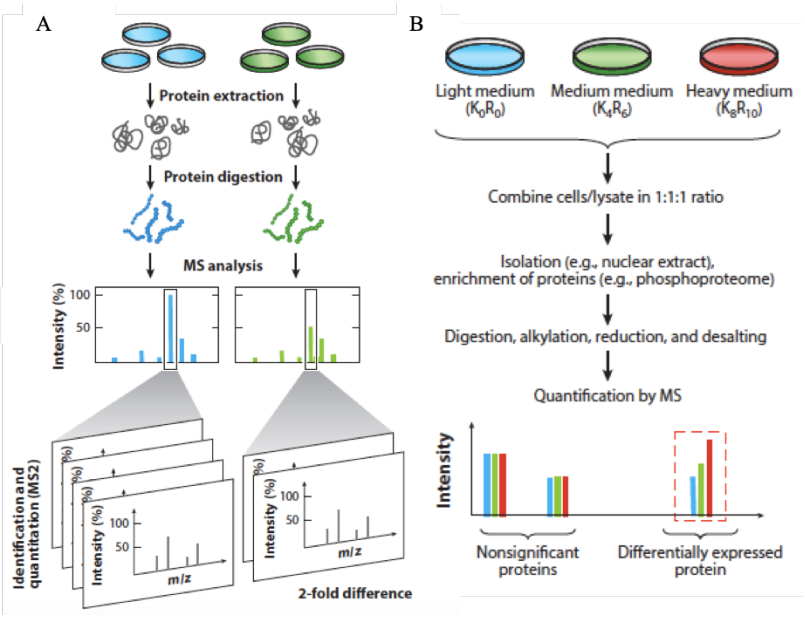

Figure 5. Labeled and label-free quantitative proteomics. (A) Spectral counting–based label free quantification (LFQ) techniques for identification and quantitation using MS/MS spectra. Quantitation is based on the number of spectra identified for each peptide. (B) Amino acid tagging and targeted proteomics strategies. Cells are grown in media containing light, medium, or heavy amino acids with stable isotopes, and lysates are combined for processing (73).

Label-free proteomics (LFP) is a simple and cost-effective application in quantitative proteomics. This approach has been used to either replace or to enhance labeling techniques. LFP can be divided in two types, ion counting, and intensity based. Ion counting determines the number of peptides of a protein in a sample and divides it by the theorical number of peptides of the identify protein. One of the disadvantages of this approach is that the number of peptides generated by proteolytic digestion (with trypsin) depends on the length of the protein. Therefore, quantitation of lighter proteins (< 20 kDa) won't be as precise as for larger proteins (73).The second LFP approach is intensity based, where the MS-signal intensity is measure, in the area under the chromatographic peak of the precursor peptide ion, while it is eluted in the liquid-chromatography (LC) column (73).

LFP is commonly used for discovery proteomics because of its simplicity, cost-effectiveness, and rapid results. However, it does not allow analysis of multiple samples, nor the differentiation of desired proteins in a sample. Variability in ion selection, retention time, and ionization efficiency are consider the major disadvantages of the approach (73, 84).

2.3. Proteomic studies of PEDV-infected cells

To the best of our knowledge, just a few reports have been published where proteomics approached were used for PEDV studies. All those reports are focused at the analysis of the PEDV-infected cells and either compared the proteomic profile of different cells lines or tissue infected with PEDV or compared the effect of different PEDV strains on the host-cell proteome (Table IV). The proteomic composition of the PEDV virions and PEDV-infection induced microvesicles were not reported to date.

Table IV. Reported proteomic studies of PEDV infected-cells

Study	Proteomic approach used	Results & Conclusion	Reference
Proteome analysis of porcine epidemic diarrhea virus (PEDV)-infected Vero cells Proteomics	The authors used the iTRAQ labeling approach to compare proteomic changes between mock- and PEDV-infected cells. An extra step of SCX (Strong Cation Exchange) chromatography, was performed before MS/MS.	HSP27 was observed to be downregulated by PEDV infection. It was speculated that this could be associated with the inhibition of host antiviral response. Authors, also showed a downregulation of caspase-8 expression in PEDV-infected Vero cells, which could explain the attenuated apoptosis at early infection phase, thus, supporting the high production of PEDV.	Zeng et al., 2015 (11).

Analysis of protein expression changes of the Vero E6 cells infected with classic PEDV strain CV777 by using quantitative proteomic technique	The proteomic profiles of PEDV-infected Vero E6 cells were analyzed using iTRAQ approach.	Among up and down regulated proteins by PEDV infection, integrin β2 was found be down-regulated, while integrin β3 was up-regulated. Validations experiments confirmed that the presence of the amino acid motifs in the sequence of PEDV S protein recognized by integrins, suggesting that integrin proteins may be involved in the PEDV attachment and entry.	Sun et al., 2015 (12).
iTRAQ-based comparative proteomic analysis of Vero cells infected with virulent and CV777 vaccine strain-like strains of porcine epidemic diarrhea virus	Using the iTRAQ-based proteomic approach, it was reported that virulent and CV777 vaccine strain of PEDV induced different proteomic profiles in Vero cells.	More than 1000 proteins were differentially regulated in virulent and CV777 infected cells. Additionally, it was found that the virulent strain activated NF-κB pathway more intensively than the CV777 vaccine strain-like isolate and caused stronger inflammatory cascades.	Guo et al., 2017 (14)
Pig jejunum protein profile changes in	The proteomic profiles of jejunum cells of *in vivo* infected with PEDV strain	The abundance of 201 proteins was dysregulated in the presence of PEDV.	Pearce et al., 2016 (16)

response to a porcine epidemic diarrhea virus challenge	USA/Iowa/18984/2013 were changed	Abundance of annexin A5 and heat shock protein 70, was up regulated in the presence of the PEDV. It was noticed, that the intracellular levels of other group of proteins, involved in bile acid metabolism, were also increased, indicating that PEDV infection affects the key proteins of the host pathways involved in cell migration, proliferation, differentiation, apoptosis, and structure, as well as in immune response.	
Comparative Proteome Analysis of Porcine Jejunum Tissues in Response to a Virulent Strain of Porcine Epidemic Diarrhea Virus and Its Attenuated Strain	iTRAQ labeling couple with liquid chromatography tandem-mass spectrometry (LC-MS/MS) was used to examine the proteomic profiles of the jejunum cells of experimentally infected piglets, with virulent and attenuated PEDV vaccine strains.	Proteins differentially regulated by two PEDV strains, were mainly involved in gastrointestinal disease, skeletal and muscular disorders, infectious diseases, and cell cycle regulation. It was also shown that infection by either virus strains downregulated proteins involved in cell structure and mobility. Furthermore, it was concluded that since	Li et al., 2016 (86)

		tubulin is involved in the process of viral entry, replication and assembly. The down-regulation of tubulin could be a molecular mechanism by which PEDV promotes its replication.	
Differential Protein Analysis of IPEC-J2 Cells Infected with Porcine Epidemic Diarrhea Virus Pandemic and Classical Strains Elucidates the Pathogenesis of Infection.	Using iTRAQ-based comparative quantitative proteomic approach, differential proteomic profiles of IPEC-J2 cells (intestinal porcine enterocytes isolated from the jejunum of a neonatal unsuckled piglet) infected with a pandemic and classical PEDV strains were evaluated.	It was found that PEDV suppressed protein synthesis of IPEC-J2 cells through the downregulation of the PI3K-AKT/mTOR signaling pathways. Moreover, it was shown that pandemic strain activated the JAK-STAT signaling pathway and the NF-κB pathway in the cells to a larger extent than the classical strain. Therefore, it was proposed that PEDV capacity to modulate the apoptosis pathway and stimulate inflammatory cascades is strain-dependent.	Lin et al., 2017 (87)
Quantitative Proteomics Reveals Changes in	Quantitate proteomic analysis (SILAC-HPLC-MS/MS) of Vero cells	The mevalonate pathway I and the super pathway of cholesterol biosynthesis were significantly up-	Ye et al. 2019 (13).

Vero Cells in Response to Porcine Epidemic Diarrhea Virus	infected with PEDV at 18 h.p.i.	relegated on PEDV infection. Furthermore, functionality was of the mevalonate pathway was tested. Inhibition assays with 25-HC, an inhibitor of this pathway, was performed and results showed PEDV infection significantly decreasing. They finally concluded that PEDV could be modulating cell metabolism, to enhance its viral life cycle.

All aforementioned studies were focused at the analysis of proteomic changes in the infected cells after a single time post-infection (p.i.). Therefore, one of the novelties of this research project is the elucidation of the dynamics of the proteomic changes of PEDV infected cells at different time of p.i. Additionally, it is proposed examining the proteomic composition of PEDV particles and host microvesicles produced by PEDV infection. The identified proteins could have key roles in viral life cycle, and, thus, could represent promising targets for antiviral therapies and PEDV control.

3. Methods to enhance PEDV viral infection

Porcine epidemic diarrhea virus was first isolated in simian cells in the presence of trypsin. This first isolation allowed to characterize chemically, physically and biologically the virus. On this first report, viral growth kinetics showed that PEDV had a peak of viral production at 15 h.p.i., and the viral titer at this time p.i was $10^{5,5}$ virus/mL (19, 20). Little has been changed since that first characterization. Routinely, PEDV production in simian cells yields up to $10^{5,5}$ to $10^{6,5}$ virus/mL. What it was not known back then, is that at these

titers, the virus even at high MOIs (multiplicity of infection) (virus per cell) can't infect significant percentage of cells. To overcome this problem, for downstream experiments, and enhance viral infection, several approaches, which will be described in the following section, could be applied to improve the PEDV production and infectivity.

3.1. Polycations

Polycations are positively charge molecules that inhibit the repulsive electrostatic forces between the membranes of the virus and cell, which are both negatively charged (88). These molecules are known to enhance the infection of retroviruses. Davis et al. in 2004 (89) discovered that depending on the biophysical characteristics of the cationic polymer, the level polycation-mediated enhancement of the infectivity will vary. Majority of the polycations enhance adsorption and transduction of retroviruses due to the charge shielding effect (89); however, the polycations with a molecular weight higher than 15 kDa are able to enhance viral infection through viral aggregation mechanism (Figure 6). Polycations can have toxic effects on cells at high concentrations, and their cytotoxicity can be cell type dependent (89).

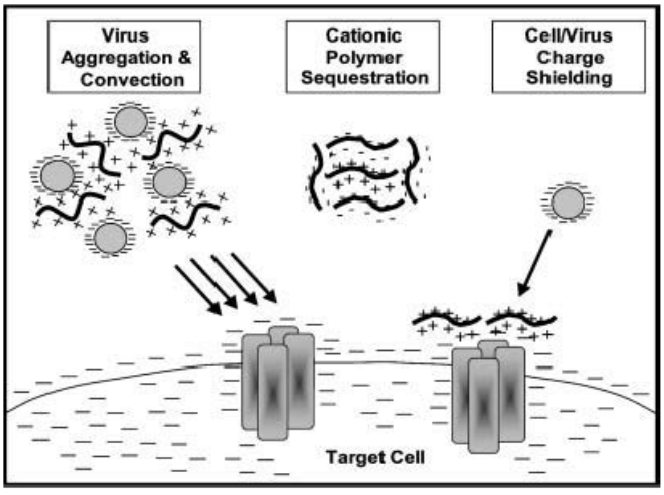

Figure 6. Biophysical model of electrostatic interactions between the virus, target cell, and charged polymer. Electrostatic interactions between virus, target cell, and polycations determine the efficiency of viral adsorption. All polycations are capable of

enhancing viral adsorption by neutralizing the negative electrostatic forces between virus and cells surface; however, the mechanism of enhancement depends on the molecular weight of the molecule. Polycations can either provide virus/ charge shielding, cationic polymer sequestration, or virus aggregation and convection (89).

DEAE-dextran is a polycation use to enhance lentiviral transduction. It is believed that it helps on virus aggregation and convection, as well as cell/virus charge shielding due to its high molecular weight. Kaplan et al. in 1967 (90), described that treatment of rabies virus with DEAE-dextran enhanced viral infectivity. The authors explained that DEAE-dextran could interact either with the membrane of the cells or with the viral membrane, making the attachment virus-cell more efficient (90). Numerous studies on HIV infectivity have reported a large ratio of defective virions in viral progeny, which explains partially the low overall rate of HIV infection (91). The effect of polycations on viral infectivity has been discovered in 1960's (92). To date, DEAE-dextran is the polycation of choice that is frequently used to increase the cells infection by HIV. At low concentrations, it can increase up to 20- 30-fold the HIV infectivity. The infectivity enhancement can be increased even further, if DEAE-dextran treatment is combined with centrifugal inoculation, i.e. spinoculation (93). Centrifugal inoculation (spinoculation) is the centrifugation-assisted inoculation of cells by virus. The spinoculation shortens the proximity between virus and cell, thus enhancing the attachment and infection. Additionally, it has been proposed that the stress caused by the spinoculation make the cell more susceptible to infection (94).

It was shown that treatment of the purified viral particles of transmissible gastroenteritis coronavirus (TGEV) with DEAE-dextran resulted in enhancement of viral infection, reaching plateau at high concentration of DEAE-dextran (95). Positive effect of this polycation on the infectivity of other coronaviruses, such as human coronavirus (HCoV) and porcine hemagglutinating encephalomyelitis virus, have been described (96, 97).

Another widely used polycation is the polybrene. Often, the effects of the DEAE-dextran and polybrene are compared, due to the different molecular mechanisms by which both polycations enhance viral infection. The polybrene's molecular weight is lower than 15 kDa, meaning that polybrene causes shielding of virus/cell charge. In contrast, the DEAE-dextran mediated enhancement of viral infection is probably due to viral aggregation.

However, it was reported that polybrene can have higher cytotoxicity in some cell lines. In a study by Denning et al., in 2013 (98) it was demonstrated that lentiviral transduction was more effective with DEAE-dextran than with polybrene, leading the authors to conclude that lentiviral transduction protocols should be optimized, depending on the cell and virus type (98). On the other hand, it was reported that avian sarcoma virus infection was enhanced by the pre-treatment of the virus with polybrene at low concentrations (99). It was shown that the positive effect of polybrene on the attachment and transduction of retroviruses was cell and virus membrane dependent (88).

III. Hypotheses and objectives

Based on the abovementioned literature review about PEDV and proteomic analyses, and the knowledge gap surrounding this virus; we hypothesized that:

1. PEDV can change the intracellular levels of host proteins in order to modify the intracellular environment, to escape host defenses and facilitate their own replication and spread
2. Host-virus interactions are highly dynamic and may involve viral-host-protein complexes. Thus, it could be expected that the compositions of PED virions are cell-type dependent.

Accordingly, the main objectives of this work were to investigate the changes in the intracellular levels of host proteins during PEDV infection, and to identify the host cell proteins associated with or encapsidated into PEDV and microvesicles/exosomes of infected cells.

To this end, the next specific aims were proposed:

1.1 To optimize PEDV infection, using polycations;

2.1 To produce and purify PEDV progeny virions using simian cell lines that are routinely used for PEDV production and studies;

2.2 To analyze the composition of virions and microvesicles/exosomes through proteomics approach.

IV. Methodology

Cell lines and viral strains

The African green monkey kidney cells Vero-76, which are routinely used for the production of porcine epidemic diarrhea virus (19), were maintained in Dulbecco modified Eagle's medium (DMEM) with L-glutamine, 4.5g/L glucose and sodium pyruvate (Corning, Tewksbury, MA, USA), containing 10% of fetal bovine serum (FBS) (Wisent Inc, QC, Canada), penicillin/streptomycin 1% (Corning, Tewksbury, MA, USA) and 250 g/L of antifungal agent, amphotericin B (Corning, Tewksbury, MA, USA). The viral strain used in all our experiments was PEDV NVSL-CO (PEDV USA/Colorado/2013). Recovered from fecal sample of a 7-day-old piglet presenting severe diarrhea (100).

Viral stocks production

To propagate PEDV, $1.7x10^7$ Vero-76 cells were seeded in T175 flasks (Corning, Tewksbury, MA, USA) and infected with the virus at MOI of 0.05, in presence of 4,5µg/mL of trypsin (Wisent Inc., QC, Canada). The viruses were harvested by three cycles of freeze-thawing when the 50% cytopathic effect (CPE) was observed (typically, after 72 h.p.i.). Virus-containing supernatant was centrifuged at 500 x g for 10 min. Viruses were semipurified by an ultracentrifugation through a 30% sucrose (Thermo Fisher Scientific, Waltham, MA, USA) cushion diluted in TNE buffer pH 7.4 (50 mM Tris–HCl, 100 mM NaCl, 0.1 mM EDTA), for 4 h at 112 000 x g, and virus-containing pellets were resuspended in the TNE buffer. Hereafter, these viral preparations are called "semipurified virus" or semipurified preparation. Viral titers were quantified by standard endpoint titration method on Vero 76- cells, using the Spearman-Karber using algorithm and expressed as 50% tissue culture infectious dose (101).

Viral titration

Spearman-Karber method

$2x10^4$ Vero-76 cells were seeded in 96-well plates. Briefly, a 50% Tissue culture Infective Dose ($TCID_{50}$) format of 10-fold serial dilutions was used to dilute the virus in DMEM medium without FBS but containing 4.5 µg/mL of trypsin. These dilutions were

added to the cells and incubated for 3 days at 37ºC and 5% of CO_2 and presence of cytopathogenic effects (CPE) were observed under a light microscope (102).

Cell viability assay

Trypan blue dye exclusion assay

The effect of polycations on Vero-76 cells was assessed by trypan blue dye exclusion assay. $3x10^5$ Vero cells were seeded per well into a 6-well plate (Sarstedt, Numbrecht, Germany). After 24 hours of incubation at 37ºC with 5% CO_2, cells were washed twice with PBS (Corning, Tewksbury, MA, USA), then treated with different concentrations of hexadimethrine bromide (polybrene) (Sigma-Aldrich, Saint Louis, MO, USA) or DEAE-dextran (Sigma-Aldrich Saint Louis, MO, USA). Cell were treated with polybrene at concentrations of 2µg/mL, 4µg/mL, 8µg/mL, 12µg/mL and 16µg/mL, or with DEAE-dextran at concentrations of 3.75µg/mL, 7.5µg/mL, 15µg/mL, 30µg/mL, 60µg/mL for 2 hours at 37ºC. Next, cells were washed twice with PBS, and fresh DMEM medium containing 10% of fetal bovine serum (FBS) and antibiotics were added. Cells were incubated for additional 24 and 48 hours. Then, cells were washed and detached from culture plate with trypsin-EDTA 0.5% (Gibco, ON, Canada) treatment for 5 minutes. Trypan blue (Thermo Fisher Scientific, Waltham, MA, USA) at concentration 0.4% was used to determine the percentage of viable cells, which was calculated as the number of viable cells per mL (manually determined by quantification of cells on a Neubauer chamber) on each condition divided by the cells per mL of the untreated control (quantified the same way), multiplied by 100%.

Cytotoxicity assay through LDH

The effect of polycations on Vero-76 cells was assessed with the CytoTox 96® Non-Radioactive Cytotoxicity Assay (Promega, Madison, WI, USA). Briefly, $8x10^4$ Vero cells were seeded per well in a 24-well plate (Sarstedt, Numbrecht, Germany). Cells were treated as described in the previous paragraph. Then following manufacturers indications CytoTox 96® Non-Radioactive Cytotoxicity Assay was performed. Briefly, 50µl aliquots from all test and control wells were transferred to a fresh 96-well flat clear bottom plate. Then, 50µl of the CytoTox 96® reagent was added to each sample aliquot, plates were incubated in absence of light for 30 minutes at room temperature. Next, 50µl of stop solution was added to each

well of the 96-well plate. Finally, the optical absorbance of the samples was read in a microplate reader at 492nm (Biotek® Synergy HT plate reader, Vermont, USA) immediately after adding the stop solution. To determine the percentage of cytotoxicity, the average values of the background absorbance of the culture medium was subtracted from all values of the experimental wells. Then, the following formula was used: Percent cytotoxicity = 100 × Experimental LDH Release (OD_{492nm}) /Maximum LDH Release (OD_{492nm}).

PEDV proliferation assay to evaluate the effects of polycations

Briefly, $3x10^5$ Vero-76 cells were seeded per well in 6-well plates. After 24 hours of incubation at 37ºC in 5% CO_2 environment, cells were washed twice with PBS. Cells were infected with PEDV at 0,05 MOI (adsorption step) in the presence of 4,5μg/mL of trypsin, and polybrene or DEAE-dextran at 4 and 8 μg/mL for 2 hours at room temperature (to partially synchronize virus adsorption and entry). After that 2-hour virus adsorption, cells were washed three times with PBS and fresh DMEM containing 4,5μg/mL of trypsin was added. Infection was stopped by freezing cells after 36 h.p.i (Figure 7). Two cycles of freezing and thawing were performed to lyse the cells, and virus-containing supernatant was centrifuged at 500 x g for 10 min. Virus proliferation was estimated as a viral titer produced by the infected cells, using the Spearman-Karber method (102).

Indirect immunofluorescence assay (IFA)

$2x10^4$ Vero-76 cells were seeded per well in a 96-well plate (Sarstedt, Numbrecht, Germany). After 24 hours of incubation at 37ºC with 5% CO_2, cells were washed twice with PBS and, then, either mock-infected or infected with PEDV at 0,5 MOI in the presence of 4,5μg/mL of trypsin for 2 hours at room temperature. To investigate the effect of polycations on viral infectivity, virus preparations were treated or untreated with polybrene or DEAE-dextran at 4 and 8 μg/mL for 1 hour prior to adding to the cells and performing the adsorption step of infection (Figure 7). After 2h of virus adsorption (or mock-adsorption), the cells were washed three times with PBS 1X, and fresh DMEM containing 4,5 μg/mL of trypsin was added. After 6 h.p.i, cells were fixed prior to the permeabilization (in 0.1% of Triton X-100 for 15 min) by 4% PFA (paraformaldehyde) (Thermo Fisher Scientific, Waltham, MA, USA)

in PBS (Figure 1). Between the steps, cells were blocked with 2% BSA (Sigma-Aldrich, Saint Louis, MO, USA) for 30 minutes. Mouse anti-PEDV N protein antibody was added to the wells and fixed cells were incubated at room temperature for 2 hours or at 4ºC overnight. The unbound antibodies were washed by PBS and cells were blocked again by the BSA for 30 minutes. To visualize infected cells, the primary anti-PEDV N antibody was detected by fluorescent secondary anti-mouse Cy5 (Jackson Immunoreseach Labs, Inc. Baltimore, PA, USA), in which cells were incubated for 1 hour at room temperature. The unbound secondary antibodies were removed by PBS washing. Cell nuclei were stained DAPI (4′,6-diamidino-2-phenylindole) staining was used to determine the number of nuclei and to assess gross cell morphology. Pictures were taken using Leica DMI 400B inverted fluorescent microscope. Two to three PBS washes were performed between steps. The efficiency of infection was calculated as the percentage of infected cells over the total number of cells.

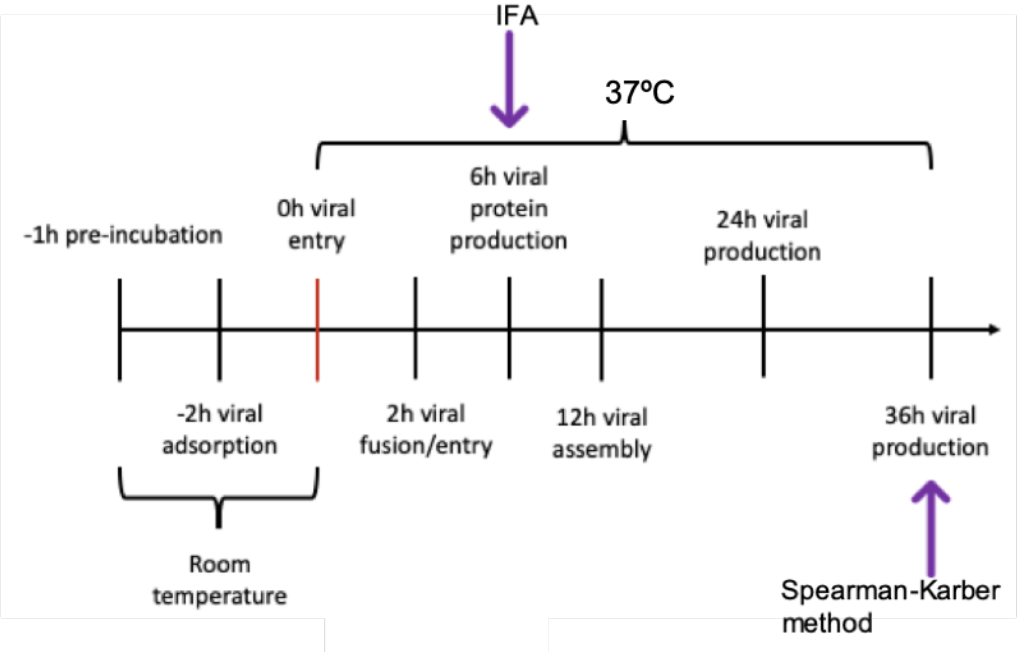

Figure 7. Schematic chart of the experimental procedure, for evaluation of polycations effect on PEDV infectivity, at different times p.i. Purple arrows show time points were polycations effect was evaluated through different techniques. -1h pre-incubation: virus preparations were treated or untreated with polybrene or DEAE-dextran at 4 and 8 µg/mL for 1 hour prior to adding to the cells. -2h viral adsorption: cells were inoculated with the

previously treated mixture of PEDV and polycations, to allow viral attachment for 2 h at room temperature. Further steps viral entry, protein production, viral assembly, virus production and massive viral production, were performed at 37ºC.

Statistical analysis

A One-way Analysis of variance (ANOVA) model followed by Tukey's Multiple Comparison was used to determine if statistically significant differences existed between data obtained for the PEDV-infected cells and PEDV-infected cells treated with polycations. This approach was used to determine the statistical significance of the data of viral propagation (viral titers defined by Spearman-Karber method) and for IFA data. The asterisks indicate significant differences (*** P<0,001, ** P<0.01, *P<0,05).

Multistep purification of the PEDV for proteomic assay

Semipurified PEDV preparation (through a 30% sucrose cushion, as it was described above) was further purified using a CsCl (Thermo Fisher Scientific, Waltham, MA, USA) 5%-45% continuous gradient. Briefly, 10 mL continuous gradients of CsCl was made by a two-chamber gradient maker (Bio-Rad, Hercules, CA, USA) and transferred into the ultra-clear tube (Beckman Coulter, Brea, CA, USA). One mL of semipurified PEDV preparation was layered on the top of the continuous gradient. Samples were spun at 107 000 x g overnight in a SW 41 rotor (Beckman Coulter, Brea, CA, USA). Ten 1-mL fractions were collected by puncturing the bottom of the tube. Each fraction was evaluated through RT-qPCR, Spearman-Karber method and Bradford assay (following manufactures instructions) for determining the fractions enriched in viral RNA, infectious viral particles, and total proteins, respectively. This step of purification is called "purified virus" hereafter.

Selected fractions (enriched in viral RNA and infectious virions) of the CsCl gradient, containing at least 50µg of protein, were treated with subtilisin at 2 g/L (Thermo Fisher Scientific, Waltham, MA, USA) dissolve in digestion buffer (40 mM Tris-HCl, pH 8.0 and 2 mM $CaCl_2$) for 18 hours, at 37ºC. Next, phenylmethyl sulfonyl fluoride (PMSF) 10 mg/mL in ethanol was added and samples were incubated for 15 minutes at room temperature to inhibit the proteases. The subtilisin-treated virions were concentrated again by

ultracentrifugation through a 30% sucrose cushion at 4ºC, 107 000 x g for 4h to eliminate any impurities and produce ultra-purified viral particles (ultra-purified preparation). Earlier reports have shown that microvesicles contamination of viral preparation can be successfully removed with subtilisin treatment (103).

Evaluation of the expression of viral RNA

In order to evaluate absence or presence of PEDV in samples, reverse transcription was performed with a quantitative PCR, all in one step. Briefly, RNA extracted with Qiamp Viral RNA Mini Kit (Qiagen N.V. Hilden, Germany) as manufactures indications, PCR with TaqMan Fast Virus 1-Step following manufactures instructions (Thermo Fisher Scientific, Waltham, MA, USA.) was performed, and detection of mRNA from ORF6 of PEDV was determined. The nucleotide sequence of the forward and reverse primers, and the probe were: CCAGCAAATTGGGTACTGGAATG, CCTGTTCCGAGGTAGTAGAAATG and [6-FAM] CCGTGGTGAGCGAATTGAACAACC [BHQ1a-Q], respectively (Eurofins Genomics LLC, Louisville, KY, USA).

Proteomic analysis

Sample Preparation

Briefly, 100 µg of proteins were transferred to a microcentrifuge tube and proteins were precipitated with a ratio of 1:5 (v: v) of ice-cold acetone. Then acetone was discarded, and protein pellet was dried at room temperature. The protein pellet was dissolved in 200 µL of 50 Tris-HCl buffer (pH 8) and the solution was vigorously mix for 2 x 3 minutes to maximize protein dissolution yield. The proteins were denatured by heating at 120˚C for 15 min using heated reaction block. The solution was allowed to cool down. Proteins were reduced with 20mM DL-dithiothreitol (DTT) and the reaction was performed at 90 ˚C for 10 minutes. Then proteins were alkylated with 40mM iodoacetamide (IAA) and the reaction was performed at room temperature for 30 min. Reaction was quenched with the addition of DTT. Two µg of proteomic-grade trypsin was added, and the reaction was performed at 37˚C for 24h. The protein digestion was quenched by adding 20 µL of a 1% trifluoroacetic acid (TFA) solution. Samples were centrifuged at 12,000 g for 10 min and 200 µL of the supernatants were transferred into injection vials for analysis.

Chromatographic conditions

The high-performance liquid chromatography (HPLC) system was a Thermo Scientific Vanquish FLEX UHPLC system (San Jose, CA, USA). The chromatography was achieved using a gradient mobile phase along with a microbore column Thermo Biobasic C18 100 × 1 mm, with a particle size of 5 µm. The initial mobile phase condition consisted of acetonitrile and water (both fortified with 0.1% of formic acid) at a ratio of 5:95. From 0 to 2 minute, the ratio was maintained at 5:95. From 2 to 92 minutes, a linear gradient was applied up to a ratio of 40:60 and maintained for 3 minutes. The mobile phase composition ratio was reverted at the initial conditions and the column was allowed to re-equilibrate for 20 minutes. The flow rate was fixed at 50 µL/min and 2 µL of sample were injected.

Mass Spectrometry conditions

A Thermo Scientific Q Exactive Plus Orbitrap Mass Spectrometer (San Jose, CA, USA) was interfaced with a Thermo Scientific Vanquish FLEX UHPLC system using a pneumatic assisted heated electrospray ion (ESI) source. MS detection was performed in positive ion mode and operating in scan mode at high-resolution, and accurate-mass (HRAM). Nitrogen was used for sheath and auxiliary gases and they were set at 10 and 5 arbitrary units. The ESI voltage was set to 4000 V and the ion transfer tube temperature was set to 300°C. The MS was operating in an acquired using a data-dependent top-10 (DDA TOP-10) method to dynamically choose the most abundant precursor ions from the survey scans (i.e. m/z 400–1500) and generate MS/MS spectra. Data was acquired at a resolving power of 70,000 (FWHM) using automatic gain control target of 1.0x106 at the MS1 level with maximum ion injection time of 100 msec and product ion spectra were acquired at resolving power of 17,500 FWHM, using automatic gain control target of $1.0x10^5$ and maximum ion injection time of 100 msec. The normalize collision energy was set to 28V and precursor were isolated using a 2 Da window. Instrument calibration was performed prior to all analysis and mass accuracy was notably below 1 ppm using Thermo Pierce calibration solution and automated instrument protocol.

Bioinformatic analyses

Comprehensive protein identification was performed using Thermo Scientific Proteome Discoverer software v2.2 (San Jose, CA, USA). Thermo raw files were imported into Proteome Discoverer v2.2. Peak lists were generated with a precursor signal-to- noise ratio of 1.5, and default settings were used to search a FASTA database containing the protein sequence sequences for the *Chlorocebus aethiops* (i.e. taxonomy #9534) extracted from UniProt. The enzyme was set to trypsin, and two missed cleavages were tolerated. Carbamidomethylation of cysteine was set as a fixed modification and oxidation of methionine as a variable modification. The precursor ion mass tolerance was set to 5 ppm, and the product ion mass tolerance was set to 0.02 Da. Data sets were further analyzed with percolator (strict false discovery rate (FDR) of 0.01 and a relaxed FDR of 0.05). Tryptic peptide identifications were accepted with high confidence, corresponding to less than 1% FDR. Relative quantification was performed using the label-free node based on peak area at the MS1 levels.

V. Results

1. Changes in the intracellular levels of host proteins during PEDV infection.

1.1. Optimization of PEDV infection by polycations

The efficiency of viral entry and infection is very low for the large majority of the viruses (104). Thus, in order to study the dynamics of the proteomic changes in the PEDV infected cells, it is desirable to reach a high level and synchronized infectivity. Previously, enhancement of the infectivity of retroviruses and a similar effect for some coronaviruses have been reported (60, 61, 62). In this study, we investigated the effect of two widely used polycations; polybrene and DEAE-dextran on the PEDV infectivity. First, we evaluated their cytotoxicity in Vero-76 cells. For such cells were treated 2 h with different concentration of polybrene or DEAE-dextran (or mock-treated) and the viability of the cells was measured after 24 and 48 hours post treatment. Percentage of viable cells treated with DEAE-dextran (Figure 8) and Polybrene (Figure 9) was measured with trypan blue staining.

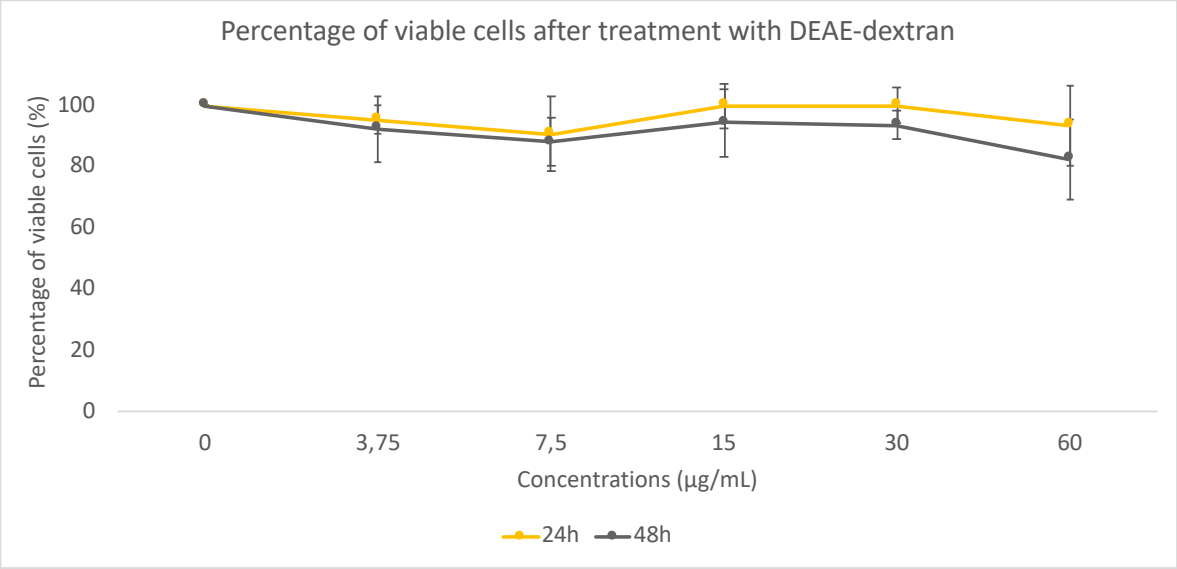

Figure 8. Effect of DEAE-dextran at different concentrations, on viability of Vero-76 cells after different times post-treatment. Cells were treated 2h with different concentration, already reported in the literature as effective concentrations, of DEAE-

dextran and viability of the cells was measured after 24 and 48 hours. Percentage of viable cells was measured by trypan blue staining. Data are express as mean ± Standard deviation (SD) (n=3).

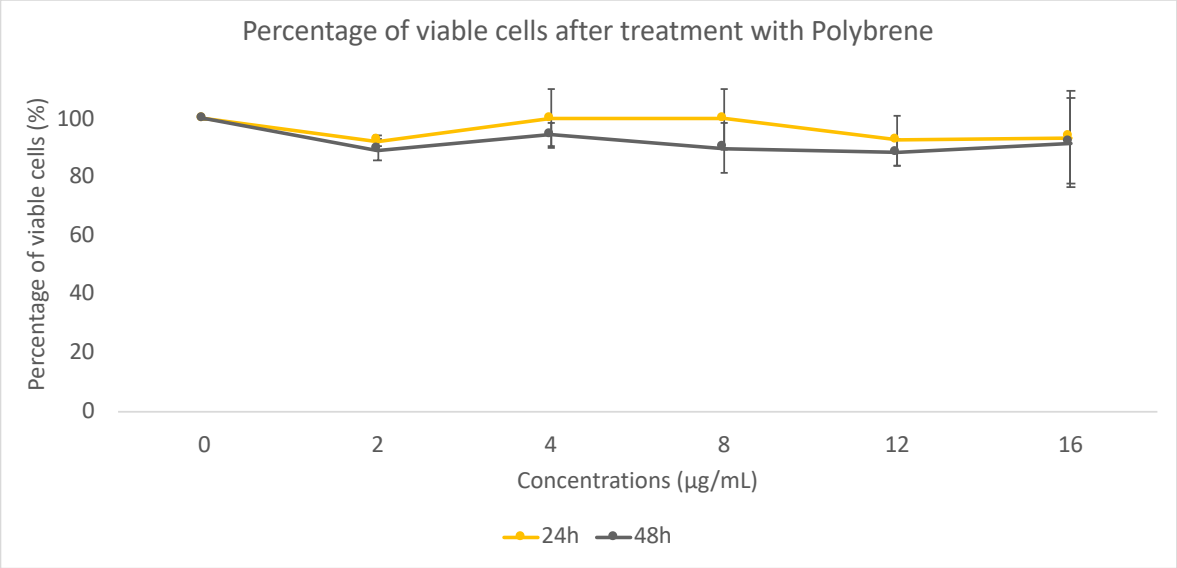

Figure 9. Effect of polybrene at different concentration on viability of Vero-76 cells after different times post-treatment. Cells were treated 2h with different concentration of polybrene, already reported in the literature as effective concentrations and viability of the cells was measured after 24 and 48 hours. Percentage of viable cells was measured through trypan blue staining. Data are express as mean ± SD (n=3).

As it was expected, the viability of cells was slightly lower at the high concentrations, due to the cytotoxic effect of these molecules. Overall, no significant decrease in viability percentage was observed after treatment with both polycations. To further confirm the cytotoxicity of polycations to Vero-76 cells, the cytotoxicity of both polycations was assessed by highly sensitive colorimetric lactate dehydrogenase (LDH)-release assay (Promega, Madison, WI, USA). The relative amounts of live and dead cells (percent cytotoxicity) within the medium of the cells treated with DEAE-dextran (Figure 10) and Polybrene (Figure 11) were determined using the manufacturer's recommendations.

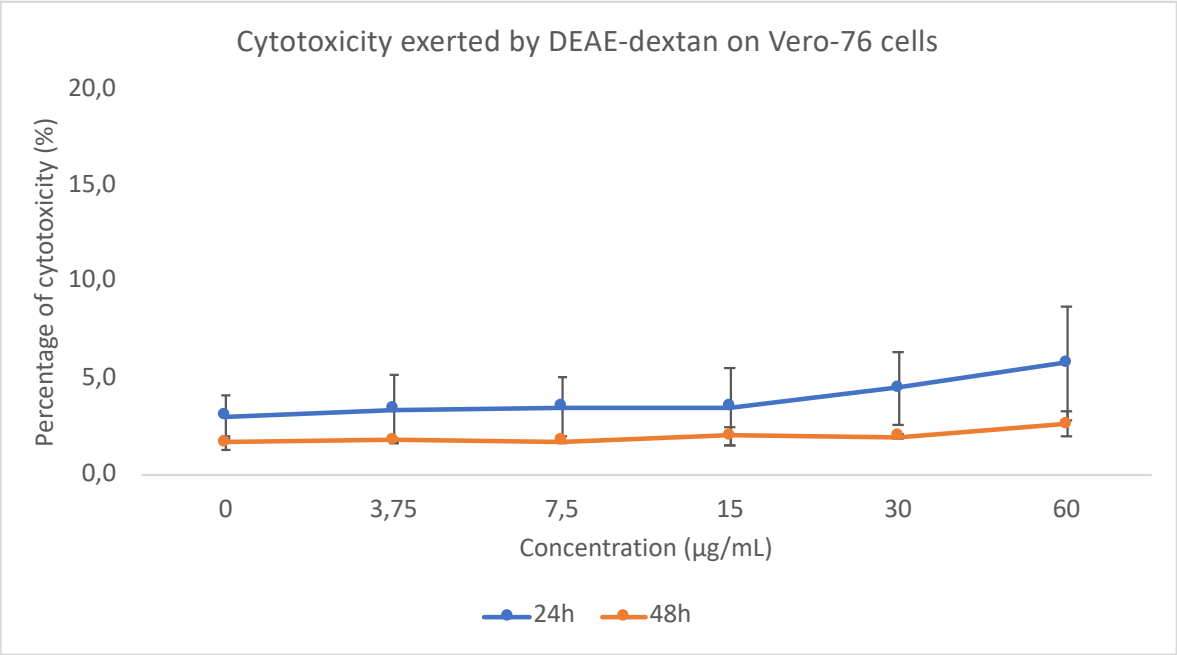

Figure 10. Cytotoxic effect of DEAE-dextran at different concentration on Vero-76 cells measured after 24- and 48-hours post-treatment. Cells were treated 2 h with different concentration of DEAE-dextran, already reported in the literature as effective concentrations and viability of the cells was measured after 24 and 48 hours. Percentage of cytotoxicity (% of dead cells) assessed by LDH assay. Data are express as mean ± SD (n=3).

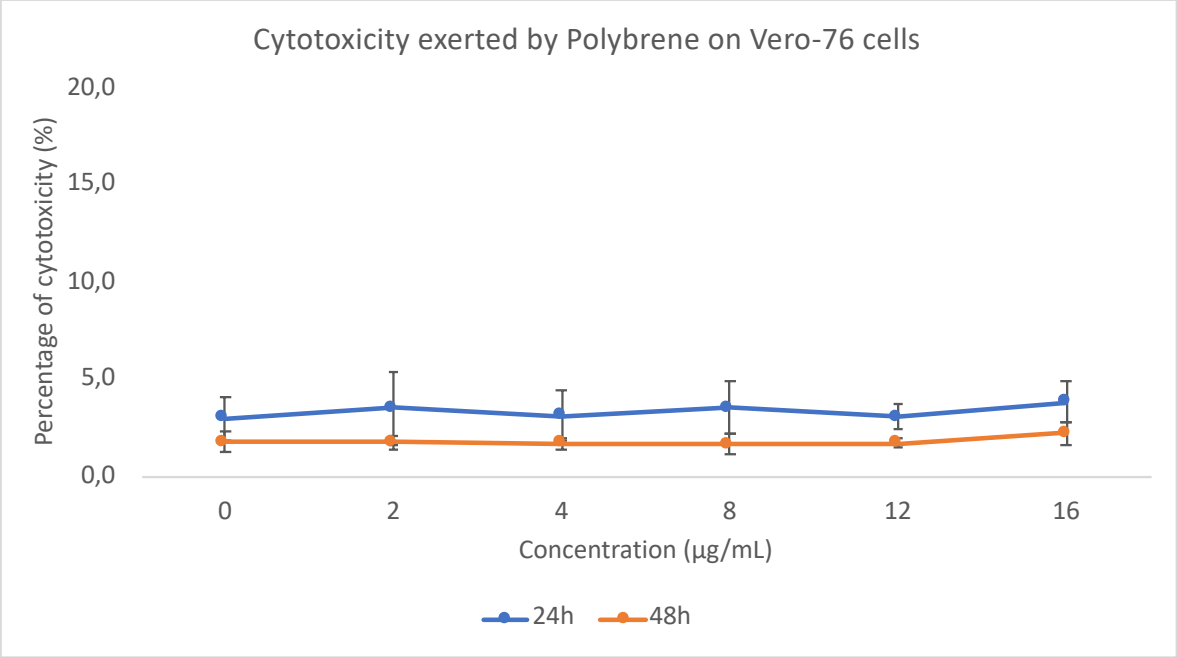

Figure 11. Cytotoxic effect polybrene at different concentration on Vero-76 cells measured after 24- and 48-hours post-treatment. Cells were treated 2 h with different concentration of polybrene, already reported in the literature as effective concentrations and viability of the cells was measured after 24 and 48 hours. Percentage of cytotoxicity (% of dead cells) assessed by LDH assay. Data are express as mean ± SD (n=3).

There was no significant difference in cell mortality among concentrations tested. Thus, there is a good agreement between results generated by two different assays. Viability of Vero-76 cells after treatment with polycations and LDH assay showed that cytotoxicity of both polycations is lower than 5%, after 24 and 48h post-treatment.

Next, we evaluated the effect of polycations on the PED viral progeny production after 36h post-treatment using the Spearmen-Karber method (105). Synchronization of infection was achieved by 2h adsorption of virus inoculum at room temperature (which does not allow viral entry and fusion), followed by a washing step to remove unbound virus and further incubation at 37ºC (Figure 12), additionally, synchronization and continuous infection were compared.

As shown in the graph (Figure 12), a non-significant effect of enhancement of PEDV infection was shown, when the virus was treated with DEAE-dextran, nor when infection

was synchronized and treated with this molecule. On the contrary, when the synchronization of infection was coupled with polybrene treatment, a significant enhancement of PEDV infection was observed ($p<0.001$). Nine-fold increase of PEDV progeny production was reached, when the virus was pretreated with polybrene and infection was synchronized (Figure 12). However, a 4-fold enhancement of viral production was observed in non-synchronized infection of a polybrene-treated viral inoculum. Thus, for further experiments with both polycations and the synchronization of infection were added to the protocol.

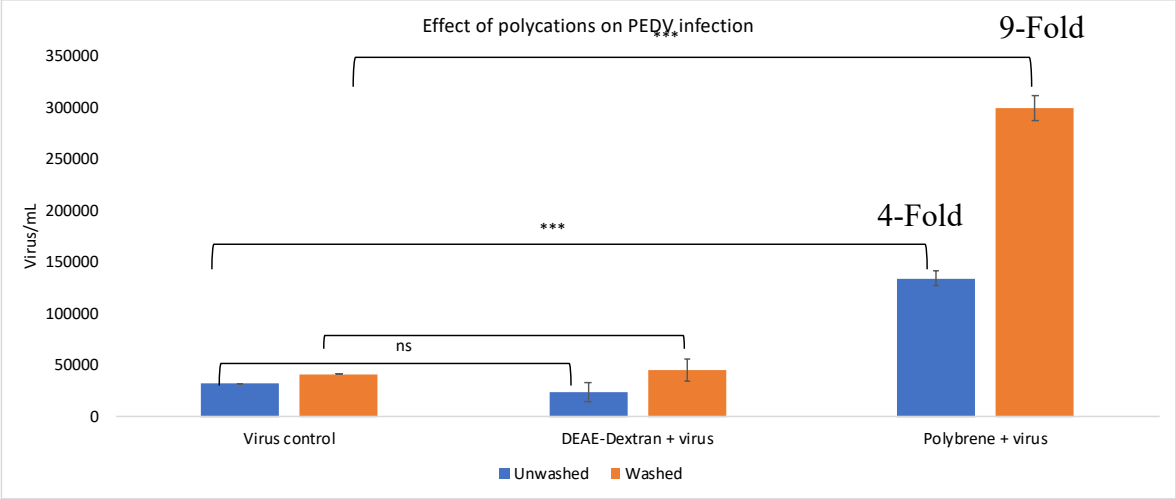

Figure 12. Synchronization of infection effect on PEDV infectivity in presence of polycations. Vero-76 cells were infected with PEDV at MOI 0,05 non-treated or treated with polycations for 2 hours at room temperature (washed/synchronized infection) (orange bars), or inoculum was left for 36 hours (unwashed/ continuous infection) (blue bars). Number of viruses per mL was assessed through Spearman-Karber method; data are express as mean ± SD (n=3). The statistic analysis performed was an ANOVA model followed by Tukey's Multiple Comparison; used for determination of statistically significant differences between data of PEDV-infected cells and PEDV-infected cells treated with polycations as well as washed and unwashed (***$p<0.001$, Ns: no significant).

To prove that polycations enhance viral entry (i.e. early stage of infection), we examined the presence of newly produced viral N protein six h.p.i. by indirect

immunofluorescence assay (IFA microscopy) and quantifying the ratio of infected cells using ImageJ software. Additionally, we investigated which molecular mechanism (viral membrane or cell membrane charge shielding) was responsible for the effects of the polycations on the infection. Pre-incubation of cells with polycations for 1h at room temperature (Figure 13) did not show a significant enhancement of PEDV N protein production. This observation suggests that polycations were not exerting their charge neutralizing effect directly at the level of the cellular plasma membrane.

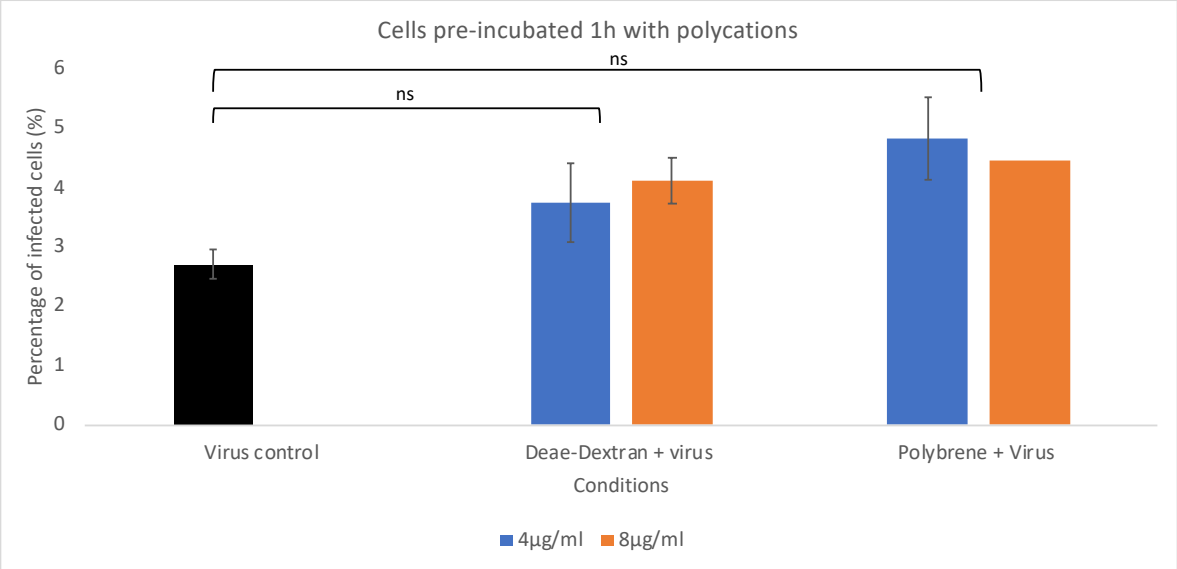

Figure 13. Effect of pre-incubation of Vero-76 cells with polycations before viral adsorption and infection. Cells were pre-incubated 1 h with polycation at 2 different concentration, reported to being effective enhancing viral attachment (106–108), at room temperature. PEDV at MOI 0,5 and polycations were then added, and synchronization of infection was performed. 6 h.p.i cells were fixed, and IFA was done. Percentage of infected cells was estimated using ImageJ software. Data are express as mean ± SD (n=3). The statistic analysis performed was an one-way ANOVA model followed by Tukey's Multiple Comparison; used for determination of statistically significant differences between data of PEDV-infected cells and PEDV-infected cells treated with polycations (ns: no significant).

Interestingly, the pre-incubation of PEDV with polycations (Figure 14) for 1 h at room temperature showed a 4-fold increase of N protein production (i.e., percentage of infected cells). This effect was more dramatic when PEDV inoculum was pre-treated with polybrene at 8 µg/mL ($p<0.001$), compared to when the virus was pre-treated with DEAE-dextran. Thus, suggesting that the molecular mechanism of the polybrene-mediated enhancement of PEDV infectivity may be due to the shielding of virions charge. Importantly, our results correlate with previous reports (89). Not only the number of infected cells was enhanced by the pre-incubation of PEDV with polybrene, but also the intensity of the fluorescence in infected cells was higher (Figure 15).

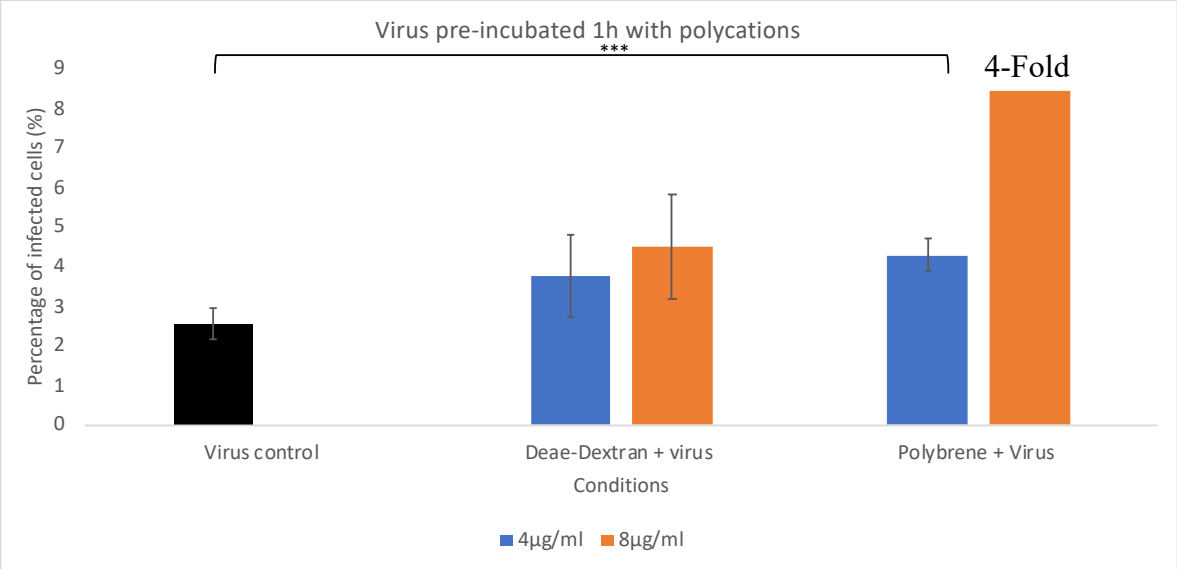

Figure 14. Effect of pre-incubation of virus with polycations before viral infection. PEDV at MOI 0,5 was pre-incubated 1 h with polycation at 2 different concentration, at room temperature. Inoculum was then added (PEDV pre-incubated with polycations), and synchronization of infection was performed. Percentage of infected cells was calculated using the ImageJ software. Data are express as mean ± SD (n=3). The statistic analysis performed was an one-way ANOVA model followed by Tukey's Multiple Comparison; used for determination of statistically significant differences between data of PEDV-infected cells and PEDV-infected cells treated with polycations (*** $p<0.001$).

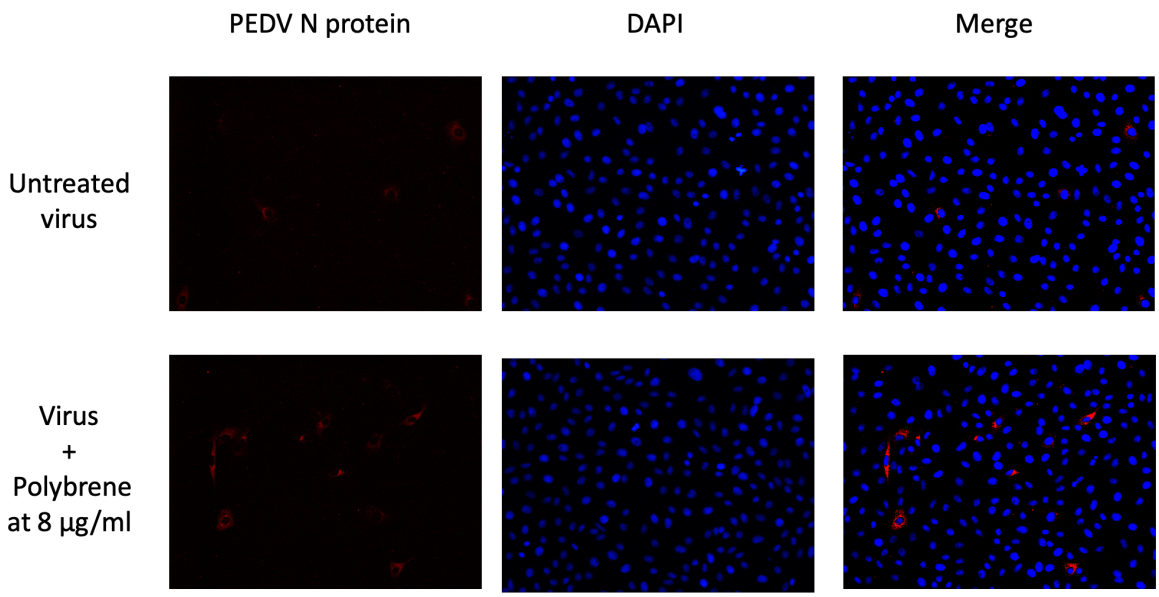

Figure 15. Polybrene at 8µg/mL significantly increased PEDV infectivity after 6 h.p.i. PEDV at MOI 0.5 was pre-incubated 1 h with polybrene at 8µg/mL, at room temperature. Inoculum was then added, and synchronization of infection was performed. IFA assay: PEDV N protein was detected by red-fluorophore-conjugated secondary antibody. Nuclei were stained by DAPI (blue).

Additionally, we investigated the potential dose-response relationship between polycations and PEDV entry using the IFA microscopy for 6 h.p.i. setting. To this end, viral inoculums were pre-incubated with polybrene or DEAE-dextran for one hour at different concentrations, followed by viral adsorption step (2 h at room temperature incubation), and synchronization of the infection (intensive washes to remove unbound viruses). It was shown that DEAE-dextran didn't have a strong impact on PEDV infectivity at any tested concentration, reaching just 5% infected cells (Figure 16). However, polybrene showed a significant effect on PEDV infection, increasing the ratio of N protein expressing cells to 8% ($p<0.001$). We observed that 8µg/mL of polybrene showed the best outcome on the efficiency of the PEDV infection (Figure 17).

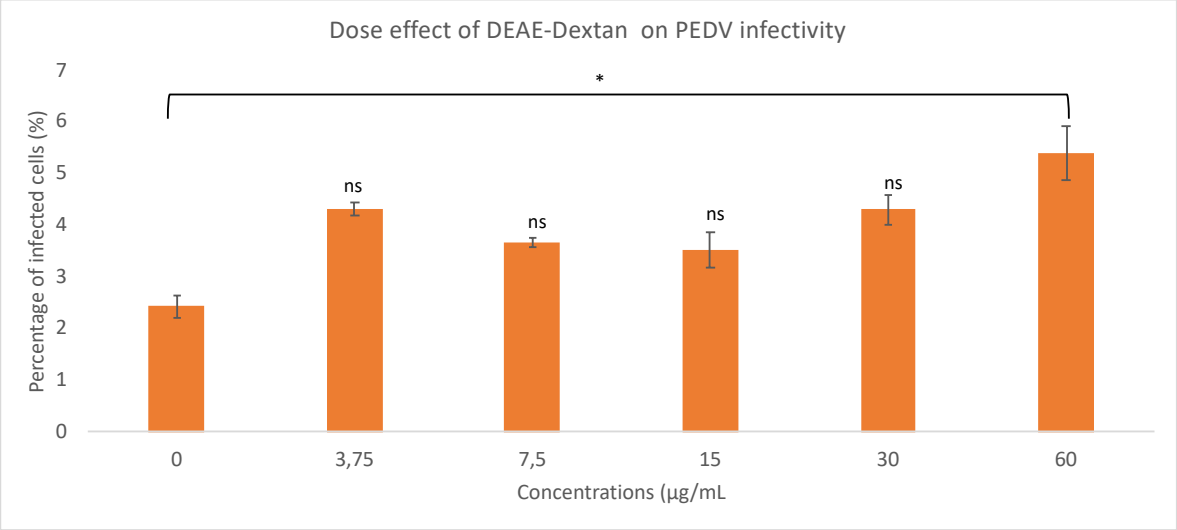

Figure 16. Dose effect of DEAE-dextran treatment on PEDV infectivity. PEDV at MOI 0,5 was pre-incubated 1 h with different concentration of DEAE-Dextran, at room temperature. Inoculum was then added, and synchronization of infection was performed. Percentage of infected cells was calculated using ImageJ software. Data are express as mean ± SD (n=3). The statistic analysis performed was an one-way ANOVA model followed by Tukey's Multiple Comparison; used for determination of statistically significant differences between data of PEDV-infected cells and PEDV-infected cells treated with different concentrations of DEAE-dextran (*$p<0.05$, ns: no significant).

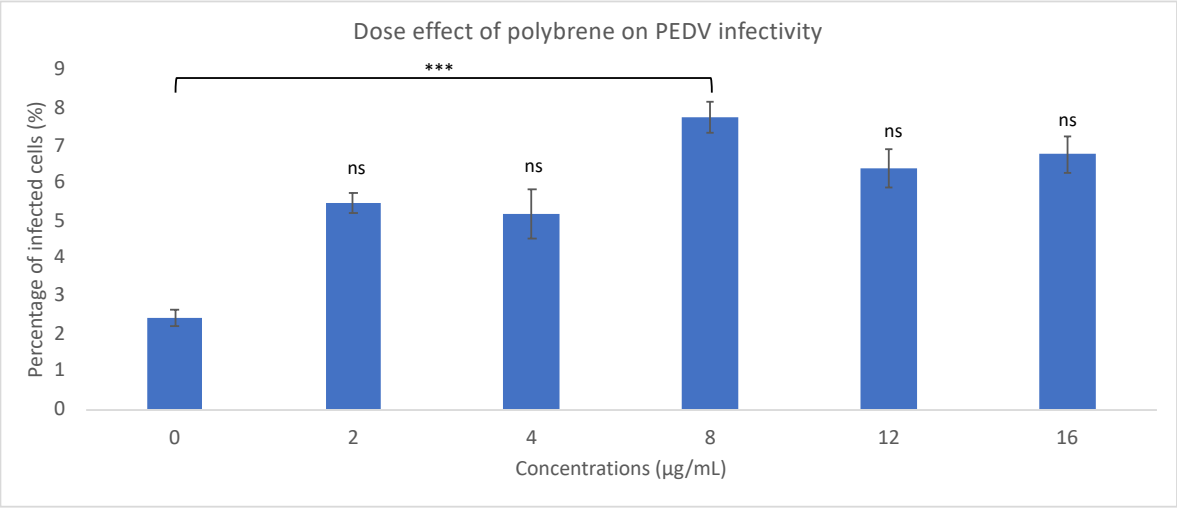

Figure 17. Dose effect of polybrene treatment on PEDV infectivity. PEDV was pre-incubated 1 h with different concentration of polybrene, at room temperature. Inoculum was then added, and synchronization of infection was performed. Percentage of infected cells was calculated using ImageJ software, Data are express as mean ± SD (n=3). The statistic analysis performed was an one-way ANOVA model followed by Tukey's Multiple Comparison; used for determination of statistically significant differences between data of PEDV-infected cells and PEDV-infected cells treated with different concentrations of polybrene (*** $p<0.001$, ns: no significant).

2. Identification of host cell proteins associated with or encapsidated into PEDV and EMV during viral infection.

2.1. Production of PEDV using simian cell lines that are routinely used for PEDV studies.

Vero-76 cells were infected with PEDV, and when cell culture showed the signs of CPE after 3 days p.i. (cell fusion, syncytia formation, rounded morphology or shrinking), they were lysed by a process of freezing-thawing. In some coronaviruses, the spike protein that remains not assembled is transferred to the cell surface and mediates cell-cell fusion. This produces a massive, multinucleated group of cells that allows the virus to spread between attached cells (25). After, the virus was harvested and submitted through a process of multistep purification described in the Methodology section.

2.2. Analysis of the composition of virions and microvesicles/exosomes through proteomics approach.

Viral particles were semipurified through a 30% sucrose cushion (semipurified preparation). Semi-purified samples were further purified (ultracentrifugation) through a 5%-45% CsCl continuous gradient and ten fractions were collected. Chosen fractions (purified viral preparation) were ultra-purified using the subtilisin-mediated removal of the EMV procedure.

During each purification step: viral RNA, protein concentration and viral titers were determined as unique quality control. The concentration of total proteins in the samples, the number of viruses per mL and the presence of viral genome were chosen as key parameters to determine the "best" fractions for mass-spectrometry analysis (Figure 18). The selected ones from the CsCl gradient were usually the fractions 6 and 7, due to their lower Ct values (i.e. reach in viral genome) high viral titers and protein concentration.

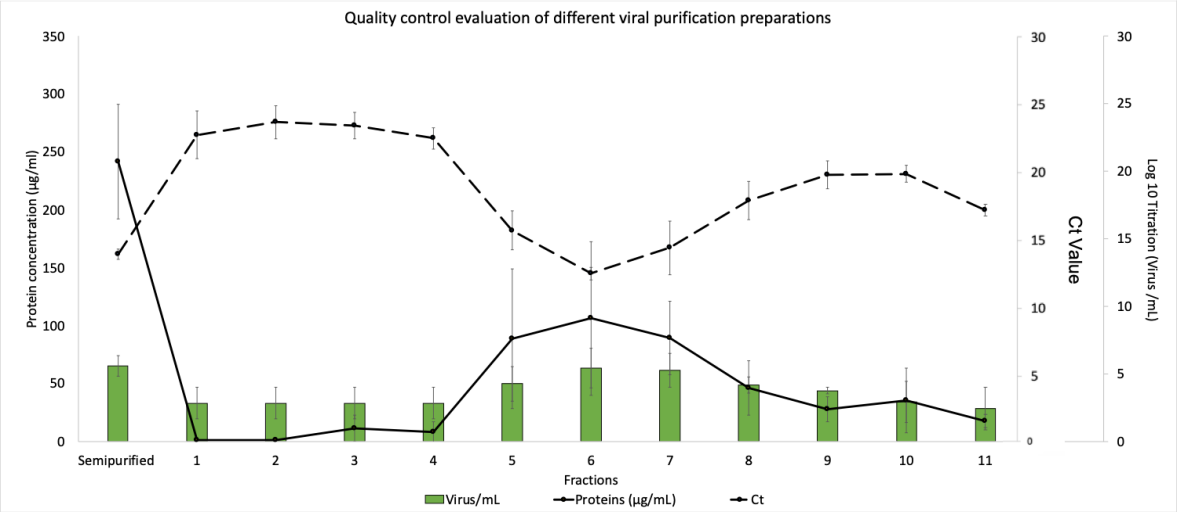

Figure 18. Comprehensive quality control assessed by Spearmen-Karber method (viral titer), RT qPCR (presence of viral RNA) and Bradford assay (protein concentration). After Semipurification with 30% sucrose cushion parameters were evaluated for further purification. CsCl continuous gradient was performed, and 11 fractions were collected. Fraction with the best quality (protein, viral RNA and viral titer) was chosen for final ultra-purification step.

Semipurified fraction (preparation)

In the semipurified samples, containing PEDV virions and microvesicles, the abundance of 63 proteins was affected: 47 were up-regulated and 16 were down-regulated (Table V) in comparison with the same fraction obtained from the mock-transfected cells. The abundance of peptides in the semipurified preparation of PEDV infected cells was mainly up-regulated, as can be evidenced by a volcano-plot (Figure 19).

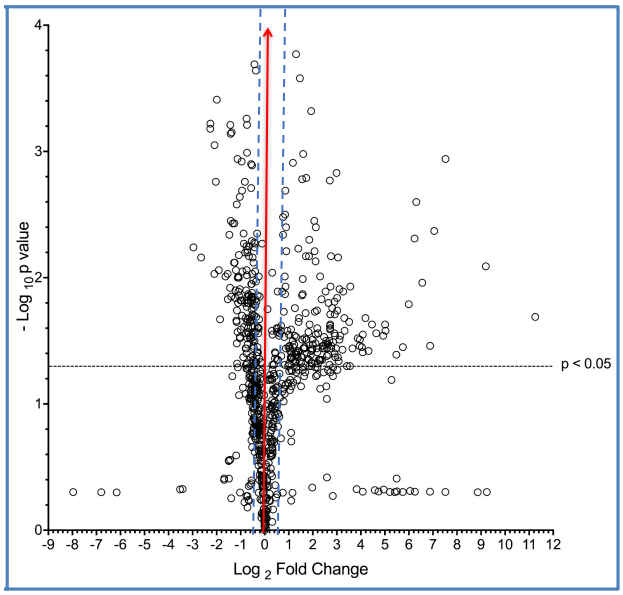

Figure 19. Volcano plot of dysregulated tryptic peptides in the semipurified preparation containing viruses and EMV after PEDV infection. The -Log 10 (Benjamin–Hochberg corrected P value) versus the log2 (fold change). The non-axial vertical dashed lines (in blue) mean ±1.5-fold change. The non-axial horizontal line indicates $p< 0.05$ the significance threshold.

The differentially expressed proteins were annotated by UniProt-GOA database and enriched by GO annotation based on three categories: Biological Process, Cellular Component, and Molecular Function. Thus, the gene ontology (GO) database has been used for describing the biological functions of the identified proteins. GO analyses revealed that majority of the proteins affected in the semipurified viral preparation were involved in nucleic acid binding (23%), metabolic process (34%), signaling (24%), and cell cycle regulation (20%) (Figure 20).

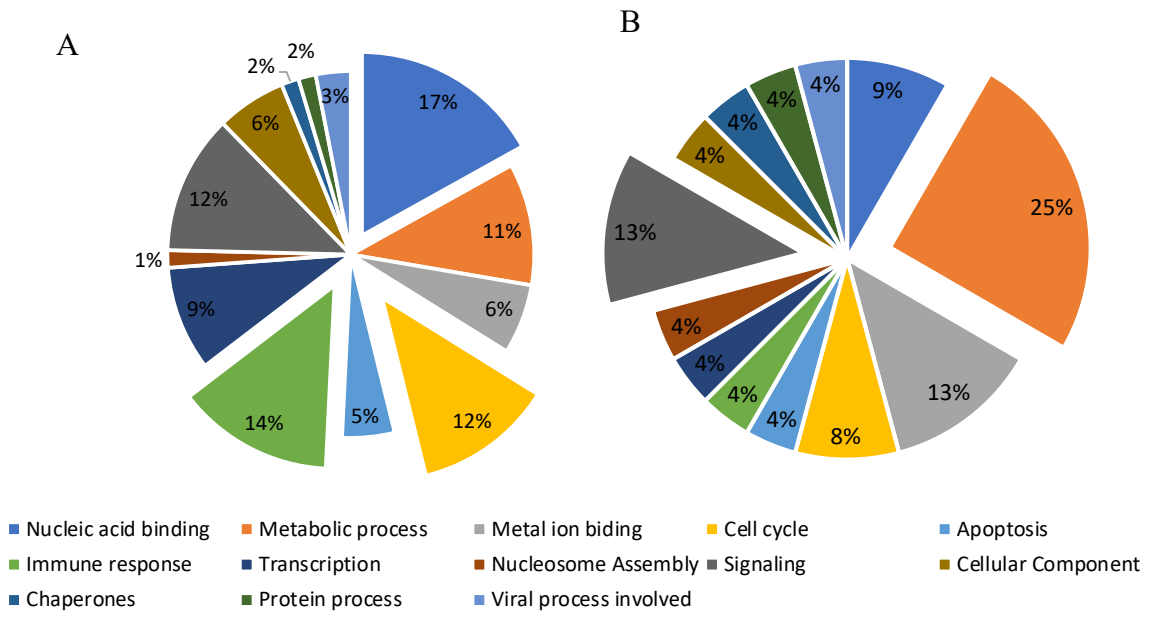

Figure 20. Functional categories of cellular proteins of the semipurified viral preparation. After LFP analysis of semipurified fraction, proteins significantly regulated were classified by their molecular functions. (A) Up-regulated proteins, (B) down-regulated proteins. Gene ontology annotation (GO).

Most of the upregulated by PEDV infection proteins belonged to the cytoplasm, nucleus and plasma membrane components (Figure 21), while negatively regulated proteins had nuclear and cytoplasm localization.

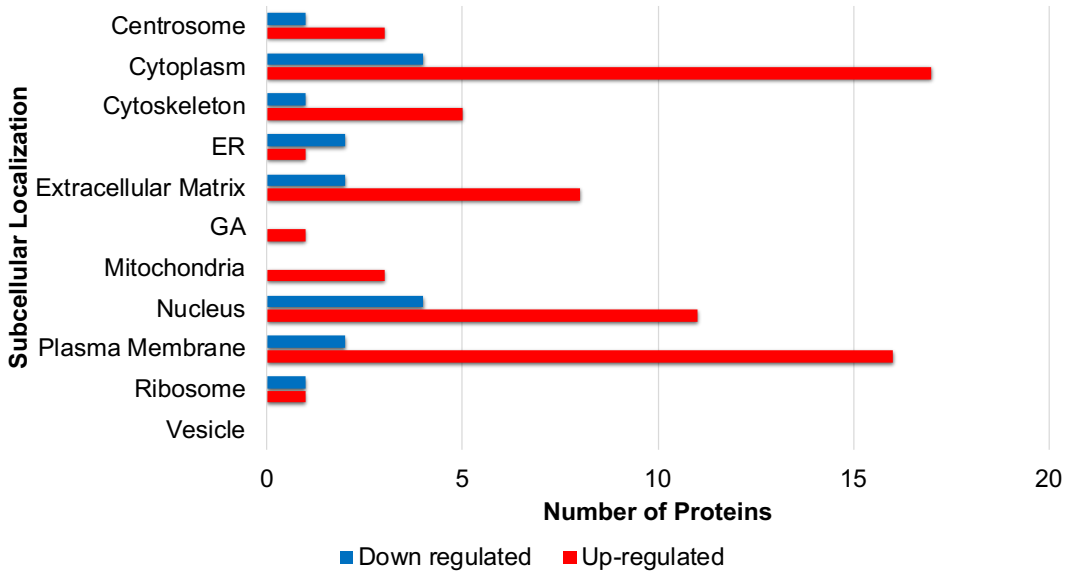

Figure 21. Subcellular localization of dysregulated host proteins identified in semipurified viral preparation. Consequent to an LFP analysis of semipurified fraction, proteins significantly regulated were classified by their subcellular localization. Gene ontology annotation.

From the proteomic analyses of five biological replicates among mock or PEDV-infected, we identified and quantified in the semipurified preparation 110 proteins differentially expressed ($p< 0.05$) (Table V). Significantly up or down-regulated proteins were determined by a fold change > 2.

Table V. Proteins of the semipurified viral preparation affected by the PEDV infection

Up-regulated proteins				
		Gene ontology annotation		
Protein name	Accession number	Cellular Localization	Molecular Function	Reported in virus
2',3'-cyclic-nucleotide 3'-phosphodiesterase	K4GWC8	Plasma membrane	• Regulate multiple cellular functions	Hepatitis B virus (109), influenza A2, NDV, VSV (110).

			• Suppress protein production by association with polyadenylation of mRNA.	
AH receptor-interacting protein	O97628	Cytoplasm	• Regulator of type I interferon • Essential for restricting virus infection and spread.	Hepatitis B virus, EBNA-3 of the Epstein-Barr virus (111).
Axl receptor tyrosine kinase	Q14UF1	Plasma membrane	Transduces signals from the extracellular matrix into the cytoplasm by binding to the vitamin K-dependent protein growth arrest-specific 6 (Gas6).	Influenza A virus, Puerto Rico/8/34(PR8) (112).
CD1d	Q4ACW7	Plasma membrane	Interacts with distinct NKT populations inducing gamma IFN-gamma production and NK-cell activation.	EMCV (113), TMEV (114), HIV-1, EBV (115), HCV (116)

Cellular tumor antigen p53	P13481	Cytoplasm, Plasma membrane, Endoplasmic reticulum, Mitochondria, Nucleus	Involved in cell cycle regulation as a trans-activator. It negatively regulates cell division	SV40 (117), adenovirus, Abelson murine leukemia virus, Friend erythroleukemia virus, HPV (118),
Centromere protein J	F8S641	Centrosome, Cytoplasm	Play essential on cell division and centrosome function by participating in centriole duplication	HSV- 1 (119)
D (3) dopamine receptor	P52703	Plasma membrane	Dopamine receptor whose activity is mediated by G proteins which inhibit adenylyl cyclase. Promotes cell proliferation.	HIV (120)
DNA topoisomerase 1	Q7YR26	Nucleus	Releases the supercoiling and torsional tension of DNA by cleaving and rejoining one strand of the DNA duplex.	Ebola virus (EBOV), SV40, HSV2, HIV (121), DHBV (122).
Fibrillarin	H6U5Q2	Nucleus	Catalyzes the site-specific 2'-hydroxyl	Tobacco mosaic virus (TMV), Potato virus X (PVX) (123)

			methylation of ribose moieties in pre-ribosomal RNA.	
G-protein coupled receptor 15	O18982	Plasma membrane	Chemokine receptor for human immunodeficiency virus type 1 and 2	(EBOV), Marburg virus (MARV), HIV-1 HIV-2 (124)
Guanylate-binding protein 1	Q5D1D6	Cytoplasm, Extracellular matrix, Plasma membrane, Golgi apparatus	Specifically binds guanine nucleotides	Dengue virus (DENV), Vesicular stomatitis virus, Encephalomyocarditis virus, Hepatitis C Virus (125), Classical Swine Fever Virus (126).
Heat shock 70 kDa protein 1	Q28222	Cytoplasm, Ribosome	Stabilizes pre-existent proteins and mediates the folding of newly translated polypeptides in the cytosol as well as within organelles.	Vesicular stomatitis virus, Measles virus (MeV) (127).
Histone H4	Q6B828	Nucleus	Core component of nucleosome. Important for transcription, regulation, DNA repair, DNA replication and	Cotesia plutellae bracovirus (128).

			chromosome stability.	
Interferon-stimulated protein	Q56B92	Cytoplasm, Plasma membrane	Interferon-induced antiviral exoribonuclease that acts on single-stranded RNA and has minor activity towards single-stranded DNA.	HCV, HIV-1, Yellow fever virus (YFV), WNV, Venezuelan equine encephalitis virus (VEEV), and Chikungunya virus (CHIKV) (129), West Nile virus (130).
MHC Class I Antigen	F6KY45	Cytoplasm, Plasma membrane, Cytoskeleton	Presents of foreign antigens to the immune system.	Adenovirus E3/19K, (HIV-1), herpesvirus family (131), (EBV), The human cytomegalovirus (hCMV) (132).
Peptidyl-prolyl cis-trans isomerase A	P62938	Cytoplasm, Extracellular matrix,	Accelerates the folding of proteins.	Vesicular stomatitis virus, influenza A virus, (HCV), Japanese encephalitis virus, severe acute respiratory syndrome (SARS), human cytomegalovirus, rotavirus (133).
Poly ADP-ribose polymerase family member 9	A0A060III8	Mitochondria, Nucleus, Plasma membrane	Induces the expression of IFN-gamma-responsive genes	HSV-1 (134).

Proheparin-binding EGF-like growth factor	Q09118	Extracellular matrix, Plasma membrane	Promotes smooth muscle cell proliferation.	Measles (MV), canine distemper (CDV), rinderpest, peste des petits ruminants (PPRV) viruses, poliovirus like receptor 4 (PVRL4) (135).
Promyelocytic leukemia protein	Q15JD5	Nucleus	Tumor suppression and viral defense stimulator.	The promyelocytic leukemia (PML), Dengue virus (DENV) (136).
RNase L inhibitor	Q6SSD8	Plasma membrane, Mitochondria, Cytoplasm	ATP binding and IFN antiviral response stimulator.	Influenza virus A, Theiler's virus L (137), (HIV-1), (EMC), vaccinia virus, reovirus (138), stomatitis virus, West Nile virus, (HSV), SV40 (139).
SCL/TAL1 interrupting locus protein	A0A060KS53	Centrosome, Cytoplasm, Cytoskeleton	• Plays an important role in cellular growth and proliferation • Decreases CDK1 population	ZIKV, CMV, (HSV-1), (HIV), and Varicella-zoster virus (VZV) (140).
Signal transducer and activator	Q1T7F0	Cytoplasm, Nucleus	Signal transducer and transcription activator that	γ-herpesviruses, Kaposi's sarcoma-associated herpesvirus

of transcription			mediates cellular responses to interferons (IFNs), cytokine KITLG/SCF.	(KSHV), (EBV), herpesvirus saimiri, (VZV) (141).
Syndecan	A4K2Z3	Plasma membrane	Regulates exosome biogenesis.	(HSV-1), (HPV), hepatitis B, C, E viruses, rotavirus, respiratory syncytial virus (142), PRRSV (143).
Vimentin	P84198	Cytoplasm, Cytoskeleton	Cell structure and transport of molecules.	African swine fever virus (ASFV), Dengue (DENV), Vaccinia virus, West Nile virus (144).
Zinc finger protein	P85977	Plasma membrane	Involve in transcriptional regulation.	Sindbis virus (SIN), Semliki Forest virus, Ross River virus, Venezuelan equine encephalitis virus, (MLV) (145).
Down-regulated proteins				
APOBEC3C	BL0W73	Cytoplasm, Plasma membrane, Nucleus	Inhibitor of retrovirus replication and retrotransposon mobility via deaminase-dependent	(HIV), HTLV, (HTLV-1), SFV (simian foamy virus), Hepatitis B virus, (HSV-1), (EBV), Human papillomaviruses (HPVs), Transfusion-

				transmitted virus (TTV) (146).
CCCH-type zinc finger antiviral protein	B0LB09	Cytoplasm, Cytoskeleton	Antiviral protein which inhibits the replication of viruses by recruiting the cellular RNA degradation machineries to degrade the viral mRNAs.	MLV, SIN, Semliki Forest virus, Ross River virus, Venezuelan equine encephalitis virus (145).
Herpesvirus entry mediator C	Q9GL74	Plasma membrane	Receptor for BTLA. Receptor for TNFSF14/LIGHT and homotrimeric TNFSF1/lymphotoxin-alpha. Involved in lymphocyte activation.	Hepatitis C virus (147).
Protein disulfide-isomerase A3	Q4VIT4	Endoplasmic reticulum	Catalyzes the rearrangement of -S-S- bonds in proteins.	Influenza virus, baculovirus, Hepatitis C, HIV, Herpes virus (148).
Radical S-adenosyl methionine domain-	I6ZYZ7	Endoplasmic reticulum	Induces type I and type II IFN.	HIV, HCV, DENV, JEV Japanese encephalitis virus, CHIKV, WNV, IFV,

containing protein 2	RSV respiratory syncytial virus (149).

In order to show the different interactions between the identified proteins significantly affected by the PEDV infection, proteins were mapped with String tool. String is a biological database containing known and predicted protein-protein interactions from different sources, such as experimental results, computational prediction and available information on published reports. The proteins found in the semipurified fraction were mapped according to what has been reported for African green monkey kidney cells (Figure 22). Out of the 63 proteins described (Table V), only 23 are reported for *Chlorocebus aethiops* (cells of African green monkey kidney). This cell line (Vero-76) is highly used for study and isolation of PEDV (19, 20). Currently, the reported interactome of the PEDV also is poorly developed, so a few PEDV-host protein-protein interactions are reported to date. We found some of them in our proteomic database. They are reviewed in the Discussion section.

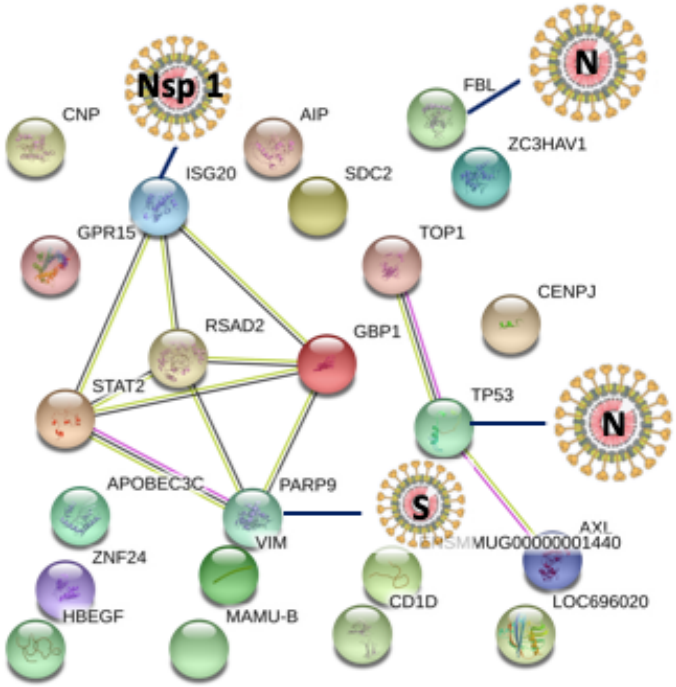

Figure 22. Network of specifically the significantly dysregulated by PEDV infection proteins present in the semipurified viral preparation. Colored nodes represent query

proteins and first shell of interactors, empty and filled notes indicate unknown or known 3D structure of the protein, respectively. Reported interactions among then (blue and pink lines) and predicted interactions (red and green lines). The reported interactions with PEDV were added manually (dark lines).

Purified viral fraction (preparation)

Similar to the semipurified viral preparation, Gene Ontology (GO) analysis was performed to determine the biological processes affected by PEDV infection in the purified viral preparation, where the presence of the EMV proteomic components were decreased by additional purifications steps. The majority of the affected proteins were members of the signaling (40%), immune response (30%) and nucleic acid binding function (30%) pathways (Figure 23).

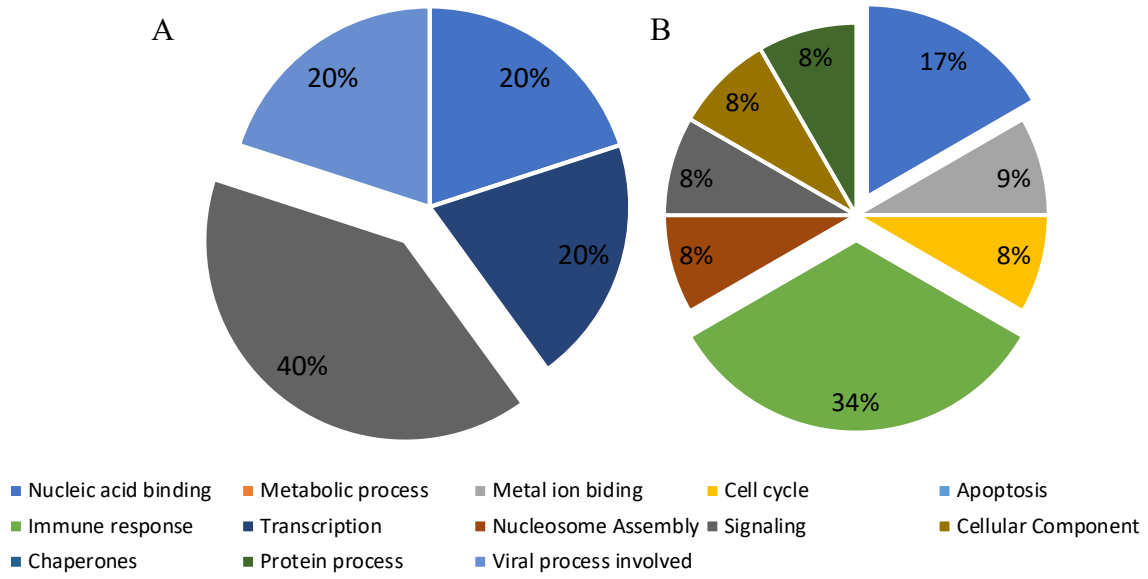

Figure 23. Functional categories of cellular proteins identified in the purified viral preparation. After LFP analysis of semipurified fraction, proteins significantly regulated were classified by their molecular functions. (A) Up-regulated proteins, (B) down-regulated proteins. Gene ontology annotation

Classification of proteins by their subcellular localization was also performed. Proteins identified in the purified viral preparation and significantly dysregulated by the PEDV infection were mainly localized in the nucleus and plasma membrane (Figure 24).

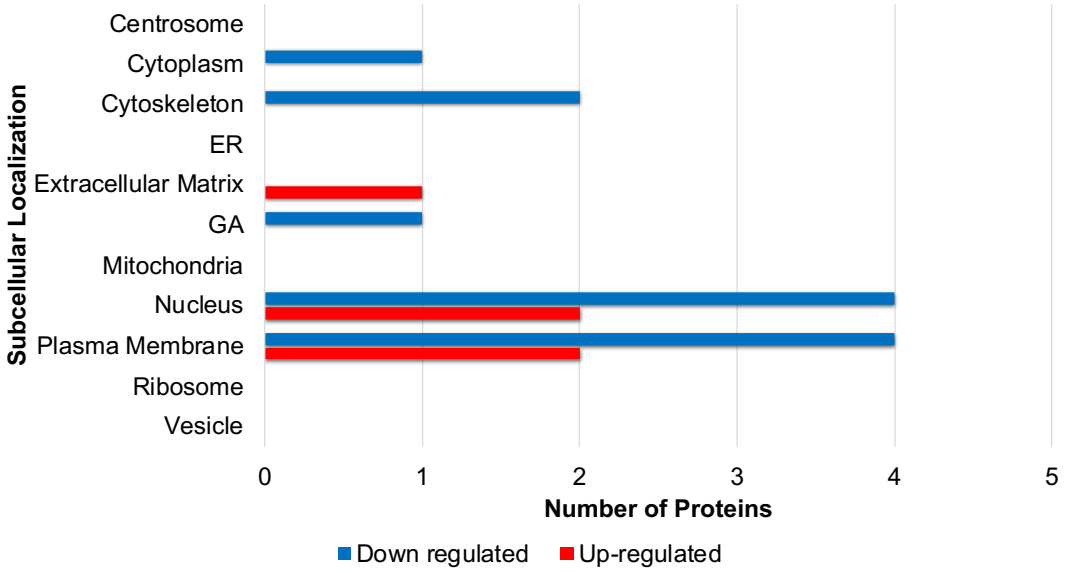

Figure 24. Subcellular localization of dysregulated host proteins identified in the purified viral preparation. Consequent to an LFP analysis of semipurified fraction, proteins significantly regulated were classified by their subcellular localization. Gene ontology annotation

In the purified viral preparations, it was expected to find lower levels of the contamination associated with the presence of microvesicles. Therefore, it was not surprising that fewer proteins were identified in this fraction. Furthermore, the biomarkers of exosomes and microvesicles, such as CD86 and HSP40, were found at lower amount in the purified fraction. This is additional proof of the efficiency of our multistep virus purification procedure and the specificity of the virus-associated set of proteins identified by our proteomic analyses.

From the proteomic analyses of five biological replicates among mock or PEDV-infected, we identified and quantified in the purified preparation 16 proteins differentially expressed ($p< 0.05$) (Table VI). Significantly up- or down-regulated proteins were

determined by a fold change > 2. As for this, 5 proteins were significantly up-regulated, and 11 were significantly down-regulated. Our data demonstrate again that our purification procedure successfully eliminated the proteins, which were non-specifically associated to the PEDV, or have been present in the semipurified preparations due to the contamination by microvesicles and exosomes. Thus, this provides us with a powerful tool to identify and distinguish the definite sets of the host proteins, which are specifically associated or encapsidated into the PEDV virions or are components of the PEDV-infection induced EMV.

Table VI. Proteins affected by PEDV infection identified in the purified viral preparation

Up-regulated proteins				
		GO annotation		
Protein name	Accession number	Cellular Localization	Molecular Function	Reported in virus
Cathelicidin antimicrobial peptide	Q1KLY6	Extracellular region	Involved in the disintegration of cell membranes of pathogens	HIV (150), RSV (151), Influenzas (152) Vaccinia virus (153)
Histone H4	Q6B828	Nucleus	Core component of nucleosome. Important for transcription, regulation, DNA repair, DNA replication and chromosome stability.	Cotesia plutellae bracovirus (128).
Promyelocytic leukemia protein	Q15JD5	Nucleus	Tumor suppression, and viral defense stimulator.	The promyelocytic leukemia (PML), Dengue

				virus (DENV) (136).
Soluble type II IL-1 receptor	Q8HRX8	Plasma membrane	Blocking receptor activity	Vaccinia Virus (154), Cowpox virus, Camel Pox virus (155)
Zinc finger protein	P85977	Plasma membrane	Involve in transcriptional regulation.	Sindbis virus (SIN), SemLiki Forest virus, Ross River virus, Venezuelan equine encephalitis virus, (MLV) (145).
Down-regulated proteins				
CD86 protein	Q9BDM2	Membrane	Signal peptide for activation of immune response	Stimulation of expression upon PEDV infection (156) PRRSV and PCoV (157)
Cyclic GMP-AMP synthase	A0A0F7DHA3	Cytosol, nucleus	Binds to microbial DNA or self-DNA present on the cytoplasm and catalyzes cGAMP synthesis. Activates immune response	HBV (158), indirectly related to PEDV, DENV, EBV, MHV68 (159)

DnaJ (Hsp40) homolog, subfamily C, member 1	A0A0A1GK97	Nucleus	Regulates negatively proteolysis and protein secretion.	Measles virus, Murine hepatitis virus, Human papillomavirus, Herpes simplex virus, HIV, HBV, Porcine circovirus, Influenza (160) Stimulation of expression upon PEDV infection (86)
MHC Class I Antigen	F6KY45	Cytoplasm, Plasma membrane, Cytoskeleton	Presents of foreign antigens to the immune system.	Adenovirus E3/19K, (HIV-1), herpesvirus family (131), (EBV), The human cytomegalovirus (hCMV) (132).
MHC DQ-alpha 1 protein	Q30336	Plasma membrane	Fragment of the heterodimer of the antigen MHC Class I. Presents of foreign antigens to the immune system.	HBV (161), EBV (162) HSV 2 (163) HPV (164)
Natural resistance-associated	Q95N77	Plasma membrane	• Iron metabolism	Sindbis virus (165)

macrophage protein 1			• Host resistance to intracellular pathogens. • Macrophage-specific membrane channel	
NPIP-like protein	Q8WNH3	Nucleus	Part of the nuclear pore complex	
Polysialyltransferase	Q9TT10	Golgi apparatus	Involved in protein glycosylation	
WD repeat domain 62 (Fragment)	A0A1D5RIS9	Cytoskeleton, nucleolus	Involved in centriole replication and mitotic organization, as well as neurogenesis	Measles Virus (166)

The interactions between the proteins identified in the purified viral preparation and significantly dysregulated by the PEDV infection were mapped using the String tool. Out of the 16 proteins affected by the PEDV infection and found in this fraction, only 9 proteins have been reported on the databases of African green monkey kidney cells (Figure 25).

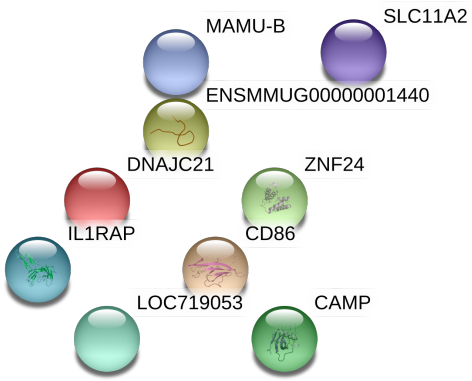

Figure 25. Network of specifically the significantly dysregulated by PEDV infection proteins present in the purified fraction. Colored nodes represent query proteins and first shell of interactors, empty and filled notes indicate unknown or known 3D structure of the protein, respectively. To date, there are no reported interactions for these proteins among them in *Chlorocebus aethiops* database. Additionally, there are no reports of interaction between the found proteins and PEDV proteins.

VI. Discussion

PEDV-caused diarrhea is clinically indistinguishable from other diarrhoeal viral diseases. To date, PEDV circulates on the Asian, American and European continents and causes outbreaks in Asia and North America, having a significant impact on the swine industry. A better understanding of the molecular interactions between PEDV and host cells will help to bust the development of safe vaccines for controlling the epidemic of PEDV. To contribute to fulfilling the knowledge gap, it was proposed to evaluate the proteomic profile of different viral preparation, in order to decipher proteins associated or encapsidated into PEDV virions. To do so, optimization of PEDV production and assessment of the host cell proteins associated with or encapsidated into PEDV and microvesicles/exosomes of infected cells was performed; then, evaluation through label-free quantitative proteomics of several viral purifications was done. This will provide valuable insight into the complex network of the host-cell protein interactions.

1. Optimization of PEDV infection by polycations

Polycations have been widely used to enhance infection of recombinant lentiviral vectors. The molecular mechanism behind the polycation-mediated enhancement of viral attachment and entry is the neutralization of the repulsive electrostatic forces between target cell and virus membrane (89). It was compared the effects of two commonly used polycations (polybrene and DEAE-dextran) on the PEDV infectivity and showed that polybrene was more effective enhancer of the PEDV infectivity. These results were proven by various techniques and at different time of post-infection.

Initially, it was investigated the cytotoxic potential of the polycations. Results showed that at the range of the previously reported for both polycations concentrations, polybrene and DEAE-dextran did not exert high cytotoxicity to Vero-76 cells and can be safely used for PEDV entry enhancement. The higher concentrations of the polycations had slightly higher the toxicity and effect of the cell viability, which was reported for these molecules (167). Interestingly, Monnery et al., in 2017 (167) demonstrated that cytotoxicity of the polycations is directly related with their molecular weight, suggesting that at higher concentrations polycations could have higher toxicity (167). On the contrary, a group of researchers from Germany didn't observe a significant decrease of cells viability at high

concentrations of the polycations. They also determined that polycations' toxicity could be related with the structure of the molecule (168). Overall, there is a consensus that cytotoxicity exerted by polycations most likely is related to their structure and molecular weight, and it is cell type dependent. Nevertheless, presence of FBS in the cell culture medium should be consider as toxicity factor. Exact composition and variability among batches of FBS are a constant problem. Depending on the cells type, the percentage of FBS will vary, having different outcomes among different cells types (169).

It was observed that viability of cells didn't decrease significantly after 24- or 48-hours post-treatment (Figure 8 and 9) for all tested concentrations. Furthermore, results (Figure 10 and 11) showed that both polycations had a low cytotoxic effect in Vero-76 cells (less than 5% after 24- or 48- hours of post-treatment). Interestingly, cytotoxicity exerted by polycations was slightly higher after 24 hours posttreatment, compare to 48 h. This can be link to the cell cycle of this cell line. Vero-76 cells take approximately 22 hours to double the population (170). Therefore, 24 hours after cells will start to die and free LDH to the medium, but 48 hours after cells would have double the population already two times, overcoming with the dead population, and for so with the LDH liberated.

Next, the effects of two non-toxic concentrations of both polycations were tested on the PEDV progeny production after 36 h.p.i. Additionally, the effect of the viral entry synchronization on PEDV infection (Figure 12) was examined. Interestingly, results showed that a) synchronization of the infection had a positive impact on the PEDV infectivity, but more importantly, b) polybrene enhanced the PEDV infectivity up to 9-fold.

PEDV infection *in vitro* (cell cultures) is trypsin-dependent (19, 20). Previous reports have demonstrated that trypsin's protease activity is indispensable for the S protein activation right after viral-host receptor binding. Fusion S peptide, which is a key element for viral entry into the cells, is exposed after that binding step (26, 171). After the synchronization step of the PEDV infection (2 hours of viral adsorption at room temperature), the medium containing trypsin and unbound virus were washed out and fresh medium with trypsin was added. Thus, the addition of fresh medium with trypsin further enhanced viral entry (Figure 12).

As it was mentioned earlier, polycations have different mechanisms for neutralizing the repulsive electrostatic forces between cell membranes and virus. It has been reported that polycations with a molecular weight higher (MW) than 15 kDa are able to enhance viral

infection through viral aggregation mechanism, while polycations with a lower MW (less than 15 kDa) can perform either cell or virus shielding (89). Experiments showed that pre-incubating cells for 1 hour at room temperature with the polycations didn't have significant impact on the PEDV infectivity, at all tested concentrations (Figure 13). In contrast, when viral inoculums were pre-incubated at the same conditions with polycations, a significant increase (4-fold) of the PEDV infectivity was observed (Figure 14 and 15). Thus, it was proposed that polybrene enhances PEDV attachment and entry through the charge shielding mechanism. Interestingly, the concentration of the polybrene that showed high performance (8μg/mL) on this report, has been earlier recommended for the optimization of lentiviral transduction (172, 173). Jang et al. in 2012 (88) demonstrated that the effect of this molecule on viral infection can be virus and cell specific (88). Although, it was observed a significant enhancement of the PEDV infectivity in Vero-76 cells by polybrene treatment, it can be expected that on other cell types the effect of polybrene may vary. To date, this is the first report of the polycation-mediated enhancement of PEDV infectivity.

Furthermore, the dose-response relationship between polycations and PEDV infectivity was examined. Various concentrations of both polycations were tested. After 1 hour of pre-incubation of the PEDV inoculums with the polycations and synchronization of the infection, the efficiency of the infection was evaluated by IFA at 6 h.p.i. Results confirmed that DEAE-dextran treatment had very modest positive effect on PEDV infectivity at all tested concentrations. For instance, even at the highest concentration of the DEAE-dextran (60μg/mL) the ratio of infected cells was about 5 % (Figure 16). In contrast, PEDV pre-incubation with polybrene at 8μg/mL was more effective treatment that enhanced PEDV infection up to 4-fold (Figure 17).

Optimization of the efficiency of viral infection is of a high importance for a variety of research applications and vaccine production. Calculation of the titers of viral stocks and the estimation of viral load in the study of many viruses often involve cytopathic effect (CPE) quantification in plaque-forming units (PFU) or similar approaches. Theoretically, the MOI predicts the number of viruses needed to infect a single cell. However, the virus infectivity is known to be uneven, and frequently the MOI becomes less practical (174). As it was shown here, the PEDV pre-treatment with polycations reproducibly increased the number of infected cells (as it was measured by IFA), suggesting that there are much more infectious

particles in the viral preparations than it was estimated by standard virus titration techniques (MOI are based on Spearman-Karber method of calculation of viral titers). In spite of the last-mentioned statement, cell permissiveness plays a key factor on viral infection (175). This has been already reported by Shirato et al., in 2016 (36), where authors infected several permissive and non-permissive cell lines with PEDV, expressing or not the aminopeptidase N (APN), that was believed to be PEDV main cellular receptor. Conclusion from this study, determined that APN is not the receptor of PEDV, but also that PEDV infection outcome on different cells lines varies (36).

It is also worth to mention that PEDV is characterized by a low viral infectivity and production compared to other coronaviruses (19, 20). The data showed that polycations can successfully contra rest this problem. it was shown that even by using a low MOI, the percentage of PEDV infected cells can be increased by polybrene pre-treatment at least four times. This suggests that using low MOIs in combination with the polycation treatment, it is possible to infect high percentage of host cells and save on viral inoculum. This can have implication in vaccine manufacturing (optimization of vaccine yield and decreasing the cost).

Nevertheless, further experiments on natural host cells (intestinal cells of pigs) are needed to understand the impact of polycations on host cells lines. More specifically, if polycations effect is cell- and virus- dependent, expected outcome on natural host cell of enhancement of PEDV infection is higher. Additionally, the study of PEDV for effective vaccine production should be carry out on natural host cells.

Following the hypothesis proposed: PEDV can change the intracellular levels of host proteins in order to modify the intracellular environment, to escape host defenses and facilitate their own replication and spread, I can't be concluded the statement, due to the lack of experiments. However, optimization of infection of PEDV was performed for further proteomic experiments, where timepoints will be performed, in order to elucidate what is happening hour by hour on infected cells, based on PEDV viral life cycle. This way understand how PEDV is shaping the intracellular environment for immune response evasion and spread.

2. Identification of host cell proteins associated with or encapsidated into PEDV and EMV induced by PEDV infection.

2.1. Multistep purification of the PEDV for proteomic assay

Multistep purifications are often performed to obtain pure viral particles. Elimination of the cellular debris, microvesicles and exosomes, and defective virions is necessary for downstream procedure such as proteomics, especially if the proteomic analysis is aimed at studying the composition of viral particles. It is known that sucrose cushion can remove part of cellular contaminants, but is less efficient for eliminating defective (empty, e.g.) virions and exosomes/microvesicles. Of note, defective particles and EMV have very similar to virions density and size. The purification through the density gradients do remove the majority, if not all, cellular contaminants, most of the exosomes/microvesicles and empty viral particles (176).

Results showed that semipurified (passed through a 30% sucrose cushion) viral preparations contained high amount of proteins, had average viral titers, and displayed a relatable Ct values (i.e., had viral RNA) (Figure 18). Viral particles were further purified by submitting the semipurified viral preparation to a CsCl density gradient and collecting 11 fractions. Some fractions displayed low amount of proteins, but some had similar Ct values and viral titers as the semipurified virus (Figure 18). Chosen purified fractions were further ultra-purified through an enzymatic digestion with subtilisin, to eliminate exosomes with a size and density close to PEDV. Fractions were selected according to their enrichment in infectious viral particles (purified viral preparation), and thus most of the contaminants were eliminated, which was the goal. Then, the semipurified and selected purified fraction were analyzed through proteomics approach to decipher host cell proteins associated with or encapsidated into PEDV and microvesicles/exosomes of infected cells.

2.2. Semipurified viral preparation

Proteomics has become an important tool for the analysis of protein interactions network. Interactions between host and host cell can be deciphered by this approach, creating a detailed map of virus-host interactions, and ultimately helping to discover novel anti-pathogen targets (177).

This research is aimed at elucidating the protein composition of microvesicles and exosomes induced by PEDV infection and the composition of pure PED virions. It was demonstrated that 63 proteins were significantly dysregulated by PEDV infection in the semipurified fraction (Table V). The majority of these proteins were up-regulated (Figure 19). These proteins were involved mainly in various cellular processes such as cell cycle regulation and acid binding among others (Figure 20). To date, this is a first report of the comparative proteomic studies of the PED viral preparations.

Results showed that proteins involved in cell cycle were significantly up-regulated by PEDV infection. One of them is the poly (ADP-ribose) polymerase (PARP), an enzyme that catalyzes the transfer of ADP-ribose to specific proteins. It plays an essential role in modulation of chromatin structure, transcription, replication, recombination, and DNA repair (178). It has been reported that PEDV induces cell apoptosis *in vivo* as well as *in vitro.* More specifically, the presence of the subunit S1 of the S protein of PEDV induced the degradation of PARP, prompting nuclear concentration and fragmentation. The exact role of the S1 subunit for PARP degradation still remains unknown (10). This correlates with the symptom piglets present after viral infection. Vomiting, diarrheas, dehydration, among others, are typical of cells destruction and apoptosis of intestinal cells. Up-regulation of this protein in presence of PEDV could indicate that it may have a specific role during viral infection.

Another well-known molecule involved in the cellular apoptosis pathway is the cellular tumor antigen P53. It was found that it also was up-regulated by PEDV infection. P53 plays a crucial role in responding to the cellular stress signaling, such as DNA damage or oncogenic stress. It is activated through a cascade of phosphorylation and posttranslational modifications (PTMs). P53 target genes involved in cell-cycle arrest, DNA repair, or apoptosis (179). Recently, it was shown that PEDV can arrest the host cell cycle in the G0/G1 stage through the P53 pathway. G0 is known to be the non-proliferative stage of the cell cycle, right after mitotic process. Epithelial cells usually don't arrest their cell cycle on this stage; they are constantly in division. G1 is a stage where cells prepare their elements, such as proteins and organelles, for the cell division step, and metabolic processes are usually at a high rate. In the PEDV-infected cells, a significant decrease in the expression of Cyclin E was observed, in return which could be involved in G0/G1 phase transition, causing the cell cycle arrest in this stage. Moreover, it was shown that PEDV infection induced accumulation

of p53and p21, which are usually expressed when there is DNA damage and cell cycle should be arrested. Authors speculate that cell cycle arrest in G0/G1 phase provides a more favorable condition for PEDV replication (180). Significant abundance of this protein in infected PEDV-cells could be due to a modulation caused by PEDV to favor its own replication.

Results showed as well that proteins involved in cell structure were significantly up-regulated. Among them, the fibrillarin that has been described to co-localize with the N protein of PEDV (181). A recent study demonstrated that PEDV N protein can also co-localized with other nuclear structural proteins such as NPM1, which is ribosome assembly protein. This is a structural protein, but also functions as a nucleic acid binding factor. Authors concluded that the interaction of the N protein with NPM1 helps to protect it from the proteolytic cleavage, by inhibiting caspase-3-mediated cleavage of NPM1, and thus enhancing the PEDV-infected cell survival (182). The nucleic acid binding was one of the cellular functions significantly affected by the PEDV infection, as it was revealed on the proteomic analysis of the semipurified fraction (Figure 20).

Importantly, the non-structural proteins of PEDV also have been reported to interact with various host cell proteins. For example, interferon-stimulated gene 20 (ISG) is a gene whose expression is stimulated by interferon and is an antiviral exoribonuclease that acts on ssRNA. It has been shown that ISG20 has antiviral activity against HCV, hepatitis A virus (HAV), and yellow fever virus (YFV). Interactions between nsp1 of the PEDV and ISGs have been reported recently. It was demonstrated that PEDV nsp1 promotes degradation CBP, a complex with the transcription co-activator CREB (cAMP responsive element binding)-binding protein (CBP)/p300 degradation, which resulted in the inhibition of the expression of ISGs, evading antiviral response of the host cell (6).

Another protein identified in our study is the peptidyl-prolyl cis-trans isomerase A (CyPA), which catalyzes proteins folding. It is known that CyPA is secreted in response to a cellular stress (for example, caused by an infection). It has been reported that CyPA enhances viral life cycle of HIV, specifically viral entry and retro transcription. Additionally, a correlation between increased production of CyPA and increased of percentage of infected cells by viruses like hepatitis and influenza was reported (183). For the PEDV infection, there is no reports about specific interaction between PEDV and CyPA. However, an interaction between PEDV and peptidyl-isomerases (PPIA), a member of the same family of proteins

very close to the CyPA protein, has been described (Figure 22). CyPA-related protein, the cyclophilin D (CyPD) is an important factor involved in the mitochondrial permeabilization transition pore (MPTP) complex, and it is also involved in the protein folding pathway. In the PEDV-infected cells, it was found that CyPD was stimulated, triggering translocation of the apoptosis-inducing factor from the mitochondria to the nucleus, which facilitated PEDV replication and pathogenesis. This allowed authors to conclude that PEDV infection stimulates caspase-independent apoptosis (184).

Interestingly, proteins up-regulated by PEDV infection and identified in the semipurified samples mostly were localized on the cytoplasm and plasma membrane (Figure 21). As it was discussed earlier, the semipurified viral preparation can still contain some cellular debris, microvesicles and exosomes, as well as empty viral particles. Proteins localized in the cytoplasm and plasma membrane can be associated with the microvesicles and exosomes (EMV), which are formed in the cytoplasm and are membrane-covered structures. Thus, the content of the EMV can depend of the molecular processes happening in the cytoplasm of infected cells. Also, microvesicles membrane is constituted by the plasma membrane of the cell. Some exosomes markers such as HSP, MHC (185), among others, were spotted in our semipurified samples, indicating the presence of these ones at this level of purification. Some of the proteins discovered in the semipurified preparation were found to interact with each other as well (Figure 22).

2.3. Purified viral preparation

Fourteen proteins were significantly down-regulated by the PEDV infection in the purified viral preparation (Table VI). These proteins are involved mainly in nucleic acid binding, signaling, and immune response (Figure 23). Some of the proteins found in the semipurified fractions were identified in the purified fraction, suggesting that these proteins could be specifically encapsidated into or association with the virions.

The protein CD86 in the purified viral fraction was found. This is an antigen presenting receptor that stimulates T cell activation and survival. To date, there is not report regarding interaction between this protein and PEDV proteins. Recently, it was shown that expression of this receptor on monocyte-derived dendritic cells (Mo-DCs) and intestinal

dendritic cells was up-regulated by the infection of classical PEDV strain, which are cell culture adapted strains (156). Authors found that Mo-DCs were more susceptible to PEDV infection than intestinal dendritic cells. Also, they demonstrated that infection of Mo-DCs with PEDV up-regulated proteins like CD1a, CD80/86 and SLA-IIDR, which stimulate immature Mo-DCs to develop antigen presentation functions (156).

Likewise, heat shock protein 40 (HSP40) has been reported to be significantly expressed in the cells infected by a highly pathogenic PEDV strain and suppressed in the cells infected with a cell culture adapted PEDV strain (classical) (86). In the case of this report, this protein was down-regulated, which corroborates the published report. The strain that was used in the study is a reference cell-adapted strain. HSPs are exploited by viruses for their protein folding and virion assembly. More specifically, the HSP40 regulates the function of HSP70, which plays an important role in cellular signaling, cell cycle, cell death, and the proteins folding during the cellular stress response (86). Therefore, the down regulation of this protein by PEDV infection might indicate that the virus is inhibiting its own replication and spread. This could be related to the low pathogenicity of the cell adapted or classical strains of PEDV.

Interestingly, in both viral preparations (semipurified and purified), the MHC (major histocompatibility complex) class I antigen was found to be affected by the PEDV infection. This protein was up-regulated in the semipurified preparation but was down-regulated in the purified viral preparation. The MHC I molecule function is to bind the antigens derived from the pathogens and present them on the cell surface, to be recognized by T-cells. MHC I mediates interactions between leukocytes (131). Previously, it was shown that assembly of the PED virion occurs in the ERGIC (2), where the MCH I can be found recognizing peptides of the proteins produced on the ERGIC. Down regulation of the expression of this molecule may indicate that PEDV is evading the antigen presentation, and, consequently, the T cell activation. Thus, this could be the mechanism of the PEDV immune response evasion, which facilitates effective infection and massive progeny production. However, further functional validations are needed to evaluate this possibility.

Down-regulated proteins in the purified viral preparation were principally localized in the nucleus and plasma membrane (Figure 24). At this stage of purification, exosomes of the same size and density as the PED virions can still be found in the sample. A few markers

of exosomes, such as CD86 and MHC, were still present in that fraction. In order to eliminate the exosomes, further ultra-purification by a non-physical method, such as a subtilisin-mediated digestion of the EMV (103), is needed. This work is in progress.

In this study, it was observed that PEDV infection modulates positively or negatively the abundance of various host proteins. Some of these have been already reported to interact with the PEDV proteins. It can be partially agreed with to our hypothesis: The compositions of PED virions are cell-type dependent. Host cell proteins were present in both viral fractions (semipurified and purified), indicating a possible association or encapsidation into PED virions. Nevertheless, final ultra-purification step is necessary to conclude the statement. Additionally, further validation experiments are needed to confirm that the reported interactions are vital for the course of PEDV infection.

VII. Conclusions and perspectives

To conclude, polycations-mediated enhancement of PEDV infection, was demonstrated for the first time on early and late stages of infection. Particularly, the pre-incubation of the PEDV with polybrene was effective in enhancing virus adsorption by cells. Polycation-mediated enhancement of virus infectivity can be used to increase virus yield and for a more cost-effective viral vaccine manufacturing.

Additionally, this is the first study of the composition of the PED virions and microvesicles produced by the PEDV infection. The abundance of the host cellular proteins classified in different subcellular compartments and of various functional groups was changed by PEDV infection. These changes should probably facilitate PEDV replication and spread. Moreover, presence of the same proteins identified in semipurified and purified viral preparations demonstrates the specificity and validity of our approach.

However, in order to have a complete map of PEDV-host molecular interactions, study of the cellular proteomic profiles along the PEDV infection in natural host cells, (e.g., porcine small intestinal epithelial cell line – IPEC), is necessary for identifying host proteins involved in viral life cycle. Also, quantitative proteomic analyses of the ultra-purified fraction will allow to determine the host proteins that are specifically encapsidated or associated with PED virions. Moreover, evaluation of the proteomic profiles of microvesicles/exosomes, produced by PEDV infection in natural host cells will reveal molecular mechanisms of virus-host interactions and pathogenesis, and will allow to identify the host biomarkers of the PEDV infection. Further functional validation experiments through diverse techniques such as overexpression, knockdown experiments, protein-protein interaction assays, etc., are necessary to validate the proteomic results presented.

Finally, the present work provides new information on important specific details of the mechanisms of PEDV-host cell interactions. This will help us to create a comprehensive and dynamic picture of the host response to virus infection. More specifically, the identified host proteins will represent attractive targets for antiviral therapies.

VIII. References

1. Song D, Moon H, Kang B. 2015. Porcine epidemic diarrhea: a review of current epidemiology and available vaccines. Clin Exp Vaccine Res 4:166–76.
2. Lee C. 2015. Porcine epidemic diarrhea virus: An emerging and re-emerging epizootic swine virus. Virol J 12:193.
3. Shirato K, Matsuyama S, Ujike M, Taguchi F. 2011. Role of Proteases in the Release of Porcine Epidemic Diarrhea Virus from Infected Cells. J Virol 85:7872–7880.
4. Wang Q, Vlasova AN, Kenney SP, Saif LJ. 2019. Emerging and re-emerging coronaviruses in pigs. Curr Opin Virol.
5. Ren X, Suo S, Jang Y-S. 2011. Development of a porcine epidemic diarrhea virus M protein-based ELISA for virus detection. Biotechnol Lett.
6. Zhang Q, Shi K, Yoo D. 2016. Suppression of type I interferon production by porcine epidemic diarrhea virus and degradation of CREB-binding protein by nsp1. Virology.
7. Lin SY, Liu CL, Chang YM, Zhao J, Perlman S, Hou MH. 2014. Structural basis for the identification of the N-terminal domain of coronavirus nucleocapsid protein as an antiviral target. J Med Chem.
8. Zhao S, Gao J, Zhu L, Yang Q. 2014. Transmissible gastroenteritis virus and porcine epidemic diarrhoea virus infection induces dramatic changes in the tight junctions and microfilaments of polarized IPEC-J2 cells. Virus Res.
9. Ding Z, Fang L, Jing H, Zeng S, Wang D, Liu L, Zhang H, Luo R, Chen H, Xiao S. 2014. Porcine Epidemic Diarrhea Virus Nucleocapsid Protein Antagonizes Beta Interferon Production by Sequestering the Interaction between IRF3 and TBK1. J Virol.
10. Chen Y, Zhang Z, Li J, Gao Y, Zhou L, Ge X, Han J, Guo X, Yang H. 2018. Porcine epidemic diarrhea virus S1 protein is the critical inducer of apoptosis. Virol J 15:170.
11. Zeng S, Zhang H, Ding Z, Luo R, An K, Liu L, Bi J, Chen H, Xiao S, Fang L. 2015. Proteome analysis of porcine epidemic diarrhea virus (PEDV)-infected Vero cells. Proteomics 15:1819–1828.
12. Sun D, Shi H, Guo D, Chen J, Shi D, Zhu Q, Zhang X, Feng L. 2015. Analysis of protein expression changes of the Vero E6 cells infected with classic PEDV strain CV777 by using quantitative proteomic technique. J Virol Methods 218:27–39.
13. Ye Y, Zhu J, Ai Q, Wang C, Liao M, Fan H. 2019. Quantitative Proteomics Reveals Changes in Vero Cells in Response to Porcine Epidemic Diarrhea Virus. J Proteome Res.
14. Guo X, Hu H, Chen F, Li Z, Ye S, Cheng S, Zhang M, He Q. 2016. iTRAQ-based comparative proteomic analysis of Vero cells infected with virulent and CV777 vaccine strain-like strains of porcine epidemic diarrhea virus. J Proteomics 130:65–75.
15. Li W, van Kuppeveld FJM, He Q, Rottier PJM, Bosch BJ. 2016. Cellular entry of the porcine epidemic diarrhea virus. Virus Res 226:117–127.
16. Pearce SCC, Schweer WPP, Schwartz KJJ, Yoon KJJ, Lonergan SMM, Gabler NKK. 2016. Pig jejunum protein profile changes in response to a porcine epidemic diarrhea virus challenge. J Anim Sci 94:412–415.
17. Moerdyk-Schauwecker M, Hwang S Il, Grdzelishvili VZ. 2014. Cellular proteins associated with the interior and exterior of vesicular stomatitis virus virions. PLoS One.
18. Rodrigues M, Fan J, Lyon C, Wan M, Hu Y. 2018. Role of extracellular vesicles in viral and bacterial infections: Pathogenesis, diagnostics, and therapeutics.

Theranostics.
19. Hofmann M, Wyler R. 1988. Propagation of the virus of porcine epidemic diarrhea in cell culture. J Clin Microbiol 26:2235–2239.
20. Hofmann M, Wyler R. 1989. Quantitation, biological and physicochemical properties of cell culture-adapted porcine epidemic diarrhea coronavirus (PEDV). Vet Microbiol.
21. Boniotti MB, Papetti A, Lavazza A, Alborali G, Sozzi E, Chiapponi C, Faccini S, Bonilauri P, Cordioli P, Marthaler D. 2016. Porcine epidemic diarrhea virus and discovery of a recombinant swine enteric coronavirus, Italy. Emerg Infect Dis.
22. Hain K. 2016. Development and Characterization of A Recombinant Orf Virus Vector Expressing the Spike Protein of Porcine Epidemic Diarrhea Virus. South Dakota State University.
23. Thomas JT, Chen Q, Gauger PC, Giménez-Lirola LG, Sinha A, Harmon KM, Madson DM, Burrough ER, Magstadt DR, Salzbrenner HM, Welch MW, Yoon KJ, Zimmerman JJ, Zhang J. 2015. Effect of porcine epidemic diarrhea virus infectious doses on infection outcomes in Naïve conventional neonatal and weaned pigs. PLoS One.
24. Sekhon SS, Nguyen PL, Ahn JY, Lee KA, Lee L, Kim SY, Yoon H, Park J, Ko JH, Kim YH. 2016. Porcine epidemic diarrhea (PED) infection, diagnosis and vaccination: A mini review. Toxicol Environ Health Sci.
25. Belouzard S, Millet JK, Licitra BN, Whittaker GR. 2012. Mechanisms of coronavirus cell entry mediated by the viral spike protein. Viruses 4:1011–1033.
26. Wicht O, Li W, Willems L, Meuleman TJ, Wubbolts RW, van Kuppeveld FJM, Rottier PJM, Bosch BJ. 2014. Proteolytic Activation of the Porcine Epidemic Diarrhea Coronavirus Spike Fusion Protein by Trypsin in Cell Culture. J Virol 88:7952–7961.
27. Sato T, Takeyama N, Katsumata A, Tuchiya K, Kodama T, Kusanagi KI. 2011. Mutations in the spike gene of porcine epidemic diarrhea virus associated with growth adaptation in vitro and attenuation of virulence in vivo. Virus Genes.
28. Lin CM, Annamalai T, Liu X, Gao X, Lu Z, El-Tholoth M, Hu H, Saif LJ, Wang Q. 2015. Experimental infection of a US spike-insertion deletion porcine epidemic diarrhea virus in conventional nursing piglets and cross-protection to the original US PEDV infection. Vet Res.
29. Xu X, Zhang H, Zhang Q, Huang Y, Dong J, Liang Y, Liu HJ, Tong D. 2013. Porcine epidemic diarrhea virus N protein prolongs S-phase cell cycle, induces endoplasmic reticulum stress, and up-regulates interleukin-8 expression. Vet Microbiol 164:212–221.
30. Cao L, Ge X, Gao Y, Ren Y, Ren X, Li G. 2015. Porcine epidemic diarrhea virus infection induces NF-kB activation through the TLR2, TLR3 and TLR9 pathways in porcine intestinal epithelial cells. J Gen Virol.
31. Liwnaree B, Narkpuk J, Sungsuwan S, Jongkaewwattana A, Jaru-Ampornpan P. 2019. Growth enhancement of porcine epidemic diarrhea virus (PEDV) in Vero E6 cells expressing PEDV nucleocapsid protein. PLoS One.
32. Sun M, Ma J, Yu Z, Pan Z, Lu C, Yao H. 2017. Identification of two mutation sites in spike and envelope proteins mediating optimal cellular infection of porcine epidemic diarrhea virus from different pathways. Vet Res 48:1–13.
33. Nam E, Lee C. 2010. Contribution of the porcine aminopeptidase N (CD13) receptor density to porcine epidemic diarrhea virus infection. Vet Microbiol 144:41–50.
34. Li BX, Ge JW, Li YJ. 2007. Porcine aminopeptidase N is a functional receptor for the

PEDV coronavirus. Virology.
35. Liu C, Tang J, Ma Y, Liang X, Yang Y, Peng G, Qi Q, Jiang S, Li J, Du L, Li F. 2015. Receptor Usage and Cell Entry of Porcine Epidemic Diarrhea Coronavirus. J Virol 89:6121–6125.
36. Shirato K, Maejima M, Islam MT, Miyazaki A, Kawase M, Matsuyama S, Taguchi F. 2016. Porcine aminopeptidase N is not a cellular receptor of porcine epidemic diarrhea virus, but promotes its infectivity via aminopeptidase activity. J Gen Virol 97:2528–2539.
37. Li W, Luo R, He Q, van Kuppeveld FJM, Rottier PJM, Bosch B-J. 2017. Aminopeptidase N is not required for porcine epidemic diarrhea virus cell entry. Virus Res 235:6–13.
38. Luo X, Guo L, Zhang J, Xu Y, Gu W, Feng L, Wang Y. 2017. Tight junction protein occludin is a porcine epidemic diarrhea virus entry factor. J Virol JVI.00202-17.
39. Buckley A, Turner JR. 2018. Cell biology of tight junction barrier regulation and mucosal disease. Cold Spring Harb Perspect Biol.
40. Meckes DG, Raab-Traub N. 2011. Microvesicles and Viral Infection. J Virol.
41. Bunggulawa EJ, Wang W, Yin T, Wang N, Durkan C, Wang Y, Wang G. 2018. Recent advancements in the use of exosomes as drug delivery systems. J Nanobiotechnology.
42. Koga Y, Yasunaga M, Moriya Y, Akasu T, Fujita S, Yamamoto S, Matsumura Y. 2011. Exosome can prevent RNase from degrading microRNA in feces. J Gastrointest Oncol.
43. Hagemeijer M, Rottier P, Haan C. 2012. Biogenesis and Dynamics of the Coronavirus Replicative Structures. Viruses.
44. Zhou X, Cong Y, Veenendaal T, Klumperman J, Shi D, Mari M, Reggiori F. 2017. Ultrastructural characterization of membrane rearrangements induced by porcine epidemic diarrhea virus infection. Viruses.
45. Wang T, Fang L, Zhao F, Wang D, Xiao S. 2017. Exosomes mediate intercellular transmission of porcine reproductive and respiratory syndrome virus (PRRSV). J Virol.
46. Montaner-Tarbes S, Borrás FE, Montoya M, Fraile L, Del Portillo HA. 2016. Serum-derived exosomes from non-viremic animals previously exposed to the porcine respiratory and reproductive virus contain antigenic viral proteins. Vet Res.
47. Sun M, Ma J, Wang Y, Wang M, Song W, Zhang W, Lu C, Yao H. 2015. Genomic and epidemiological characteristics provide new insights into the phylogeographical and spatiotemporal spread of porcine epidemic diarrhea virus in asia. J Clin Microbiol.
48. Carvajal A, Argüello H, Martínez-Lobo FJ, Costillas S, Miranda R, de Nova PJG, Rubio P. 2015. Porcine epidemic diarrhoea: New insights into an old disease. Porc Heal Manag.
49. Bjustrom-Kraft J, Woodard K, Giménez-Lirola L, Rotolo M, Wang C, Sun Y, Lasley P, Zhang J, Baum D, Gauger P, Main R, Zimmerman J. 2016. Porcine epidemic diarrhea virus (PEDV) detection and antibody response in commercial growing pigs. BMC Vet Res.
50. Poonsuk K, Cheng TY, Ji J, Zimmerman J, Giménez-Lirola L. 2018. Detection of porcine epidemic diarrhea virus (PEDV) IgG and IgA in muscle tissue exudate ("meat juice") specimens. Porc Heal Manag.
51. Song D, Park B. 2012. Porcine epidemic diarrhoea virus: A comprehensive review of molecular epidemiology, diagnosis, and vaccines. Virus Genes.

52. Pyo HM, Kim IJ, Kim SH, Kim HS, Cho SD, Cho IS, Hyun BH. 2009. Escherichia coli expressing single-chain Fv on the cell surface as a potential prophylactic of porcine epidemic diarrhea virus. Vaccine.
53. Jung K, Kang BK, Kim JY, Shin KS, Lee CS, Song DS. 2008. Effects of epidermal growth factor on atrophic enteritis in piglets induced by experimental porcine epidemic diarrhoea virus. Vet J.
54. Gerdts V, Zakhartchouk A. 2017. Vaccines for porcine epidemic diarrhea virus and other swine coronaviruses. Vet Microbiol 206:45–51.
55. Frederickson D, Bandrick M, Taylor L, Coleman D, Pfeiffer A, Locke C. 2014. Safety and antibody response of pigs to an experimental porcine epidemic diarrhea virus (PEDV) vaccine, killed virus.North American PRRS Symposium.
56. Schwartz TJ, Rademacher CJ, Zimmerman LG, Gimenez-Lirola J, Sun Y. 2016. Evaluation of the effects of PEDV vaccine on PEDV naïve and previously PEDV exposed sows in a challenge model comparing immune response and preweaning mortality. 2016 AASV Annu Meet Standing shoulders giants Collab teamwork 363–363.
57. Makadiya N, Brownlie R, Van Den Hurk J, Berube N, Allan B, Gerdts V, Zakhartchouk A. 2016. S1 domain of the porcine epidemic diarrhea virus spike protein as a vaccine antigen Susanna Lau. Virol J.
58. Chen JF, Feng L, Shi HYJ, Cui S. 2010. Update on vaccines of porcine epidemic diarrhea virus. Swine Ind Sci 12: 51. (i.
59. Sato T, Oroku K, Ohshima Y, Furuya Y, Sasakawa C. 2018. Efficacy of genogroup 1 based porcine epidemic diarrhea live vaccine against genogroup 2 field strain in Japan. Virol J.
60. Turner MD, Nedjai B, Hurst T, Pennington DJ. 2014. Cytokines and chemokines: At the crossroads of cell signalling and inflammatory disease. Biochim Biophys Acta - Mol Cell Res.
61. Chatel-Chaix L, Cortese M, Romero-Brey I, Bender S, Neufeldt CJ, Fischl W, Scaturro P, Schieber N, Schwab Y, Fischer B, Ruggieri A, Bartenschlager R. 2016. Dengue Virus Perturbs Mitochondrial Morphodynamics to Dampen Innate Immune Responses. Cell Host Microbe.
62. Zhao L, Jha BK, Wu A, Elliott R, Ziebuhr J, Gorbalenya AE, Silverman RH, Weiss SR. 2012. Antagonism of the interferon-induced OAS-RNase L pathway by murine coronavirus ns2 protein is required for virus replication and liver pathology. Cell Host Microbe.
63. Laurent-Rolle M, Morrison J, Rajsbaum R, Macleod JML, Pisanelli G, Pham A, Ayllon J, Miorin L, Martínez-Romero C, Tenoever BR, García-Sastre A. 2014. The interferon signaling antagonist function of yellow fever virus NS5 protein is activated by type i interferon. Cell Host Microbe.
64. Theofilopoulos AN, Kono DH, Baccala R. 2017. The multiple pathways to autoimmunity. Nat Immunol.
65. InvivoGen. 2005. Type I IFN Production and Signaling.
66. Devasthanam AS. 2014. Mechanisms underlying the inhibition of interferon signaling by viruses. Virulence.
67. Yu L, Dong J, Wang Y, Zhang P, Liu Y, Zhang L, Liang P, Wang L, Song C. 2019. Porcine epidemic diarrhea virus nsp4 induces pro-inflammatory cytokine and chemokine expression inhibiting viral replication in vitro. Arch Virol.

68. Xu X, Zhang H, Zhang Q, Dong J, Liang Y, Huang Y, Liu H-J, Tong D. 2013. Porcine epidemic diarrhea virus E protein causes endoplasmic reticulum stress and up-regulates interleukin-8 expression. Virol J 10:26.
69. Rees MA, Stinear TP, Goode RJA, Coppel RL, Smith AI, Kleifeld O. 2015. Changes in protein abundance are observed in bacterial isolates from a natural host. Front Cell Infect Microbiol.
70. Collado-Romero M, Aguilar C, Arce C, Lucena C, Codrea MC, Morera L, Bendixen E, Moreno Á, Garrido JJ. 2015. Quantitative proteomics and bioinformatic analysis provide new insight into the dynamic response of porcine intestine to Salmonella Typhimurium. Front Cell Infect Microbiol.
71. Herweg J-A, Hansmeier N, Otto A, Geffken AC, Subbarayal P, Prusty BK, Becher D, Hensel M, Schaible UE, Rudel T, Hilbi H. 2015. Purification and proteomics of pathogen-modified vacuoles and membranes. Front Cell Infect Microbiol.
72. Zhang W, Sun J, Ding W, Lin J, Tian R, Lu L, Liu X, Shen X, Qian P-Y. 2015. Extracellular matrix-associated proteins form an integral and dynamic system during Pseudomonas aeruginosa biofilm development. Front Cell Infect Microbiol.
73. Ankney JA, Muneer A, Chen X. 2018. Relative and Absolute Quantitation in Mass Spectrometry–Based Proteomics. Annu Rev Anal Chem.
74. Pumfery A, Berro R, Kashanchi F. 2008. Proteomics of viruses, p. 309–343. *In* Medical Applications of Mass Spectrometry.
75. de Chassey B, Meyniel-Schicklin L, Vonderscher J, André P, Lotteau V. 2014. Virus-host interactomics: new insights and opportunities for antiviral drug discovery. Genome Med 6:115.
76. Cravatt BF, Simon GM, Yates JR. 2007. The biological impact of mass-spectrometry-based proteomics. Nature.
77. Graves PR, Haystead T a J. 2002. Molecular Biologist's Guide to Proteomics. Microbiol Mol Biol Rev Microbiol Mol Biol Rev 66:39–63.
78. Todd DA, Zich DB, Ettefagh KA, Kavanaugh JS, Horswill AR, Cech NB. 2016. Hybrid Quadrupole-Orbitrap mass spectrometry for quantitative measurement of quorum sensing inhibition. J Microbiol Methods.
79. Michalski A, Damoc E, Hauschild J-P, Lange O, Wieghaus A, Makarov A, Nagaraj N, Cox J, Mann M, Horning S. 2011. Mass spectrometry-based proteomics using Q Exactive, a high-performance benchtop quadrupole Orbitrap mass spectrometer. Mol Cell Proteomics.
80. Ho CS, Lam CWK, Chan MHM, Cheung RCK, Law LK, Lit LCW, Ng KF, Suen MWM, Tai HL. 2003. Electrospray ionisation mass spectrometry: principles and clinical applications. Clin Biochem 24:3–12.
81. Clark AE, Kaleta EJ, Arora A, Wolk DM. 2013. Matrix-Assisted laser desorption ionization-time of flight mass spectrometry: A fundamental shift in the routine practice of clinical microbiology. Clin Microbiol Rev 26:547–603.
82. Perry RH, Cooks RG, Noll RJ. 2008. Orbitrap mass spectrometry: Instrumentation, ion motion and applications. Mass Spectrom Rev 27:661–699.
83. Thiede B, Höhenwarter W, Krah A, Mattow J, Schmid M, Schmidt F, Jungblut PR. 2005. Peptide mass fingerprinting. Methods 35:237–247.
84. Lindemann C, Thomanek N, Hundt F, Lerari T, Meyer HE, Wolters D, Marcus K. 2017. Strategies in relative and absolute quantitative mass spectrometry based proteomics. Biol Chem.

85. Strmiskova M, Desrochers GF, Shaw TA, Powdrill MH, Lafreniere MA, Pezacki JP. 2016. Chemical Methods for Probing Virus-Host Proteomic Interactions. ACS Infect Dis.
86. Li Z, Chen F, Ye S, Guo X, Muhanmmad Memon A, Wu M, He Q. 2016. Comparative Proteome Analysis of Porcine Jejunum Tissues in Response to a Virulent Strain of Porcine Epidemic Diarrhea Virus and Its Attenuated Strain. Viruses 8:323.
87. Lin H, Li B, Chen L, Ma Z, He K, Fan H. 2017. Differential Protein Analysis of IPEC-J2 Cells Infected with Porcine Epidemic Diarrhea Virus Pandemic and Classical Strains Elucidates the Pathogenesis of Infection. J Proteome Res 16:2113–2120.
88. Jang J, Lee J, Kim ST, Lee KY, Cho JY, Kweon DH, Kwon ST, Koh YH, Kim S, Yoon K. 2012. Polycation-mediated enhancement of retroviral transduction efficiency depends on target cell types and pseudotyped Env proteins: Implication for gene transfer into neural stem cells. Neurochem Int 60:846–851.
89. Davis HE, Rosinski M, Morgan JR, Yarmush ML. 2004. Charged Polymers Modulate Retrovirus Transduction via Membrane Charge Neutralization and Virus Aggregation. Biophys J.
90. Kaplan MM, Wiktor TJ, Maes RF, Campbell JB, Koprowski H. 1967. Effect of polyions on the infectivity of rabies virus in tissue culture: construction of a single-cycle growth curve. J Virol 1:145–151.
91. Ran X, Ao Z, Trajtman A, Xu W, Kobinger G, Keynan Y, Yao X. 2017. HIV-1 envelope glycoprotein stimulates viral transcription and increases the infectivity of the progeny virus through the manipulation of cellular machinery. Sci Rep.
92. Bailey CA, Miller DK, Lenard J. 1984. Effects of DEAE-dextran on infection and hemolysis by VSV. Evidence that nonspecific electrostatic interactions mediate effective binding of VSV to cells. Virology 133:111–118.
93. Platt EJ, Kozak SL, Durnin JP, Hope TJ, Kabat D. 2010. Rapid Dissociation of HIV-1 from Cultured Cells Severely Limits Infectivity Assays, Causes the Inactivation Ascribed to Entry Inhibitors, and Masks the Inherently High Level of Infectivity of Virions. J Virol 84:3106–3110.
94. Hughes JH. 1993. Physical and chemical methods for enhancing rapid detection of viruses and other agents. Clin Microbiol Rev.
95. Nguyen TD, Bottreau E, Aynaud JM. 1987. Transmissible gastroenteritis (TGE) of swine: In vitro virus attachment and effects of polyanions and polycations. Vet Microbiol.
96. Sato K, Inaba Y, Miura Y, Tokuhisa S, Matumoto M. 1983. Inducement of cytopathic changes and plaque formation by porcine haemagglutinating encephalomyelitis virus. Vet Microbiol.
97. Bradburne AF, Tyrrell DAJ. 1969. The propagation of ``coronaviruses'' in tissue-culture. Arch Gesamte Virusforsch 28:133–150.
98. Denning W, Das S, Guo S, Xu J, Kappes JC, Hel Z. 2013. Optimization of the transductional efficiency of lentiviral vectors: Effect of sera and polycations. Mol Biotechnol.
99. Toyoshima K, Vogt PK. 1969. Enhancement and inhibition of avian sarcoma viruses by polycations and polyanions. Virology 38:414–426.
100. Marthaler D, Jiang Y, Otterson T, Goyal S, Rossow K, Collins J. 2013. Complete Genome Sequence of Porcine Epidemic Diarrhea Virus Strain USA/Colorado/2013 from the United States. Genome Announc.

101. Yang DK, Kim HH, Lee SH, Yoon SS, Park JW, Cho IS. 2018. Isolation and characterization of a new porcine epidemic diarrhea virus variant that occurred in Korea in 2014. J Vet Sci.
102. Trudel PP and M. 1989. Manuel de techniques virologiques. L'Université de Québec, Quebec.
103. Ott DE. 2009. Purification of HIV-1 virions by subtilisin digestion or CD45 immunoaffinity depletion for biochemical studies. Methods Mol Biol.
104. Marsh M, Helenius A. 2006. Virus entry: Open sesame. Cell.
105. Debouck P, Pensaert M. 1980. Experimental infection of pigs with a new porcine enteric coronavirus, CV 777. Am J Vet Res.
106. Madani N, Kabat D. 2002. Cellular and Viral Specificities of Human Immunodeficiency Virus Type 1 Vif Protein. J Virol.
107. Pace MJ, Graf EH, Agosto LM, Mexas AM, Male F, Brady T, Bushman FD, O'Doherty U. 2012. Directly infected resting CD4+T cells can produce HIV Gag without spreading infection in a model of HIV latency. PLoS Pathog.
108. Janas AM, Wu L. 2009. HIV-1 interactions with cells: From viral binding to cell-cell transmission. Curr Protoc Cell Biol.
109. Ma H, Zhao XL, Wang XY, Xie XW, Han JC, Guan WL, Wang Q, Zhu L, Pan X Ben, Wei L. 2013. 2',3'-cyclic nucleotide 3'-phosphodiesterases inhibit hepatitis B virus replication. PLoS One.
110. Rosenbergova M, Pristasova S. 1991. Relationship of 2',3'-cyclic nucleotide 3'-phosphohydrolase activity of large enveloped RNA viruses to host cell activity. Acta Virol 35:401–407.
111. Zhou Q, Lavorgna A, Bowman M, Hiscott J, Harhaj EW. 2015. Aryl hydrocarbon receptor interacting protein targets IRF7 to suppress antiviral signaling and the induction of type I interferon. J Biol Chem.
112. Fujimori T, Grabiec AM, Kaur M, Bell TJ, Fujino N, Cook PC, Svedberg FR, Macdonald AS, Maciewicz RA, Singh D, Hussell T. 2015. The Axl receptor tyrosine kinase is a discriminator of macrophage function in the inflamed lung. Mucosal Immunol.
113. Ilyinskii PO, Wang R, Balk SP, Exley MA. 2006. CD1d Mediates T-Cell-Dependent Resistance to Secondary Infection with Encephalomyocarditis Virus (EMCV) In Vitro and Immune Response to EMCV Infection In Vivo. J Virol.
114. Tsunoda I, Tanaka T, Fujinami RS. 2008. Regulatory Role of CD1d in Neurotropic Virus Infection. J Virol.
115. Diana J, Lehuen A. 2009. NKT cells: Friend or foe during viral infections? Eur J Immunol.
116. Durante-Mangoni E, Wang R, Shaulov A, He Q, Nasser I, Afdhal N, Koziel MJ, Exley MA. 2004. Hepatic CD1d Expression in Hepatitis C Virus Infection and Recognition by Resident Proinflammatory CD1d-Reactive T Cells. J Immunol.
117. Ahuja D, Sáenz-Robles MT, Pipas JM. 2005. SV40 large T antigen targets multiple cellular pathways to elicit cellular transformation. Oncogene.
118. Levine AJ, Oren M. 2009. The first 30 years of p53: Growing ever more complex. Nat Rev Cancer.
119. Gross S, Catez F, Masumoto H, Lomonte P. 2012. Centromere Architecture Breakdown Induced by the Viral E3 Ubiquitin Ligase ICP0 Protein of Herpes Simplex Virus Type 1. PLoS One.

120. Gupta S, Bousman CA, Chana G, Cherner M, Heaton RK, Deutsch R, Ellis RJ, Grant I, Everall IP. 2011. Dopamine receptor D3 genetic polymorphism (rs6280TC) is associated with rates of cognitive impairment in methamphetamine-dependent men with HIV: Preliminary findings. J Neurovirol.
121. Takahashi K, Halfmann P, Oyama M, Kozuka-Hata H, Noda T, Kawaoka Y. 2013. DNA Topoisomerase 1 Facilitates the Transcription and Replication of the Ebola Virus Genome. J Virol.
122. Pourquier P, Jensen AD, Gong SS, Pommier Y, Rogler CE. 1999. Human DNA topoisomerase I-mediated cleavage and recombination of duck hepatitis B virus DNA in vitro. Nucleic Acids Res.
123. Kim SH, MacFarlane S, Kalinina NO, Rakitina D V., Ryabov E V., Gillespie T, Haupt S, Brown JWS, Taliansky M. 2007. Interaction of a plant virus-encoded protein with the major nucleolar protein fibrillarin is required for systemic virus infection. Proc Natl Acad Sci.
124. Cheng H, Lear-Rooney CM, Johansen L, Varhegyi E, Chen ZW, Olinger GG, Rong L. 2015. Inhibition of Ebola and Marburg Virus Entry by G Protein-Coupled Receptor Antagonists. J Virol.
125. Pan W, Zuo X, Feng T, Shi X, Dai J. 2012. Guanylate-binding protein 1 participates in cellular antiviral response to dengue virus. Virol J.
126. Li L-F, Yu J, Li Y, Wang J, Li S, Zhang L, Xia S-L, Yang Q, Wang X, Yu S, Luo Y, Sun Y, Zhu Y, Munir M, Qiu H-J. 2016. Guanylate-Binding Protein 1, an Interferon-Induced GTPase, Exerts an Antiviral Activity against Classical Swine Fever Virus Depending on Its GTPase Activity. J Virol.
127. Kim MY, Oglesbee M. 2012. Virus-Heat Shock Protein Interaction and a Novel Axis for Innate Antiviral Immunity. Cells.
128. Hepat R, Song J-J, Lee D, Kim Y. 2013. A Viral Histone H4 Joins to Eukaryotic Nucleosomes and Alters Host Gene Expression. J Virol.
129. Schoggins JW, Rice CM. 2011. Interferon-stimulated genes and their antiviral effector functions. Curr Opin Virol.
130. Schneider WM, Chevillotte MD, Rice CM. 2014. Interferon-Stimulated Genes: A Complex Web of Host Defenses. Annu Rev Immunol.
131. Hewitt EW. 2003. The MHC class I antigen presentation pathway: Strategies for viral immune evasion. Immunology.
132. Yewdell JW, Bennink JR. 1999. Mechanisms of Viral Interference with MHC Class I Antigen Processing and Presentation. Annu Rev Cell Dev Biol.
133. Unal CM, Steinert M. 2014. Microbial peptidyl-prolyl cis/trans isomerases (PPIases): virulence factors and potential alternative drug targets. Microbiol Mol Biol Rev 78:544–571.
134. Kuny C V, Sullivan CS. 2016. Virus–Host Interactions and the ARTD/PARP Family of Enzymes. PLOS Pathog 12:1–7.
135. Melia MM, Earle JP, Abdullah H, Reaney K, Tangy F, Cosby SL. 2014. Use of SLAM and PVRL4 and identification of Pro-HB-EGF as cell entry receptors for wild type phocine distemper virus. PLoS One.
136. Giovannoni F, Damonte EB, García CC. 2015. Cellular promyelocytic leukemia protein is an important dengue virus restriction factor. PLoS One.
137. Drappier M, Michiels T. 2015. Inhibition of the OAS/RNase L pathway by viruses. Curr Opin Virol.

138. Martinand C, Montavon C, Salehzada T, Silhol M, Lebleu B, Bisbal C. 1999. RNase L inhibitor is induced during human immunodeficiency virus type 1 infection and down regulates the 2-5A/RNase L pathway in human T cells. J Virol.
139. Liang SL, Quirk D, Zhou A. 2006. RNase L: Its biological roles and regulation. IUBMB Life.
140. Rolfe AJ, Bosco DB, Wang J, Nowakowski RS, Fan J, Ren Y. 2016. Bioinformatic analysis reveals the expression of unique transcriptomic signatures in Zika virus infected human neural stem cells. Cell Biosci.
141. Sen N, Che X, Rajamani J, Zerboni L, Sung P, Ptacek J, Arvin AM. 2011. Signal transducer and activator of transcription 3 (STAT3) and survivin induction by varicella-zoster virus promote replication and skin pathogenesis. Proc Natl Acad Sci U S A.
142. Shi Q, Jiang J, Luo G. 2013. Syndecan-1 Serves as the Major Receptor for Attachment of Hepatitis C Virus to the Surfaces of Hepatocytes. J Virol.
143. Wang R, Wang X, Ni B, Huan CC, Wu JQ, Wen L Bin, Liao Y, Tong GZ, Ding C, Fan HJ, Mao X. 2016. Syndecan-4, a PRRSV attachment factor, mediates PRRSV entry through its interaction with EGFR. Biochem Biophys Res Commun.
144. Teo CSH, Chu JJH. 2014. Cellular Vimentin Regulates Construction of Dengue Virus Replication Complexes through Interaction with NS4A Protein. J Virol.
145. Guo X, Carroll J-WN, Macdonald MR, Goff SP, Gao G. 2004. The Zinc Finger Antiviral Protein Directly Binds to Specific Viral mRNAs through the CCCH Zinc Finger Motifs Downloaded from. J Virol.
146. Willems L, Gillet NA. 2015. APOBEC3 interference during replication of viral genomes. Viruses.
147. Allen SJ, Rhode-Kurnow A, Mott KR, Jiang X, Carpenter D, Rodriguez-Barbosa JI, Jones C, Wechsler SL, Ware CF, Ghiasi H. 2014. Interactions between Herpesvirus Entry Mediator (TNFRSF14) and Latency-Associated Transcript during Herpes Simplex Virus 1 Latency. J Virol.
148. Stolf BS, Smyrnias I, Lopes LR, Vendramin A, Goto H, Laurindo FRM, Shah AM, Santos CXC. 2011. Protein disulfide isomerase and host-pathogen interaction. ScientificWorldJournal.
149. Helbig KJ, Beard MR. 2014. The role of viperin in the innate antiviral response. J Mol Biol.
150. Wang G, Watson KM, Buckheit RW. 2008. Anti-human immunodeficiency virus type 1 activities of antimicrobial peptides derived from human and bovine cathelicidins. Antimicrob Agents Chemother.
151. Currie SM, Findlay EG, McHugh BJ, Mackellar A, Man T, Macmillan D, Wang H, Fitch PM, Schwarze J, Davidson DJ. 2013. The Human Cathelicidin LL-37 Has Antiviral Activity against Respiratory Syncytial Virus. PLoS One.
152. Tripathi S, Tecle T, Verma A, Crouch E, White M, Hartshorn KL. 2013. The human cathelicidin LL-37 inhibits influenza a viruses through a mechanism distinct from that of surfactant protein d or defensins. J Gen Virol.
153. Howell MD, Gallo RL, Boguniewicz M, Jones JF, Wong C, Streib JE, Leung DYM. 2006. Cytokine milieu of atopic dermatitis skin subverts the innate immune response to vaccinia virus. Immunity.
154. Symons JA, Alcamí A, Smith GL. 1995. Vaccinia virus encodes a soluble type I interferon receptor of novel structure and broad species soecificity. Cell.

155. Alcami A, Smith GL, Alcamí A. 1995. Vaccinia, cowpox, and camelpox viruses encode soluble gamma interferon receptors with novel broad species specificity. J Virol.
156. Gao Q, Zhao S, Qin T, Yin Y, Yang Q. 2015. Effects of porcine epidemic diarrhea virus on porcine monocyte-derived dendritic cells and intestinal dendritic cells. Vet Microbiol.
157. Richmond O, Cecere TE, Erdogan E, Meng X., Piñeyro P, Subramaniam S, Todd SM, LeRoith T. 2015. The PD-L1/CD86 ratio is increased in dendritic cells co-infected with porcine circovirus type 2 and porcine reproductive and respiratory syndrome virus, and the PD-L1/PD-1 axis is associated with anergy, apoptosis, and the induction of regulatory T-cells in porcine lymphocytes. Vet Microbiol 180:223–229.
158. Dansako H, Ueda Y, Okumura N, Satoh S, Sugiyama M, Mizokami M, Ikeda M, Kato N. 2016. The cyclic GMP-AMP synthetase-STING signaling pathway is required for both the innate immune response against HBV and the suppression of HBV assembly. FEBS J.
159. Ni G, Ma Z, Damania B. 2018. cGAS and STING: At the intersection of DNA and RNA virus-sensing networks. PLOS Pathog.
160. Knox C, Luke GA, Blatch GL, Pesce ER. 2011. Heat shock protein 40 (Hsp40) plays a key role in the virus life cycle. Virus Res.
161. Jiang DK, Sun J, Cao G, Liu Y, Lin D, Gao YZ, Ren WH, Long XD, Zhang H, Ma XP, Wang Z, Jiang W, Chen TY, Gao Y, Sun LD, Long JR, Huang HX, Wang D, Yu H, Zhang P, Tang LS, Peng B, Cai H, Liu TT, Zhou P, Liu F, Lin X, Tao S, Wan B, Sai-Yin HXG, Qin LX, Yin J, Liu L, Wu C, Pei Y, Zhou YF, Zhai Y, Lu PX, Tan A, Zuo XB, Fan J, Chang J, Gu X, Wang NJ, Li Y, Liu YK, Zhai K, Zhang H, Hu Z, Liu J, Yi Q, Xiang Y, Shi R, Ding Q, Zheng W, Shu XO, Mo Z, Shugart YY, Zhang XJ, Zhou G, Shen H, Zheng SL, Xu J, Yu L. 2013. Genetic variants in STAT4 and HLA-DQ genes confer risk of hepatitis B virus-related hepatocellular carcinoma. Nat Genet.
162. Haan KM, Kwok WW, Longnecker R, Speck P. 2000. Epstein-Barr virus entry utilizing HLA-DP or HLA-DQ as a coreceptor. J Virol.
163. Kwok WW, Liu AW, Novak EJ, Gebe JA, Ettinger RA, Nepom GT, Reymond SN, Koelle DM. 2000. HLA-DQ Tetramers Identify Epitope-Specific T Cells in Peripheral Blood of Herpes Simplex Virus Type 2-Infected Individuals: Direct Detection of Immunodominant Antigen-Responsive Cells. J Immunol.
164. Piersma SJ, Welters MJP, Van Der Hulst JM, Kloth JN, Kwappenberg KMC, Trimbos BJ, Melief CJM, Hellebrekers BW, Fleuren GJ, Kenter GG, Offringa R, Van Der Burg SH. 2008. Human papilloma virus specific T cells infiltrating cervical cancer and draining lymph nodes show remarkably frequent use of HLA-DQ and -DP as a restriction element. Int J Cancer.
165. Rose PP, Hanna SL, Spiridigliozzi A, Wannissorn N, Beiting DP, Ross SR, Hardy RW, Bambina SA, Heise MT, Cherry S. 2011. Natural resistance-associated macrophage protein is a cellular receptor for Sindbis virus in both insect and mammalian hosts. Cell Host Microbe.
166. Cattaneo R, Ma D, Samuel CE, Pfaller CK, Nomburg JL, George CX. 2017. Upon Infection, Cellular WD Repeat-Containing Protein 5 (WDR5) Localizes to Cytoplasmic Inclusion Bodies and Enhances Measles Virus Replication. J Virol.
167. Monnery BD, Wright M, Cavill R, Hoogenboom R, Shaunak S, Steinke JHG, Thanou M. 2017. Cytotoxicity of polycations: Relationship of molecular weight and the

hydrolytic theory of the mechanism of toxicity. Int J Pharm.
168. Fischer D, Li Y, Ahlemeyer B, Krieglstein J, Kissel T. 2003. In vitro cytotoxicity testing of polycations: influence of polymer structure on cell viability and hemolysis. Biomaterials.
169. van der Valk J, Bieback K, Buta C, Cochrane B, Dirks WG, Fu J, Hickman JJ, Hohensee C, Kolar R, Liebsch M, Pistollato F, Schulz M, Thieme D, Weber T, Wiest J, Winkler S, Gstraunthaler G. 2018. Fetal Bovine Serum (FBS): Past - Present - Future. ALTEX 35:99–118.
170. VERO C1008 [Vero 76, clone E6, Vero E6] (ATCC® CRL-1586™). ATCC.
171. Park JE, Cruz DJM, Shin HJ. 2011. Receptor-bound porcine epidemic diarrhea virus spike protein cleaved by trypsin induces membrane fusion. Arch Virol 156:1749–1756.
172. Chen C, Akerstrom V, Baus J, Lan MS, Breslin MB. 2013. Comparative analysis of the transduction efficiency of five adeno associated virus serotypes and VSV-G pseudotype lentiviral vector in lung cancer cells. Virol J.
173. Kim BJ, Kim KJ, Kim YH, Lee YA, Kim BG, Cho CM, Kang HR, Kim CG, Ryu BY. 2012. Efficient enhancement of lentiviral transduction efficiency in Murine spermatogonial stem cells. Mol Cells.
174. Mistry BA, D'Orsogna MR, Chou T. 2018. The Effects of Statistical Multiplicity of Infection on Virus Quantification and Infectivity Assays. Biophys J.
175. Albrecht T, Fons M, Boldogh I, Rabson. AS. 1996. Chapter 44 Effects on CellsMedical Microbiology. 4th edition.
176. James KT, Cooney B, Agopsowicz K, Trevors MA, Mohamed A, Stoltz D, Hitt M, Shmulevitz M. 2016. Novel High-throughput Approach for Purification of Infectious Virions. Sci Rep.
177. Maxwell KL, Frappier L. 2007. Viral Proteomics. Microbiol Mol Biol Rev 71:398–411.
178. Morales J, Li L, Fattah FJ, Dong Y, Bey EA, Patel M, Gao J, Boothman DA. 2014. Review of Poly (ADP-ribose) Polymerase (PARP) Mechanisms of Action and Rationale for Targeting in Cancer and Other Diseases. Crit Rev Eukaryot Gene Expr.
179. Joerger AC, Fersht AR. 2016. The p53 Pathway: Origins, Inactivation in Cancer, and Emerging Therapeutic Approaches. Annu Rev Biochem.
180. Sun P, Wu H, Huang J, Xu Y, Yang F, Zhang Q, Xu X. 2018. Porcine epidemic diarrhea virus through p53-dependent pathway causes cell cycle arrest in the G0/G1 phase. Virus Res 253:1–11.
181. Shi Da, Chen Jian-fei, Shi Hong-yan, Zhang Zhi-bang FL. 2011. Subcellular localization analysis between porcine epidemic diarrhea virus nucleocapsid protein and fibrillarin. Chinese J Prev Vet Med 11.
182. Shi D, Shi H, Sun D, Chen J, Zhang X, Wang X, Zhang J, Ji Z, Liu J, Cao L, Zhu X, Yuan J, Dong H, Wang X, Chang T, Liu Y, Feng L. 2017. Nucleocapsid Interacts with NPM1 and Protects it from Proteolytic Cleavage, Enhancing Cell Survival, and is Involved in PEDV Growth. Sci Rep.
183. Nigro P, Pompilio G, Capogrossi MC. 2013. Cyclophilin A: A key player for human disease. Cell Death Dis.
184. Kim Y, Lee C. 2014. Porcine epidemic diarrhea virus induces caspase-independent apoptosis through activation of mitochondrial apoptosis-inducing factor. Virology.
185. Ståhl A lie, Johansson K, Mossberg M, Kahn R, Karpman D. 2019. Exosomes and

microvesicles in normal physiology, pathophysiology, and renal diseases. Pediatr Nephrol.

IX. Communications and founding

Communications

Sánchez Mendoza, L. J., Valle Tejada, C. A., Provost, C., Gagnon, C. A., Beaudry, F., and L. Abrahamyan. (2016, December). Dissection of Complex Molecular Interactions between Important Animal Nidoviruses and the Host. Presented in the North American PRRS Symposium. Chicago, IL.

Sánchez Mendoza, L. J., Valle Tejada, C. A., Provost, C., Gagnon, C. A., Beaudry, F., and L. Abrahamyan. (2016, December). Dissection of Complex Molecular Interactions between Important Animal Nidoviruses and the Host. Presented at the Conference of Research Workers in Animal Diseases (CRWAD). Chicago, IL.

L. Abrahamyan, Sánchez Mendoza. L.J., Valle Tejada C. A., Provost, C., Beaudry, F., and C. A. Gagnon. (2017, May). Decoding Proteins Network During Porcine Nidoviral Infection by Quantitative Proteomics. Presented at 10e symposium du CRIPA. Saint-Hyacinthe, QC.

Valle Tejada C. A., Sánchez Mendoza, L.J., Provost, C., Gagnon, C.A., Beaudry, F., and L. Abrahamyan. (2017, June). Decoding Proteins Networks During Porcine Nidoviral Infection by Quantitative Proteomics. Presented in XIVth International Nidovirus Symposium (Nido2017). Kansas City, MO.

Valle Tejada C. A., Sánchez Mendoza, L.J., Provost, C., Gagnon, C.A., Beaudry, F., and L. Abrahamyan. (2018, May). Optimization of the efficiency of viral infection of two porcine nidoviruses (PRRSV and PEDV) of veterinary importance. Presented at 11e symposium du CRIPA. Saint-Hyacinthe, QC.

Sánchez Mendoza, L. J., Valle Tejada, C. A., Provost, C., Gagnon, C. A., Beaudry, F., and L. Abrahamyan. (2018, June) Decoding Intraviral and Virus-Host Protein Interaction Networks of Porcine Nidoviruses by Quantitative Proteomics". Presented at 2nd Symposium of the Canadian Society for Virology (CSV2018). Halifax, NS.

Sánchez Mendoza, L. J., Valle Tejada, C. A., Provost, C., Gagnon, C. A., Beaudry, F., and

L. Abrahamyan. (2018, December). Dissection of Complex Molecular Interactions between Important Animal Nidoviruses and the Host. Presented at the Conference of Research Workers in Animal Diseases (CRWAD). Chicago, IL.

Valle Tejada C. A., Sánchez Mendoza, L.J., Provost, C., Gagnon, C.A., Beaudry, F., and L. Abrahamyan. (2019, May). Dissection of Complex Molecular Interactions between Important Animal Nidoviruses and the Host. Canadian animal health laboratorians network (CAHLN) 18th CAHLN Annual Meeting. Saint-Hyacinthe, QC.

Valle Tejada C. A., Provost, C., Gagnon, C.A., Beaudry, F., and L. Abrahamyan. (2019, June). Decoding protein networks during Porcine Epidemic Diarrhea Virus infection through proteomics. American society for microbiology (ASM) Microbe 2019. San Francisco, CA.

Scholarships and founding

2017-Short-term financial support for graduate students at the CRIPA, September-December. Centre de recherche en infectiologie porcine et avicole (CRIPA).

2017-Bourse d'exemption de droits scolarité supplémentaires pour le trimestre d'été 2017. Faculté des études supérieures et postdoctorales.

2017-Bourse de soutien pour étudiant international sans bourse d'exemption. Faculté des études supérieures et postdoctorales.

2018-Bourse d'exemption de droits scolarité supplémentaires pour le trimestre d'automne 2017. Faculté des études supérieures et postdoctorales.

2018-Bourse de soutien financier. Faculté des études supérieures et postdoctorales.

2019-Short-term financial support for graduate students at the CRIPA, January-April. Centre de recherche en infectiologie porcine et avicole (CRIPA).

2019-Bourse spéciale. Faculté des études supérieures et postdoctorales.

2019-Travel fellowship for attending the American Society for Microbiology 2019 congress, June 20-24, 2019.Centre de recherche en infectiologie porcine et avicole (CRIPA).